COUPLING GIS WITH HEC-RAS MODEL TO DEVELOP RETURN PERIOD BASED FLOOD HAZARD MAP: A CASE STUDY OF LOWER MEKONG RIVER, CAMBODIA

VANTHAN KIM

A Thesis Submitted to the Graduate School of Naresuan University
in Partial Fulfillment of the Requirements
for the Master of Science in (Disaster Management - (Plan A Type A2) International Program)
2019

COUPLING GIS WITH HEC-RAS MODEL TO DEVELOP RETURN PERIOD BASED FLOOD HAZARD MAP: A CASE STUDY OF LOWER MEKONG RIVER, CAMBODIA

VANTHAN KIM

A Thesis Submitted to the Graduate School of Naresuan University
in Partial Fulfillment of the Requirements
for the Master of Science in (Disaster Management - (Plan A Type A2) International Program)
2019

Thesis entitled "Coupling GIS with HEC-RAS Model to Develop Return Period Based Flood Hazard Map: A Case Study of Lower Mekong River, Cambodia"

By VANTHAN KIM

has been approved by the Graduate School as partial fulfillment of the requirements for the Master of Science in Disaster Management - (Plan A Type A2) International Program of Naresuan University

Oral Defense Committee

..... Chair
(Bhichit Rattakul, Ph.D.)

..... Advisor
(Associate Professor Sarintip Tantanee, Ph.D.)

..... Co Advisor
(Assistant Professor Panu Buranajarukorn, Ph.D.)

..... Co Advisor
(Charatdao Kongmuang, Ph.D.)

..... Internal Examiner
(Polpreecha Chidburee, Ph.D.)

Approved

.....
(Professor Paisarn Muneesawang, Ph.D.)

for Dean of the Graduate School

Title COUPLING GIS WITH HEC-RAS MODEL TO DEVELOP RETURN PERIOD BASED FLOOD HAZARD MAP: A CASE STUDY OF LOWER MEKONG RIVER, CAMBODIA

Author VANTHAN KIM

Advisor Associate Professor Sarintip Tantanee, Ph.D.

Co-Advisor Assistant Professor Panu Buranajarukorn, Ph.D. , Charatdao Kongmuang, Ph.D.

Academic Paper Thesis M.S. in Disaster Management - (Plan A Type A2) International Program, Naresuan University, 2019

Keywords Flood Hazard HEC-RAS Model Geographic Information System and Return Period

ABSTRACT

Over the last decade, societies have been exposed to the danger of natural events such as earthquakes, droughts, and floods that cannot be avoided completely even with modern-day scientific and technological facilities, preparedness, mitigation, and early warning systems. The most hazardous extreme natural event is the occurrence of floods not only due to the effects of intensive rainfall, but more significantly, due to human settlement in areas that could be affected by flooding such as floodplains, adjacent to riverbanks, and valleys. Flood models are essential to assess human, economic, and financial impacts of flood inundations.

In order to achieve successful measures to reduce the danger of flooding, it is essential to know the fundamental aspects of flooding, the definition of flooding, and the generation processes. This paves the way for methodological procedures to predict and prepare for possible future events and to take the precautions necessary to mitigate future events. Moreover, the coordination of emergency activities during flood events can be positively affected by the correct use of flood extent information. It is also very important for the calibration and validation of hydraulic models to reconstruct what happened during the flood and to determine and monitor the extent of flooded areas. These descriptions are either empirically, or physically based, or

combined conceptual physically-based descriptions of the physical processes involved. Although, in general, the conceptualizations may neglect or simplify some of the underlying hydrologic transport processes, the resulting models are quite useful in practice because they are simple and provide adequate estimates of flood hydrographs. GIS and HEC-RAS hydraulic models are a powerful tool in river flood applications like flood hazard analysis and mapping at various scales.

This study indicates the use of flood frequency analysis integrating with 1-D HEC-RAS hydraulic model and Geographic Information System (GIS) to prepare flood hazard maps of different return periods in the Lower Mekong River, Cambodia. Log-Pearson type III, Log-Normal, Normal and Gumbel distribution were used to calculate the peak flood of multi return periods, namely, 10, 20, 50, and 100-years. The peak flood from frequency analysis is entered into the HEC-RAS model to find the corresponding flood level and extents in the study area. The model results are used in integrating with ArcGIS to generate flood hazard maps. Flood depths and extents could be identified through flood hazard maps. Nevertheless, the coupling between HEC-RAS and GIS provides a capability to flood mapping for the study along the river. The flood hazard map from 10, 20, 50, and 100-year return periods provides satisfactory samples for this process. As well as, the calibration of the resulting model requires knowledge of the study area are used NSE, RSR, R2, and PBIAS by computed using daily average flow. In short, this study is in proving the necessity of GIS and HEC-RAS hydraulic modeling before flood mitigation measures realization in the territory. Because both models are improving the prediction of flood events and flood prevention system, the aims were to reduce damage from floods and providing a better quality of life along the community river.

ACKNOWLEDGEMENTS

Firstly, I would like to express my gratitude to my advisor, Associate Professor Dr. Sarintip Tantanee, and my co-advisor Assistant Professor Dr. Panu Buranajarukorn and Dr. Charatdao Kongmuang for their scientific guidance and supervision in a calm manner throughout this thesis work.

I am grateful for the Royal Scholarship provided by Her Royal Highness Princess Sirindhorn for my Royal Scholarship, with which I was able to complete this thesis. Furthermore, I would like to express their deepest gratitude to the Department of Hydrology and River Works Cambodia for providing the necessary data of the study.

Many thanks go to the dean of engineering, the head of Civil Engineering Department, lecturers, and staff of the Department of Civil Engineering, Naresuan University for their help and assistance.

Finally, my greatest gratitude is dedicated to my respectful parents and sibling, for their encouragement and inspiration during the difficult time of my study.

VANTHAN KIM

TABLE OF CONTENTS

Page

List of tables

Page

List of figures

Page

ABBREVIATIONS

ADB	=	Asian Development Bank
DEM	=	Digital Elevation Model
CRED	=	Centre for Research on the Epidemiology of Disasters
EM-DAT	=	Emergency Evens Database
MoWRM	=	Ministry of Water Resource and Meteorology
MODIS	=	Moderate Resolution Imaging Spectroradiometer
MRC	=	Mekong River Commission
NCDM	=	National Committee for Disaster Management (Cambodia)
NFFC	=	National Flood Forecasting Center
ISIS	=	Software Package Used for River Modeling
LU/LC	=	Land Use and Land Cover
Lao PDR	=	Lao People's Democratic Republic
HEC-RAS	=	Hydraulic Engineering Center River Analysis System
HEC-GeoRAS	=	Hydraulic Engineering Center Geo-River Analysis System
HEC-HMS	=	Hydraulic Engineering Center Hydrologic Modeling System
GIS	=	Geographical Information System
RAS	=	River Analysis System
TIN	=	Triangulated Irregular Network
EWS	=	Early Warning System
FAO	=	Food and Agriculture Organization
NGO	=	Nongovernment Organization
OECD	=	Organization for Economic Co-operation and Development
USACE	=	US Army Corps of Engineers
SWAT	=	Soil & Water Assessment Tool
IQQM	=	Integrated Quantity Quality Model
IHA	=	Indicators of Hydrologic Alteration
UMRB	=	Upper Mekong River Basin
LMRB	=	Lower Mekong River Basin

CHAPTER I

INTRODUCTION

Background

Natural disasters can occur almost anywhere in the world at any time. The world has many gaps in its ability to respond to natural disasters. These gaps could significantly increase the intensity and frequency of extreme geophysical, climate and weather-related disasters (Su, 2011; Tan et al., 2017; Try et al., 2018; Chen et al., 2019). They also mean that the ability to respond to impacts in terms of human physical and economic losses (Petit-Boix et al., 2017; Dagli & Ferrarini, 2019) is unequal. By 2018 the world population had soared to more than 7 billion, and is expected to increase in the future (UNFPA, 2018). Natural resource supplies are a major concern, due to the growth of the population and its subsequent effects (Usher et al., 2015). According to the International Disaster Database who comprehensively reported in 2011, that 4,022 natural disasters had occurred between 2001 to 2010 worldwide, and had apparently killed 1,221,332 people (Manfre et al., 2012). In 2017, 335 natural disasters affected over 95.6 million people, killing 9,697 and cost a total of 335 billion US dollars (Kishore et al., 2018). The economic losses caused by floods alone, cost 65.600 billion US dollars which was 23% of the total natural disasters, such as tropical storms and earthquakes (Criado et al., 2018). Hence, to address environmental problems, people need to learn how to survive during natural disasters (Lyu et al., 2019). However, 34% of natural disasters are directly related to floods. Floods led to 1254 deaths and cost more than 2.5 billion US dollars in socioeconomic losses per year from 1960 to 2014 worldwide Petit-Boix et al. (2017) as cited by Guha-Sapir et al., 2009. Flooding is a serious natural disaster which has many socioeconomic and environmental consequences within the affected floodplain (Yousuf Gazi et al., 2019). Every year between 2000 and 2008, floods affected nearly 99 million people worldwide (El-Naqa & Jaber, 2018). Among natural disasters, flooding is one of the most devastating phenomena that has serious and negative effects to life, property loss, economic impact, social-civil conflicts and

environmental problems (Vathana, 2013; Bhola, Leandro, et al., 2018; El-Naqa & Jaber, 2018; Kishore et al., 2018; Wang et al., 2018; Xu et al., 2018; Abdelkarim et al., 2019; Chen et al., 2019; Lyu et al., 2019; Qiang, 2019) and affects more people than all other natural hazards (Quirogaa et al., 2017; Xu et al., 2018). According to the Organization for Economic Cooperation and Development (OECD), flooding is one of the most common, widespread and destructive natural perils, affecting approximately 250 million people worldwide and causing more than 40 billion dollars in damage and losses on an annual basis (OECD, 2016). From 1996 to 2015, approximately 150,061 flood events occurred throughout the world and were responsible for 11.1% of all disaster fatalities, based on information received from the United Nations Office for Disaster Risk Reduction (UNISDR) (Hong et al., 2018). Asia is a continent that consists mainly of developing countries which are extremely vulnerable to flooding (Usher et al., 2015; Kishore et al., 2018; Sarann et al., 2018; Dagli & Ferrarini, 2019), with the majority of victims being poor and living in rural areas (Rishiraj et al., 2015). Cambodia is one of the developing countries in the Asian region which is affected by hazardous floods every year and is ranked as one of the top flood-prone countries in the region.

Research Problem

Cambodia is susceptible to natural disasters and is categorized as one of the most disaster-prone countries in Southeast Asia (Rishiraj et al., 2015; Mishra et al., 2018), where flooding is ranked as the most common annual natural phenomenon (Okazumi et al., 2013; Sarann et al., 2018). Its exposure and vulnerability depend on location, precipitation, and characteristics of the region, and the adaptive capacity of how the people respond (Nyda & Millington, 2015). Over the last few decades, the frequency and magnitude of floods in Cambodia have increased rapidly (Liu et al., 2019) due to the activities of the catchment areas such as physical characteristics, hydrological features (rainfall, storage, evapotranspiration), and human activities (infrastructure and land-use change) combined, intensified the flood flow (Vathana, 2013; Sarann et al., 2018). Hence, floods seriously affect people's lives and productivity, causing considerable economic loss and serious damage to towns and agriculture (Ghanbarpour et al., 2013). The flood in Cambodia in 2000, caused by the

Mekong River, were reported to be the worst in more than 70 years (CFE-DM, 2017), while the floods in 2011 only killed 250 people, it affected 350,000 households of over 1.5 million people causing 52,000 households to be evacuated and cost the economy 521,000 million US dollars, which are ranked as the worst natural disasters in Cambodia (Mochizuki et al., 2015; NCDM, 2018). (Rishiraj et al., 2015; CFE-DM, 2017) reported the Cambodian floods of 2013, affected 20 out of 24 provinces, 377,354 households, claimed 168 lives, and forced 31,314 households to evacuate to safer areas. Compared to floods in 2011, the ones in 2013 appeared to have been on a less extensive in scale, although in some provinces the impact, including the number of evacuated families, damaged crops, and damaged infrastructure, were more significant due to a combination of factors such as the unexpected gravity of the floods, both in extent and intensity, longer time for the water to recede, repeated floods and flash floods, limited preparedness undertaken in advance and limited early warning. According to (Mochizuki et al., 2015) whose study assessment about the natural disaster of floods and cyclones risk to public and private buildings including educational structures, health facilities, and housing, estimates the total direct economic damage to range from approximately 304 million US dollars for a 5-year return period event, to 2.26 billion US dollars for a 1000-year return period event. Furthermore, according to (Vathana, 2013; Mochizuki et al., 2015; CFE-DM, 2017; NCDM, 2018) floods are the worst natural disaster in Cambodia, because they create major disruptions to the population, including loss of life, and damage to infrastructure since records started in 1900. The records by the National Committee Disaster Management (NCDM) of Cambodia showed that extreme flooding from the Mekong River mostly affected the country in 1978, 1991, 1994, 1996, 2000, 2001, 2002, 2011, and 2013, as well as Mochizuki et al. (2015) review of CRED, 2014. Likewise, the Cambodian Disaster and Risk Profile (EM-DAT) for 2017 concluded that floods with drought and storms, especially when focusing on frequency, mortality and economic loss, that flooding has the most complicated impact, even over that of drought and storms (CFE-DM, 2017; CRED, 2017). On the other hand, recorded by NCDM in Cambodia, it is comprehensive that floods are the negative consequence that contributes to loss of life and damaged property **(Figure 1).**

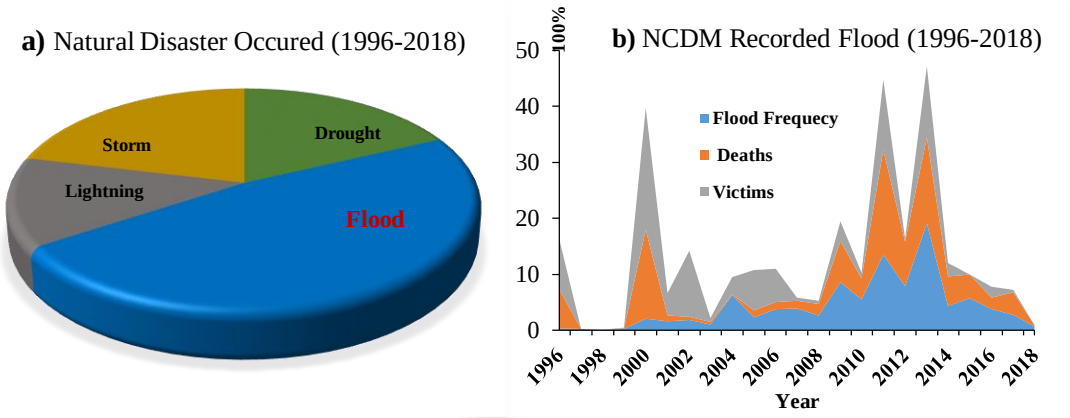

Figure 1 a) Natural hazards b) Flood frequency, deaths, and victim

Sources: National Committee Disaster Management in Cambodia (NCDM, 2018)

Most of the problem remains, flood studies and management strategies are being conducted. It has been shown that the most significant floods of recent years have occurred along the lower Mekong River. To evaluate the flood hazard, the flood inundation zone is typically used for estimating the extent of the flooding, the depth of flooding, and the flood zone (Mokhtar et al., 2018; Macchione et al., 2019). Consequently, the flood hazard and the inundation studies have been estimated accurately to minimize damage and inform the authorities responsible for flood response of the elevation zone (Habte et al., 2017; Bhola, Leandro, et al., 2018; Mokhtar et al., 2018).

Scientists have developed technologies such as hydraulic modeling, hydrology modeling, remote sensing and geographic information system (GIS) methods to estimate flood hazard exposures along rivers, infrastructures, agricultural areas and understanding land-use development (Abdelkarim et al., 2019; Massazza et al., 2019; Muthusamy et al., 2019). Many recent publications, (Habte et al., 2017; Logah et al., 2017; Mokhtar et al., 2018; Dysarz et al., 2019; Oubennaceur et al., 2019; Vojtek et al., 2019; Zeleňáková et al., 2019) assessed flood hazard, flood risk, and flood inundation by using geospatial techniques and hydraulic modeling to identify different hydrologic components, prepare hydrologic designs, and develop strategies to overcome hazards from flooding. The Hydrologic Engineering Center

River Analysis System (HEC-RAS) model and GIS have been purposefully employed to delineate flood depth, flood extent and flood feaster in a specific area.

According to these problems and possible modeling capable of considering the flood hazard, current research is attracted to preparation flood hazard maps to identify, flood inundation areas, flood extent, and flood depth using HEC-RAS modeling and GIS methods. The scope of the finding is focused on flooded river related to the ability of methods applied to design return period based on floods hazard map and data series. In this study, HEC-RAS modeling and GIS are used for efficiency flood hazard mapping in the study area. There are also other elements potentially important for the accuracy and reliability of flood hazard maps, e.g., digital elevation models (DEM), type of hydraulic simulation software, data stream flow, etc. The result will help to assess the physical build of a physical land area and formulate development strategies according to the available flood hazard data focusing on relevant aims and scope.

Research Question

1) How to determine the magnitude of flooding from indifferent return periods?
2) How to apply HEC-RAS modeling to produce flood hazard maps?
3) How to prepare flood hazard maps for multi return period?

Research Aims

The main research aim is to apply the flood simulation model using GIS and HEC-RAS modeling to produce a flood hazard map**.** The HEC-RAS model and GIS method are the most common applied by scientists. 1-D HEC-RAS modeling is mentioned in conducting the model requesting production flood hazards of the lower Mekong River basin in Cambodia. The specific objectives of this research are below:

1) To determine the magnitude of flooding return periods by using differences in flood frequency analysis methods.
2) To evaluate the efficiency of the HEC-RAS model to identify the flood hazard map area.
3) To generate the flood hazard map for multi return periods (10, 20, 50, 100-year).

Research Significance

Floods are among the most disastrous phenomena devastating and recurring natural hazards around the world (El-Naqa & Jaber, 2018; Abdelkarim et al., 2019; Farooq et al., 2019). Floods constitute a real and continuous threat to the maintenance of infrastructure, and urban development and pose a threat of economic loss and the possible loss of life, worldwide, especially as regards lowland areas and areas along the river (Sohan, 2013; Rishiraj et al., 2015; Shrestha & Lohpaisankrit, 2017; Abdelkarim et al., 2019; Farooq et al., 2019). Prediction and calculation of flood hazards is essential to informed decisions on how to manage the flood event (Criado et al., 2018; Abdelkarim et al., 2019). Hence, flood models can play an important role in understanding flood hazards (inundation depth and extent) (Logah et al., 2017; Bhola, Nair, et al., 2018; Criado et al., 2018; Erena et al., 2018; Kim et al., 2018; Farooq et al., 2019). Flood hazard management is presently shifting from total protection against flooding through a structured approach to management of the consequences of flooding through a non-structured approach (Farooq et al., 2019) and flood hazard mapping is an effective non-structural measure for sustainable urban planning, protecting property, lives, and disaster risk reduction (Zin et al., 2018). Further, flood hazard mapping is an essential part of flood risk analysis and management, it results in the visualization of flood hazards in terms of flood depth and extent (Vojtek et al., 2019). It provides an understanding of the categories, frequency, and magnitude of the flood return period events which could cause great damage to life and property (Wan Deraman et al., 2017). Farooq et al. (2019) & Lazare et al. (2019) recommended that the HEC-RAS 1-D/2-D couple model be verified in studies, once river cross-sections are available. Moreover, the combination of HEC-RAS and GIS are capable of simulating flood hazard zoning (Echogdali et al., 2018).

This study develops a return period based on flood hazard maps to help appropriate mitigation and management strategies to reduce risk and vulnerability downstream. Besides, the results will enable policymakers to perform mainstream flood hazard analysis in the planning and development process for mitigating flood hazards and the application performance of models concerning the Mekong basin, Cambodia.

Research Scope

There are many methods applied in this study. GIS and HEC-RAS modeling are the main packages for generating output while ArcMap plays a vital role to determine, interpolate, and simulate database export from RAS Map results. The scope is subdivided into a data-related model.

1. Study Area and Data Related Scoping

1) The lower part of the Mekong River in Cambodia, starting from the Kampong Cham reach to Chruy Changvar station (Phnom Penh)
2) Water discharge in Kampong Cham and Chruy Changvar station
3) Water levels over 10 years provided by the MRC
4) Water bodies provided by Open Development Cambodia (2016)
5) MODIS flood observed (https://floodmap.modaps.eosdis.nasa.gov)
6) Digital Elevation Model (DEM) series resolution 30×30 m.
7) River cross-section data is computing to TIN by RAS Mapper.

2. Models and Methods Input

1) Apply flood frequency analysis in a multi return period using Log-Pearson type III, Log-Normal, Normal, and, Gumbel distribution.
2) Applies HEC-RAS hydraulic model Version 5.0.7, GIS Version 10.5 techniques and Microsoft Excel Version 2019 analysis.
3) Critical analysis flood hazard map to determining the flooding area.

3. Instrument for Usages

1) Hardware: (Computer CORE i5, 8th Generation)
2) Microsoft Office version 2019 Generation
3) Software ArcGIS version 10.5 License
4) Easyfit software analysis
5) HEC-RAS Modeling version 5.0.7 free License

Keywords

Flood Hazard is the comprehensive areas with a probability of a flooding event for a defined return period depends on several hydrological factors such as flood velocity and inundated depths (Shrestha & Lohpaisankrit, 2017)**.** Likewise, Miller and French (2012) and Ahmad et al. (2018) defined that flood hazard is the probability of occurrence of a potentially damaging flood event of a certain magnitude within a given time and area.

GIS (Geographic Information Systems) is a mathematical construct for representing geographic objects or surfaces as data. For example, the vector data model represents geography as collections of points, lines, and polygons; the raster data model represents geography as cell matrices that store numeric values; and the TIN data model represents geography assets of contiguous, non-overlapping triangles (Tomaszewski, 2015).

HEC-RAS Model is an integrated system of software, designed for interactive use in a multi-tasking, multi-user network environment (USACE, 2018) https://www.hec.usace.army. The HEC-RAS system contains four hydraulic analysis components for (1) steady flow water surface profile computations; (2) one and two-dimensional unsteady flow simulations; (3) moveable boundary sediment transport computations; and (4) water temperature and constituent transport modeling (US Army Corps of Engineers, 2016) (Horritt & Bates, 2002; Moya Quiroga et al., 2016).

Return Period is known as a recurrence interval which is an estimate of the interval of time between events like an earthquake, flood or river discharge flow of a certain intensity or size (Vivekanandan, 2015; Wan Deraman et al., 2017; Parhi, 2018). The probability that events such as floods, wind storms or tornadoes will occur is often expressed as a return period. The inverse of probability (generally expressed in %), it gives the estimated time interval between events of a similar size or intensity. A return period, also known as a recurrence interval (sometimes repeat interval) is an estimate of the likelihood of an event, such as an earthquake, flood, landslide, or a river discharge flow to occur.

Mekong River is the 12th longest river in the world. The river flows for almost 4800 km from its source in Tibet through China, Myanmar, Lao PDR,

Thailand, Cambodia, and Viet Nam via a large delta into the East Sea, draining a basin area of 795,000 km^2 (MRC, 2018).

Structure of the Research

The research work is composed of five chapters. The chapters are synchronized starting with the introduction, followed by the literature review, methodology, results and discussion, and finally the conclusion. Contents are described as follows,

Chapter 1 Introduction: The first chapter of the thesis provides an overview of the study presented, followed by the purpose, significance, objectives, and scope of finding.

Chapter 2 Literature Review: The second chapter includes discussions about flood modeling and past studies on it, Hydraulic modeling, the history of flood in the Mekong River, and the flood study in Cambodia.

Chapter 3 Methodology: The methods and procedures used in the study are elaborated in this section. The chapter provides a detailed discussion on the organization of the data used, the description of the study area, sources of the datasets used, steps involved in the development of the hydraulic simulations of the models and calibration approach of the models used in this study. Water discharge data is the main parameter in hydraulic modeling conduct of the flood hazards.

Chapter 4 Results and Discussion: The second last chapter is a description of the results of simulations run by the hydraulic model. The chapter also covers the vulnerability assessments of the study area and the hazard maps.

Chapter 5 Conclusion and Recommendations: The last chapter summarizes the findings of the study and talks about the future contribution of this type of study.

CHAPTER II

LITERATURE REVIEW

The literature review for this research is ordered into four sections which are the definition of flood hazard, flood histories in Cambodia, flood management in Cambodia, and flood modeling (GIS, Remote sensing, HEC-RAS modeling, and generating GIS with HEC-RAS modeling components).

Definition of Flood

Floods are a natural disaster with the highest frequency and the widest geographical distribution worldwide (CRED, 2017). According to the Organization for Economic Cooperation and Development, presented that flooding is one of the most common, widespread and destructive natural perils, affecting, and damage to people and animals (OECD, 2016). Likewise, Macchione et al. (2019) and Ahmad et al. (2018) flooding occurs most frequently from heavy rainfall when natural watercourses river the capacity to transport excess water. Flooding can also result from other phenomena, particularly in coastal areas (storm surge associated with a tropical cyclone), a tsunami or a high wave, dam failure, triggered by an earthquake, etc. Floods are the common name for extreme overflow volumes after an intensive storm rainfall event over a drainage river basin (Sein, 2016; Shao et al., 2019). The previous definition indicates two components for flood occurrences, which are the rainfall intensity and the drainage area geographies. It does not suggest that intensive rainfall events will lead to floods. For flood occurrence, certain geographies of the drainage river basin are important and without them even though the rainfall might be very intensive, but there might not be any flood event (Şen, 2018). Among the most significant drainage, basin features are drainage basin areal extent, slope, and especially cross-sectional area variations along the main channel course (Brimicombe, 2010; Şen, 2018). Floods also occur when water levels of lakes, ponds, reservoirs, aquifers, and estuaries exceed some critical value and inundate the adjacent land, or when the sea surges on coastal lands are much above the mean sea level (Akbari et al.,

2014; Trung et al., 2018; Walalite et al., 2018). Nevertheless, floods are the most destructive of natural disasters and cause the greatest number of deaths (Maskong, 2019). Spatial and temporal flood scales are generally linked with the corresponding scales of the flood-generating thunderstorm events breach in flood-protection structures and rapid melting of ice in the mountains (Yousuf Gazi et al., 2019).

Flood is a natural hazard that caused by a combination of hydrological and meteorological factors (Abdelkarim et al., 2019; Yousuf Gazi et al., 2019). Hence, floods are not just nature-related disasters, rather they may be the result of meteorological and hydrological factors aggravated by human actions (Abebe et al., 2019a). To define 'flood' is difficult as floods are complex phenomena and partly because they are viewed differently by different people. Flood may be defined as the inundation of land surface that is usually dry following the exceedance of river flow channel conveyance capacity, damage to the river geometry, or obstruction of water flow (Ahmad et al., 2018; Ali, 2018). Shortly by (Chow et al., 1988), the flood is a relatively high flow that overtakes the natural channel provided for the runoff. Likewise, Proverbs and Soetanto (2004) defined flood as any high streamflow which overtops natural or artificial banks of a stream. According to IAEA (2003), 'flood' is a series of parameters that maximize the challenge to plant safety as a consequence of a flood: the parameters may be associated, for example, with the maximum water level, the maximum dynamic effect on the protection or the maximum rate of increase in water level. A flood may occur in various ways. The most prevalent are an overflow of rivers/streams, excessive rain, the breach in flood-protection structures and rapid melting of ice in the mountains (Yousuf Gazi et al., 2019). In consequence, a flood is one of the most commonly occurring environmental hazards that may not necessarily be caused by natural events but can also be due to, or, aggravated by human activities such as deforestation, pollution or uncontrolled urbanization that changes or disrupts the natural landscape (Chen et al., 2019). Flood has been categorized into different types based on the location of occurrence and what causes them. The categories of the flood are described below.

A **River flood** occurs when the river basin is filled with too much water; that is, more than the capacity of the river channel. River floods may be an expected event if it occurs seasonally, normally during the rainy season (Akbari et al., 2014; Trung et

al., 2018; Walalite et al., 2018). But depending on other authors (i.e.Akbari et al., 2014; Trung et al., 2018; Walalite et al., 2018), a river flood may be defined as a general and temporary condition of partial or complete inundation of a normally dry land area from rapid runoff of surface water from rainfall (Wang, Y. et al., 2019). A river flood is characterized by a low amplitude wave that progressively attenuates downstream due to energy loss (Bamberg et al., 2017). Floods are high magnitude events; thus, the longitudinal flow component is dominant. Despite this predominant longitudinal flow, natural river flow is composed of complex flow processes in three dimensions that are amplified at varying sections of the river network such as meanders and bends (Bezak et al., 2018). River floods are the kind of flood that occurs when the water in the river rises and overflows its bank channels.

A c**oastal flood** occurs in coastal areas due to the drive of the ocean waters inland (Buchori et al., 2018; Yin et al., 2019). Natural phenomena such as tropical storms, hurricanes or intense offshore low pressure can cause massive amounts of ocean water to be driven towards the land resulting in coastal flooding (Coquet et al., 2019; Hadipour et al., 2019). Also, tidal sea waves that are due to earthquakes or volcanic activities in the sea can cause coastal flood (Doyle, 2003). Coastal flood hazard mapping is a tool used to determine the flood zone limits inland and in other areas exposed to coastal floods due to different hazards such as storm, surge waves, sea-level rise caused by climate change, inland storm surge, heavy rainfall, among others (Batista, 2018). Coastal flooding is considered as the main risk regarding the possible losses it can inflict in human, environmental and financial term.

Urban flood is the type of flood that occurs because of heavy rainfall and changes in runoff behavior. The changes in runoff behaviors are mostly due to the development of land use and the building of paved roads which have less absorbing ability compared to an undeveloped area or natural fields (Park & Lee, 2019; Zhou et al., 2019). Urban floods have great adverse socioeconomic impacts and can cause disruptions to city facilities (e.g., transport, sewerage, communication, and electricity supply) and damage to urban structures. Urban drainage is an essential part of city infrastructure that is designed to transport excess water away from urban areas and to limit flooding (Systems et al., 2007; Rojas et al., 2017; Zhao et al., 2019). Urban flooding is increasingly problematic in developing countries, thus sympathetic flood

dynamics are necessary to establish guidelines for urban development and flood management.

Flash floods normally occurs locally and suddenly without or with little warning. Flash floods could happen due to immoderate rainfall or a sudden release of water from a dam (Taha et al., 2017; Abdulrazzak et al., 2019). Currently, the studies of urban flooding have mainly focused on the floods occurring in metropolitan regions. In these regions, it was demonstrated that the dominant cause of urban flood disasters is water-logging induced by impeded drainage systems and extreme rainfall (Wang, Z. et al., 2019). A flash flood is a specific type of flood that appears and transfers quickly across the land. Many parameters could cause flash floods including heavy rainfall concentrated over an area, thunderstorms, hurricanes, and tropical storms. Flash floods are short-term inundations of small areas such as a town or parts of a city, often near streams and creeks (Elkhrachy, 2015; Cao et al., 2016). Heavy rain in a few hours can produce flash flooding even in places, where little rain has fallen over a prolonged period. If heavy rainfall occurs frequently over a wide area, then river or mainstream flooding becomes more likely, where the main rivers of a region could swell and inundate large areas (Mahmoud & Gan, 2018).

1. Hazard Description

The concept of disaster management is important to this discussion. In the study of hazards and their management, there are a variety of terms and they need to be clearly defined and understood. However, there are different terms and used in the literature for ‘hazard and flood hazards. Below is the defining term of ‘hazard’.

Hazard is a potentially damaging natural physical event, phenomenon and/or human activity, which may cause loss of life, property damage, economic disruption and/or environmental degradation (Shao et al., 2019). H**azard** is related to magnitude (susceptibility to risk from the conditioning or passive factors such as the topography or geological substrate) and the severity and frequency with which the agent that causes the risk is expressed (probability of triggering factors). Therefore, to determine the hazardousness, we analyze the magnitude and probability of the occurrence of each event (Criado et al., 2018). **Hazard** is a dangerous phenomenon, substance, human activity or condition that may cause: loss of life, livelihoods and

services, injury or other health impacts; property or environmental damage; and social and economic disruption (Smith & Petley, 1991). Another method for recognizing hazards are through the review of general design safety criteria, precepts, and principles. By considering the reasoning and logic behind specific safety criteria, precepts, and principles, some types of hazards can be more easily recognized. For example, there is a good safety reason for the following safety criteria. This safety criterion is a clue that aids in recognizing hazards in systems involving redundancy. **Hazard** is defined as "a process, phenomenon or human activity that may cause loss of life, injury or other health impacts, property damage, social and economic disruption or environmental degradation" (Liu et al., 2019). Most of the previous studies have failed to consider both the physical hazard together with the human dimension of the hazard at specific locations as they often focus on a single dimension, either the flood hazard and risk or societal mitigation (Zin et al., 2018). Correctly describing the hazard is an essential aspect of hazard theory and analysis (Motevalli & Vafakhah, 2016). The hazard description must contain all three components such as hazardous elements, initiating mechanisms, and target/threat.

Natural hazards are complex and vary greatly in their frequency, speed of onset, duration and area affected. Natural hazards include both meteorological events, such as blizzards, drought, fog, extreme temperatures, hail, tornados and other severe storms, and earth processes such as avalanches, earthquakes, floods, landslides, tsunamis, and volcanic eruptions, although the dichotomy is not clear-cut since floods and landslides have meteorological causes and volcanic eruptions can have serious climatic consequences (Carrara, 1995). Yet, the Scientifics have been pointing out that flooding is one of the most occurring natural hazards every year risking the lives and properties of the affected communities worldwide.

2. Flood Hazard Description

Among all environmental hazards, flooding is the most common in societies all over the world (Speckhann et al., 2018; Yin et al., 2019). The main reasons for this are the widespread geographical distribution of river valleys in humid regions or wade courses in arid and semiarid regions, and low-lying coasts, together with their longstanding attractions for human settlement, and the availability of

surface and groundwater resources (Zeleňáková et al., 2019). Although in many cases, the threat is limited to comparatively well-defined floodplains and low-lying areas such as estuaries, no country is immune from flood hazards (Smith & Petley, 1991). **Flood hazard** is the intensity of the flood corresponding to an exceedance probability (Miller & French, 2012; Yousuf Gazi et al., 2019). Flood intensity is determined by the flow depth and velocity. Flood probability is inversely related to flood magnitude i.e.; large flood events occur less frequently. Flood hazard is defined as a discrete combined function of the event intensity (severity of the event) and return period (Miller & French, 2012). Normatively, flood events peaks and corresponding return periods that are displayed are obtained from a statistical analysis of extremes (Micah, 2016; Farooq et al., 2018). In general, flood hazard is the result that the combination of physical exposure represented by the type of flood and their statistical pattern at a particularsite, and human vulnerability to geophysical processes. Human vulnerability is associated with key socio-economic factors such as the number of people at risk on the floodplain and the ability of the population to anticipate and cope with the hazard (Micah, 2016; Zin et al., 2018; Shao et al., 2019). Understanding the **flood hazard map** is an important instrument in the management of floods, providing people with advance notice of flooding in an effort to save lives and help people prepare before it happens (Rahmati et al., 2016; Orton et al., 2018; Abdelkarim et al., 2019). Flood hazard maps are provided to reduce the impact of flooding on people's homes and businesses. Through such means as moving belongings and equipment to safer places and putting in place temporary measures to prevent floodwater from entering buildings. In these ways, physical loss, damage to property and infrastructure and loss of life can be minimized or prevented (Sami et al., 2016; Shrestha & Lohpaisankrit, 2017; Zin et al., 2018). These measures contribute to the saving of money, the lessening of stress, and the saving of time during the recovery period (Motevalli & Vafakhah, 2016; Xiao et al., 2017; Shao et al., 2019).

Flood Hazard Mapping is an important component for appropriate land use planning in flood-prone areas (Vojtek & Vojtekova, 2016; Zin et al., 2018). It creates easily-read, rapidly-accessible charts and maps which facilitate the identification of areas at risk of flooding and also helps priorities mitigation and response efforts (OECD, 2016; Dagli & Ferrarini, 2019). Flood hazard maps are

designed to increase awareness of the likelihood of flooding among the public, local authorities and other organizations. They also encourage people living and working in flood-prone areas to find out more about the local flood risk and to take appropriate action (Wing et al., 2019). Flood hazard mapping will allow quantification of what is at risk of being flooded such as the number of houses or businesses. The creation of flood hazard maps should promote greater awareness of the risk of flooding. This can be beneficial in encouraging hazard zone residents to prepare for the occurrence of flooding (Kumar et al., 2018). To realize the full benefits of flood hazard mapping, it is important to provide people in the hazard zone with information about emergency procedures and ways of reducing flood risk (Agency, 2013). Flood hazard assessment is the crucial first step towards effective flood-risk management and constitutes the basis for taking preventive conservation measures for risk mitigation (Liu et al., 2019), thus contributing to the sustainable development of likelihood along Mekong river. Thus, flood map can be defined as a map presents the area prone to flooding at one or more floods with given return periods (Xinjiang & Minghui, 2018; Vojtek et al., 2019). **Flood hazard maps** show areas which could be flooded according to three probabilities (low, medium, high) complemented with: type of flood, the flood extent; water depths or water level where appropriate; where appropriate, flow velocity or the relevant water flow direction (Şen, 2018; Talisay et al., 2019). Hence, Flood hazard maps present information on the characteristic dangerous aspects of floods that are important for i.e. evacuation and rescue operations (Erena et al., 2018; Farooq et al., 2019).

Flood hazard map shows the spatial distribution of the flood hazard, i.e. information on flood intensity and the probability of occurrence for single or several flood scenarios (Demir & Kisi, 2016; Ahmad et al., 2018; Yousuf Gazi et al., 2019). Flood hazard maps are based on digital elevation models (DEM) and geomorphic features (e.g. slope, distance to the nearest divide and topographical indices) that have been developed as a rapid low-cost difference in the absence of detailed hydrological and hydraulic data and for each region.

Table 1 Summaries of using flood hazard map

Content	Flood extent according to probability and according to past events. - Flood depth. - Flow velocity. - Flood propagation. - Degree of danger.
Purpose and Using	- Land-use planning and Watershed management. - Water management planning. - Hazard assessment on the local level. - Emergency planning and management. - Planning of technical measures. - Overall awareness building.
Target User	- National, regional or local land-use planning. - Flood managers. - Emergency services. - Forest services (watershed management). - Public. - And another researcher

Flood Histories in Cambodia

1. Flood Damage

Natural disasters are part of to the economic, social, and environmental features of Cambodia and many other countries in Asia as well (Dagli & Ferrarini, 2019; Liu et al., 2019; Vichet et al., 2019; Waghwala & Agnihotri, 2019). Cambodia experiences almost all types of hydrological hazards such as floods, drought, heavy storms, typhoons and flooding is the most common natural disaster in Cambodia and other Asian countries (Vathana, 2013; Rishiraj et al., 2015; CFE-DM, 2017; CRED, 2017; Sarann et al., 2018; Dagli & Ferrarini, 2019; Vichet et al., 2019). Moreover,

flooding is the main natural disaster that affects many parts of the world including developed countries. The Mekong River that enters the country from Laos and the Great Tonle Sap Lake in the middle has created unique features of flooding (MRC, 2018; Trung et al., 2018). Mochizuki et al. (2015) applied CATSIM modeling to analyze economic losses in natural disasters, found that in Cambodia gaps are estimated to rise as events become rarer but gain intensity, from 123 million dollars for a 50-year return period event to 290 million US dollars for a 100-year return period event and to 533 million US dollars for a 500-year return period event. For instance, the official report compiled by the National Committee for Disaster Management (NCDM) dated 16 November 2000, put the death toll resulting from the 2000 flood at 347 of whom (80%) were children, of the 750,618 families (3,448,629 individuals) affected by the 2000 flood, some 85,000 families (387,000 individuals) had to be temporarily evacuated. According CFE-DM (2017), government officials reported that 247 people were killed and 1.6 million people affected and more than 46,000 families were evacuated and 214,000 displaced and the UN's Food and Agriculture Organization (FAO) estimated that more than 716,000 acres of rice paddy (28% of the total crop) were destroyed in flood of 2011. Cambodia's NCDM estimates that the total economic damage from natural disasters in 2011 amounted to around 500 million US dollars, largely due to flooding (NCDM, 2018). More than eight million people in Laos, Cambodia, and Vietnam were affected and over two million in Thailand. It was estimated that economic damage in Cambodia were $157 million US dollars, with 3.5 million people affected and 347 killed.

Based on the reports compiled by the Mekong River Commission (MRC), the deaths in Cambodia constituted 43% of total deaths (800) in all the countries affected, while direct damage represented 40% of the total damage (estimated at $ 400 million US dollars) in all affected countries (CFE-DM, 2017; MRC, 2018). The flooding affected 1.3 million people with over half requiring emergency aid and more than 600,000 hectares of crops and 50,000 homes were damaged or destroyed. Damage related to floods in September and October 2013 caused 356 million US dollars of damages, affecting some 370,000 households, destroyed over 125,000 hectares of rice crops, damaged 440 kilometers of national roads, and caused 168 people to lose their lives (MRC, 2018). Floods affected Cambodia in 1961, 1966,

1978, 1991, 1999, 2000, 2001, 2011 and 2013 (CFE-DM, 2017; Mishra et al., 2018) and continuing in 2016 (MRC, 2018). Hence, more than 2 million hectares of the lower Mekong River inundation (Cambodian Plain), which extends from southern Cambodia to the border with Vietnam, is cultivated with rice; and more than 60% of the population in the flood plain are farmers involved in rice cultivation (Okazumi et al., 2013, p. a; Mishra et al., 2018). In Cambodia, flood is one of the most significant natural disasters as it is the main source of problems for the residents. However, historical extreme flood events, especially the 2011 and 2013 floods, caused significant damage to property due to insufficient flood preparedness and mitigation.

2. Factors Effecting the Floodplain

Flooding occurs most commonly from heavy rainfall when natural river channels no longer have the capacity to convey additional water (Speckhann et al., 2018; Chung et al., 2019). Floods can also be the consequence of other phenomena, coastal areas, dam failure, and changes in land-use (Samanta et al., 2018; Abebe et al., 2019b). For instance, Kawasaki et al. (2010) studied the impact of precipitation and land-use change on streamflow in the Srepok River Basin (sub-basin of the Mekong river in Cambodia) used the precipitation scenario with land use and land cover. The model simulation suggested that under Scenario 2 conditions, the predicted annual discharge decreases by 18% in 2025 and by 52% in 2050 compared to the 2000 level at Ban Don (a Vietnamese station); at the basin outlet (a Cambodian station), predicted annual discharge decreases by 10% in 2025 and by 30% in 2050. However, under Scenario 1 conditions, the annual discharge increases with the assumed precipitation increase by 2% and 3% in Ban Don and by 3% and 6% in the basin outlet in 2025 and 2050, respectively. Ty et al. (2012) published a scenario-based impact assessment of LU/LC and climate change on water resources and demand. Their assessment predicted that LU/LC change would increase from 15.3% in 1997 to 28.1% in 2050, while the urban area is forecasted to increase to 2.2% in 2050. In contrast, the thin forest area is likely to decrease from 49.0% to 34.2% between 1997 and 2050. A large percentage of future agriculture will be on land converted from the thin forest (42%) and grassland (16%). LU/LC change is found to have the largest impact on the increased inundated zone, high peak water flow and thus increase flood

frequency during the wet season. For instance, (Chim et al., 2019) stated that land use in this watershed along the river has changed considerably over the last few decades, which is thought to have influenced the river.

Furthermore, Markert et al. (2018) used spatial modeling of land cover/land-use change to study its effect on hydrology within the lower Mekong basin. They found that forest increases were shown to affect a decrease in discharge whereas increases in agricultural areas increased the discharge that runs at a 5-year increment from 2015 to 2050 with multiple scenarios. land use land cover changes of 5% to 10% will affect hydrology and increase water flow during the rainy season and the effect the inundation area. The model can be expected to see land cover changes in the lower portions of the basin around Cambodia and these changes can have implications for flooding within the flood inundation parts of the region. On the other hand, studies based on large scale modeling and scenario analysis suggest that future hydropower development would dramatically alter the Mekong flow and Tonle Sap Lake (TSL). Likewise, the Mekong River Commission (MRC), suggests a reduction in flood depth during the wet season, which could potentially reduce the total flooded areas by 400-900 km^2, forest-covered flood areas by 22-100 km^2, grasslands by 50-150 km^2, rice fields by 300-630 km^2. According to Pokhrel et al. (2018), during the high flood season (August–October), 51.3% more areas are flooded in wet years compared to the average year. Similarly, during the dry season (April–June), 17.1% more areas are flooded in wet years. Furthermore, for the 10% flow alteration scenario, marked differences are not found in downstream flood occurrence between dry, normal, and wet years. However, varying patterns of change in flood occurrence become readily discernable between dry and wet years for the 30%, and even more so for the 50% scenario. In the wet year, significant areas in the western vicinity of the Tonle Sab do not experience an increase in flood occurrence by up to 6 months for a 50% scenario. Note that the scenarios of reformed timing are analyzed only for 10%, 30%, and 50% peak streamflow attenuation scenarios (CFE-DM, 2017). Consequently, the histories of flooding that occurred in Cambodia has been concerned at lower topographic locations. Besides, without having efficient modern technology to predict the flood situation in Cambodia, the flood disaster would be more severe.

Flood Management in Cambodia

1. National Strategies

The flood management measures are complex. But the flood hazard map is a significant tool of mitigation (non-structure) because they require a comprehensive evaluation framework (Islam et al., 2015; Abdelkarim et al., 2019). The appropriate flood mitigation alternatives in reducing the flood risk along the River were suggested, modeled and compared. The first step was the development of flood hazard maps, which show inundated areas and flood depths. The second step was to select the most appropriate alternative based on a multi-criteria approach. The currently ongoing project of the flood management and mitigation program (FMMP) of MRC started in January 2005 with the following five key components: (1) establishment of a regional flood center; (2) structural measures and flood proofing; (3) mediation of trans boundary flood issues; (4) flood emergency management strengthening; and (5) land management. Although components 2 and 5 address issues related to flood vulnerability, these studies did not identify specific localities where flood vulnerability is high (Okazumi et al., 2013). 1991 to 2014, Cambodia received USD 785.34 million in foreign aid for disaster management with 55 % used for emergency responses, 35 % for reconstruction and rehabilitation, and 10 % for disaster preparedness projects. The average project size, in terms of investment, is 1.49 million dollars for emergency response, 45.61 million dollars for reconstruction and rehabilitation, and 3.81 million dollars for disaster preparedness and prevention. As will be shown below, response-oriented disaster management will likely pose an increasing challenge as continued urbanization and asset accumulation in hazard-prone areas may well increase the country's economic risk following a natural disaster (CFE-DM, 2017).

According to the National Flood Forecasting Center of the Ministry of Water Resources and Meteorology, indicated that during the June-November flood season, the Regional Flood Management and Mitigation Centre issues daily flood forecasts and warnings. Data from 138 hydro-meteorological stations are used to predict water levels at 23 forecast points on the Mekong River system. The MRC shares these daily bulletins by fax, e-mail, and on the MRC home page and dedicated

Flood Forecasting Website to National Mekong Committees, Non-Governmental Organizations, the media, and, most importantly, the public (MoWRM, 2019) see in **Figures 2 and 3**.

The daily warnings provide government agencies and communities in Cambodia and Lao PDR with advanced notice of rising water levels. Other preparedness tools include flood markers and community billboards that provide clear information on the current and predicted water levels. Through online postings, radio communication, dissemination of guidebooks as well as workshops, the MRC strives to reach a wide audience throughout the entire Mekong Basin. In the Mekong's tributaries, flash flooding from intense rainfall is the largest risk for people and infrastructure. The Mekong River Committee (MRC) is an important organization that responds to the hazards posed by the river. The Mekong River Committee sets the scenario relating to climate and other factors along the Mekong river as below see in **Figures 2 and 3**.

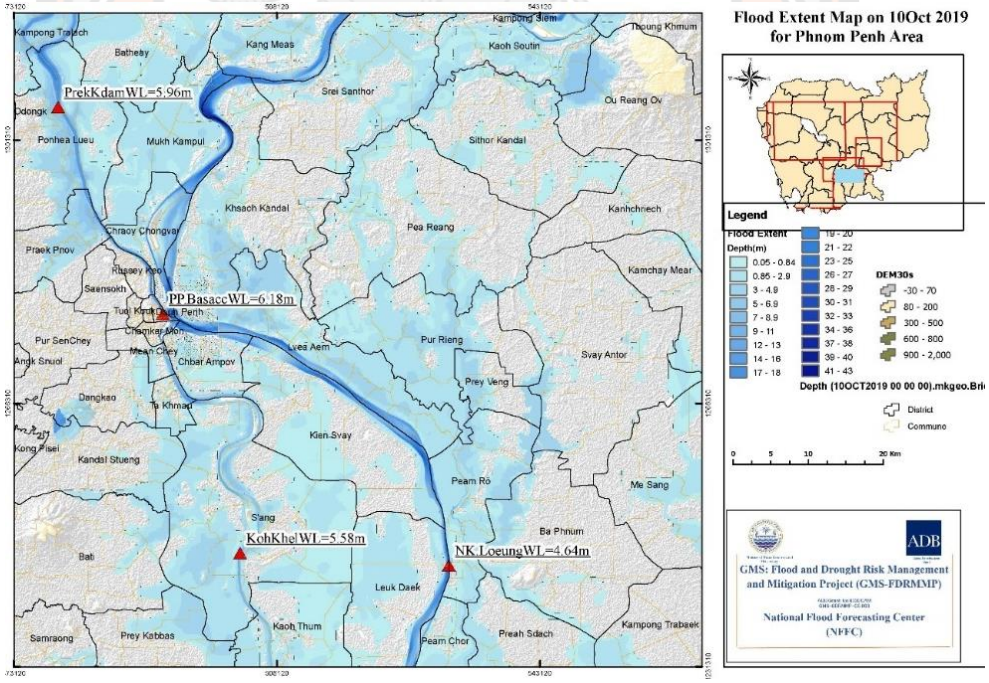

Figure 2 Flood extent map on 10, October 2019

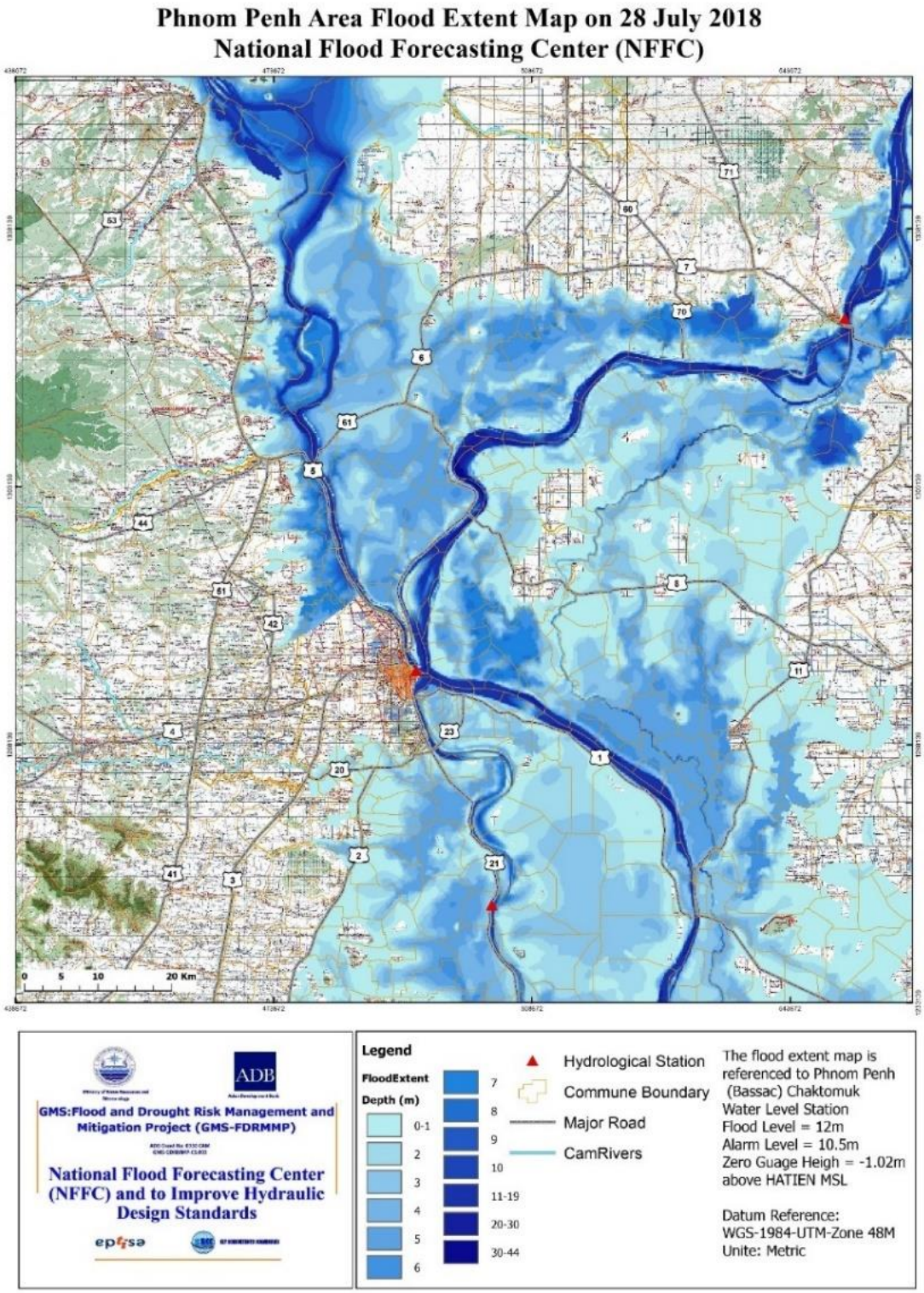

Figure 3 Flood Extent Map on 28 July 2018

2. Mekong River Commission

The Mekong River is one of the world's great river systems and the tenth-largest river in the world. The basin of the Mekong River drains a total land area of 795,000 km^2 from the eastern watershed of the Tibetan Plateau to the Mekong Delta. The Mekong River flows approximately 4,909 km through three provinces of China, continuing into Myanmar, which is called Upper Mekong River Basin (UMB) and continues its path to Lao PDR, Thailand, Cambodia, and Viet Nam before emptying into the South China Sea, which is called Lower Mekong River Basin (LMB). The Upper Mekong River Basin is mainly mountainous while the LMB is lowlands and floodplains while Mekong River's runoff is 475,000 million m3 per year towards the South China Sea (The Flow of the Mekong, MRC Secretariat, Lao PDR, 2009) see in **Figure 4**.

Figure 4 Mekong River through Southeast Asia

Source: https://cruisesmekongriver.net/mekong-river-map.html

Table 2 The contributions of the Mekong River flow systems.

River Reach	Left Bank (%)	Right Bank (%)	Total (%)
China	16		16
China – Chiang Saen	1	3	4
Chiang Saen – Luang Prabang	6	2	8
Luang Prabang – Vientiane	1	2	3
Vientiane – Nakhon Phanom	18	4	22
Nakhon Phanom – Mukdahan	3	1	4
Mukdahan – Pakse	4	6	10
Pakse – Kratie	22	2	24
Tonle Sap	9		9
Total	55	20	100

Source: http://www.mrcmekong.org/mekong-basin/hydrology

The annual flood season normally starts in June and ends in early November. The annual floods carry nutrient-rich silt to farmland around the river and provide the moisture needed to grow vast fields of rice. Although the Mekong annual flood is considered beneficial, there can sometimes be too much water in the wrong place, causing loss of human lives and damage to property (MRC, 2018).

According to the Annual Mekong Flood Report 2011, the losses in Cambodia and Viet Nam are mainly caused by high water levels in the mainstream Mekong, causing long-term flooding of the Cambodian plains and the Delta. The losses here account for about 70% of the economical flood damage losses in the region (CFE-DM, 2017). The Mekong River Committee (MRC) is an important organization that responds to the hazards posed by the river. The Mekong River Committee sets the scenario relating to climate and other factors along the Mekong river as below.

Table 3 Flood risk damage by scenario for CS Corrido in Cambodia

Corridor Cambodia	Socio-economic Development	Water infrastructure	Annual average Damage ($m)			AAD Defenses AG 10yr Prop 100 year	($m) Event Damage in Extreme Flood
	Year	Year	Agriculture	Other & Urban	Total	With Defenses	1:100yr+
Scenario M1	2010	2007	4.6	4.1	8.7	2.6	21.3
Scenario M1	2040	2007	6.4	34.4	40.9	3.5	213.6
Scenario M2	2010	2020	2.8	2.6	5.4	1.6	10.2
Scenario M2	2040	2020	3.9	21.6	25.5	2.1	109.8
Scenario M3	2010	2020	2.8	2.6	5.4	1.6	10.5
Scenario M3	2040	2040	3.9	21.7	25.6	2.2	113.0
Sce-M3 CC	2010	2040	6.5	5.3	11.8	4.1	31.7
Sce-M3 CC	2040	2040	9.1	44.0	53.1	5.5	325.0
Scenario M2	2010	2040	14.4	14.1	28.5	7.0	117.1
Scenario M2	2040	2040	20.0	118.2	138.2	9.3	557.2
Scenario F1	2010	2040	8.9	7.2	16.1	4.5	75.7
Scenario F1	2040	2040	12.4	60.1	72.4	6.0	325.0
Scenario F2	2010	2040	3.8	0.6	4.5	Already	75.7
Scenario F2	2040	2040	5.3	0.7	6.0	Already	329.7
Scenario F3	2010	2040	16.8	16.8	33.6	7.0	117.1
Scenario F3	2040	2040	23.4	$ 141.16	$ 164.52	9.3	557.2

Source: Mekong River Committee (MRC, 2018)

3. Previous Studies Related to the Mekong River

The rise of disastrous flood impact at an alarming rate stipulates the need to adopt approaches for flood disaster prevention and management. The publication of flood hazard mapping is the basis for providing fundamental information on flood mitigation strategies (Wierzbicki et al., 2018). Flood hazard maps are usually generated by modeling the inundation process combined with a hydrological analysis of past flood events (Degiorgis et al., 2012). Inundation models require a large amount of data for the simulation process, including potential hazard reaches, the geometry and characteristics of the channel, and observed hydrograph data for a particular return period (Try et al., 2019). This need has given birth to many research

topics worldwide including extensive use of flood modeling. Flood modeling alludes to the processes of transformation of rainfall into a flood hydrograph and the translation of that hydrograph throughout a watershed (Abdulrazzak et al., 2019; Talisay et al., 2019). Moreover, (Sarann et al., 2018) is applied HEC-RAS software to simulate flood inundation area along downstream Mekong River, Cambodia, was present the results that flooding varied from year to year; however, the greatest flood was during 2000 and again in 2011. In particular, (Mohammed, Ibrahim Nourein et al., 2018) used the SWAT model to examine streamflow variability of the Lower Mekong River Basin (LMRB). This stream flow variability is associated with changes in the Upper Mekong River Basin (UMRB). This inflow has shown results which suggest that the Lower Mekong River streamflow is highly variable and has a low predictability (Colwell index of about 32%) and releasing more flows from upstream Mekong would also affect flood duration and the frequency of flood occurrences downstream. However, Li et al. (2017) used metrics and indicators of hydrologic alteration (IHA) to observe changes in flow regimes in the Mekong River basin was indicate that the operation of dams reduces the streamflow in wet seasons and increases the streamflow in dry seasons. The construction and operation of dams has a significant impact on low pulse duration. It is observed that climate change dictated the changes in the annual streamflow during the transition period 1992 to 2009 (82.28%), whereas human activities contributed more in the post-impact period 2010 to 2014 (61.88%). Mostly, the flood modeling approach using SWAT (Soil Water Assessment Tool) and HEC-RAS simulations along the Mekong River Basin of Lower Cambodia was conducted to predict the flood hazard areas. Flood modeling further assists the flood risk assessment that magnifies the vulnerability of the region and reinforces the notion that land use planning decisions in the floodplains should make informed choices by incorporating scientifically derived information in their decision-making process. This study is conducted in two ways to identify effective of flood hazard mapping

Flood hazard assessment is the crucial first step towards effective flood-risk management and constitutes the basis for taking preventive conservation measures for risk mitigation, thus contributing to the sustainable development of livelihood (Vathana, 2013; Liu et al., 2019). The SWAT (Soil & Water Assessment

Tool), IQQM (Integrated Quantity-Quality Model) and ISIS models were used as a basis for simulation runs to analyses and prediction situations flood along the river that developed by Mekong River Committee (MRC, 2018). PCR-GLOBWB hydrological model, are used to generate monthly and sub-monthly terrestrial water storage (TWS) estimates and quantify flood events over the Tonle Sap basin between 2002 and 2014 (Tangdamrongsub et al., 2016). However, HEC-RAS modeling was used to simulate with the aid of flood histories Sarann et al. (2018) and Hazarika et al. (2007). Overall, the flood hazard map is necessary to monitor the lower Mekong River in Cambodia. The hydraulic model can be applied along with other models to monitor the lower Mekong River system.

Flood Modeling

Flood modeling is a simulation of an actual event. It is able to simulate a real flood event using actual hydrological data from past events including the basin's hydrological characteristics and boundary conditions (Ahmed et al., 2014; USACE, 2018; Xinjiang & Minghui, 2018; Yu et al., 2019). Those models can be used to show the results based on different boundary conditions or data input (Şen, 2018; Xinjiang & Minghui, 2018; Maskong, 2019). The performance of hydraulic models can be conducted to determine and investigate inundation areas.

The development of flood mapping, with recent advances in technology, computation time has been extremely reduced. It is becoming necessary to simulate flood inundations in the flood plains caused by different magnitudes of flood events. Different types of flood models exist and approaches have been made by various researchers using various hydraulic models (Xinjiang & Minghui, 2018). One of the most important developed tools for hydraulic modeling is a geographical information system that allows 1-D, 2-D, and 3-D representation of computed hydraulic parameters. A variety of software has been used widely for dynamic 1-D flow simulation in rivers such as MIKE 11, HEC-RAS, SOBEK 1-D, etc. (Ahmed et al., 2014; Ali, 2018; Şen, 2018). Even though, the 1-D models are modest to use and provide information on streamflow characteristics. However, it is failed to provide information, particularly on the flow field. The 2-D model whereas it requires

substantial computer time to provide the information. As there are limits in using 1-D or 2-D numerical models, attempts have been made to couple 1-D river flow models and 2-D floodplain flow models. The use of the two numerical models, together, offer a great advantage for the real-time simulation of flood events. The combined models are HEC-RAS modeling 1-D and 2-D as developed by the US Army Corps of Engineers (USACE, 2018). Consequently, Hydraulic models are commonly applied to observe the performance of flood events, especially along the river. This study is applied only to the 1-D part of the model.

1. Geographic Information System

The GIS is a computer system for capturing, storing, checking, and displaying data related to positions on Earth's surface. By relating seemingly unrelated data, GIS can help individuals and organizations better understand spatial patterns and relationships (Carrara & Guzzedi, 1993; Brimicombe, 2010). GIS has been providing two files of formats (raster and vector). Raster formats are grids of cells or pixels, such as elevation or satellite imagery. Vector formats are polygons that use points (called nodes) and lines, such as school districts or streets (Brimicombe, 2010; Weng, 2010). GIS is powerful tool accurate and timely spatial information due to integrating many maintenances of GIS show in **Figures 5 & 6.**

Figure 5 Elements of Geography Information System

Source: https://www.cleanpng.com/free/gis,2.htm

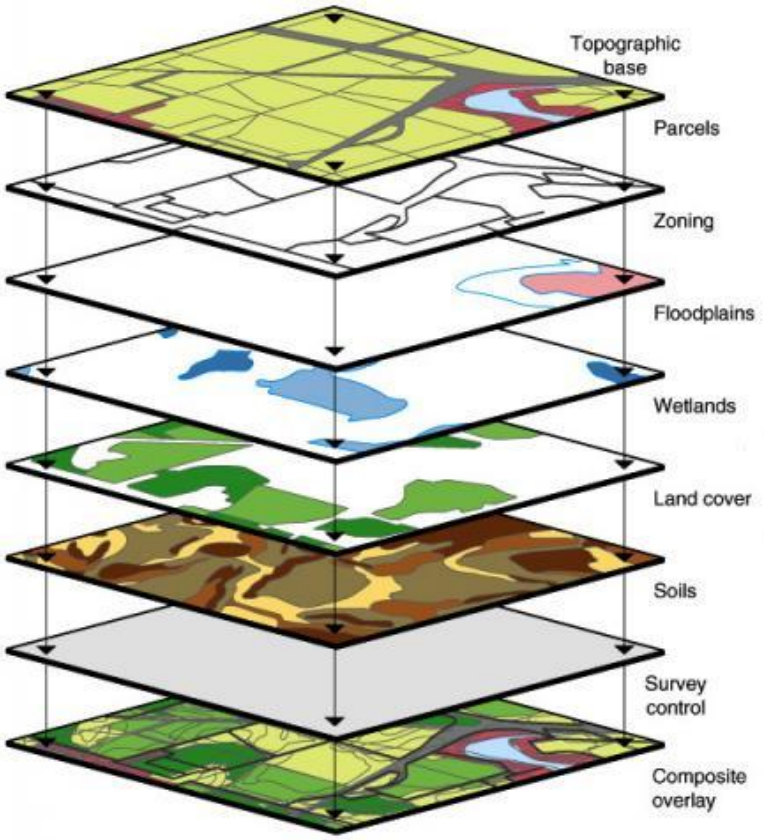

Figure 6 GIS Data Layers Images (https://www.pdx.edu/geography/GIS)

2. Remote Sensing (RS)

Remote sensing refers to the activities of recording/observing/perceiving (sensing) objects or events in remote places (Weng, 2010). Remote sensing is defined as the science and art of obtaining information about an object, area, or phenomenon through the analyses of data acquired by the sensor that is not in direct contact with the target of the investigation (Schultz and Engman, 2000; Ritchie and Rango, 1996). The information needs a physical carrier to travel from the objects/events to the sensors through an intervening medium. Electromagnetic radiation is normally used as an information carrier in remote sensing (Lunetta & Lyon, 2000). The output of a remote sensing system is usually an image representing the scene being observed. A further step of image analysis and interpretation is required to extract useful information from the image (Puno et al., 2019). The human visual system is an

example of a remote sensing system in this general sense (Carrara & Guzzedi, 1993). Remote sensing usually refers to the technology of acquiring information about the earth's surface (land and ocean) and atmosphere using sensors onboard airborne (aircraft, balloons) or space borne (satellites, drones, space shuttles) platforms.

Remote sensing instruments are of two primary types, active and passive. Active sensors, provide their source of energy to illuminate the objects they observe. An active sensor emits radiation in the direction of the target under investigation (Shamsi, 2005, p. 53). The sensor then detects and measures the radiation that is reflected or backscattered from the target. Passive sensors, on the other hand, detect natural energy (radiation) that is emitted or reflected by the object or scene being observed (Lunetta & Lyon, 2000). The remote sensing method considers high spatial and temporal resolution is light detection and ranging (LiDAR) technology. This state-of-the-art technology is considered a breakthrough in the mapping industry as it provides accurate and precise surface models needed for the detailed simulation of flooding. Reflected sunlight is the most common source of radiation measured by passive sensors in **Figures 7 and 8**.

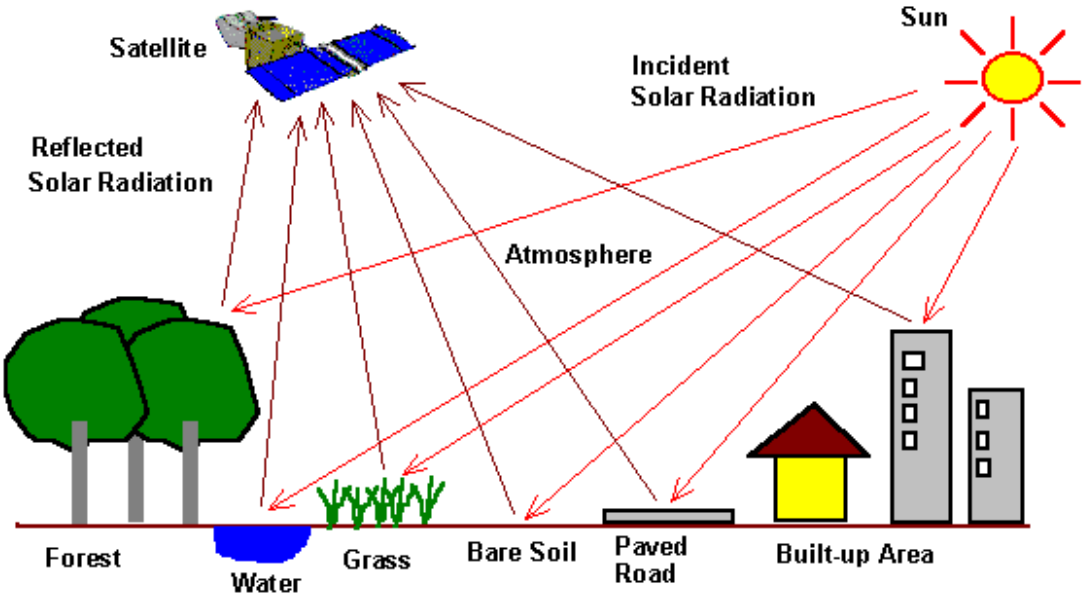

Figure 7 The process of remote sensing, Source: Chukiat, J, 2015

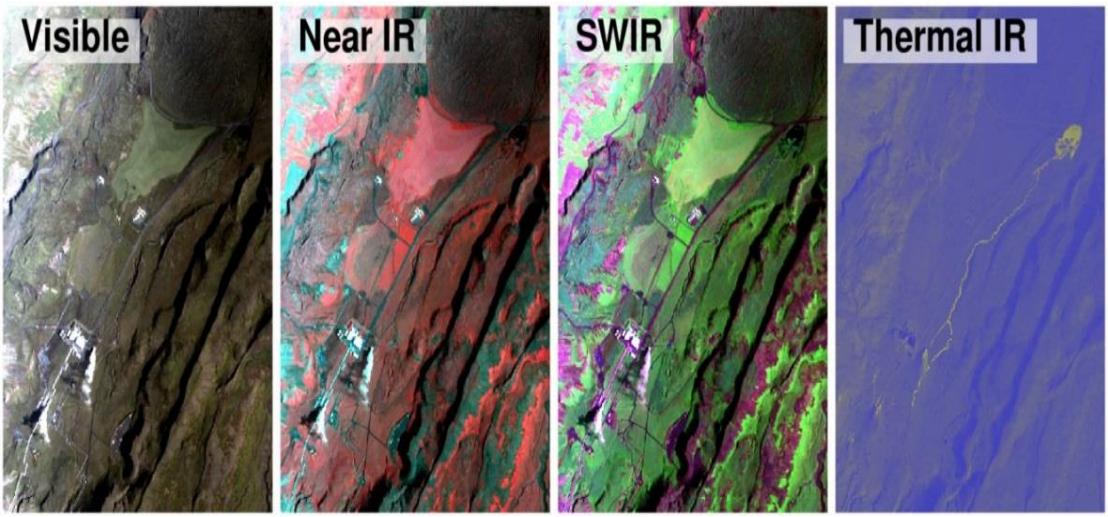

Figure 8 Multispectral infrared data channels combined by satellite image

3. Digital Elevation Model (DEM)

A Digital Elevation Model (DEM) is a specialized database that represents the relief of a surface between points of known elevation (Dysarz et al., 2019). By interpolating known elevation data from sources such as ground surveys and photogrammetric data, a rectangular digital elevation model grid can be create (Shamsi, 2005, p. 75). A DEM can be represented as a raster (a grid of squares, also known as a heightmap when representing elevation) or as a vector-based triangular irregular network (TIN). The TIN DEM dataset is also referred to as a primary (measured) DEM, whereas the Raster DEM is referred to as a secondary (computed) DEM (Brimicombe, 2010).

DEMs are commonly built using data collected using remote sensing techniques, but they may also be built from land surveys. DEMs are used often in geographic information systems and are the most common basis for digitally produced relief maps. While a DSM may be useful for landscape modeling, city modeling, and visualization applications, a DTM is often required for flood or drainage modeling, land-use studies, geological applications, and other applications (Weng, 2010). To sum up, DEM is very important technology when investigating flooding. Moreover, the researchers have been encouraged to find out the best resolution in various studies such as hydraulic models, hydrology models, etc.

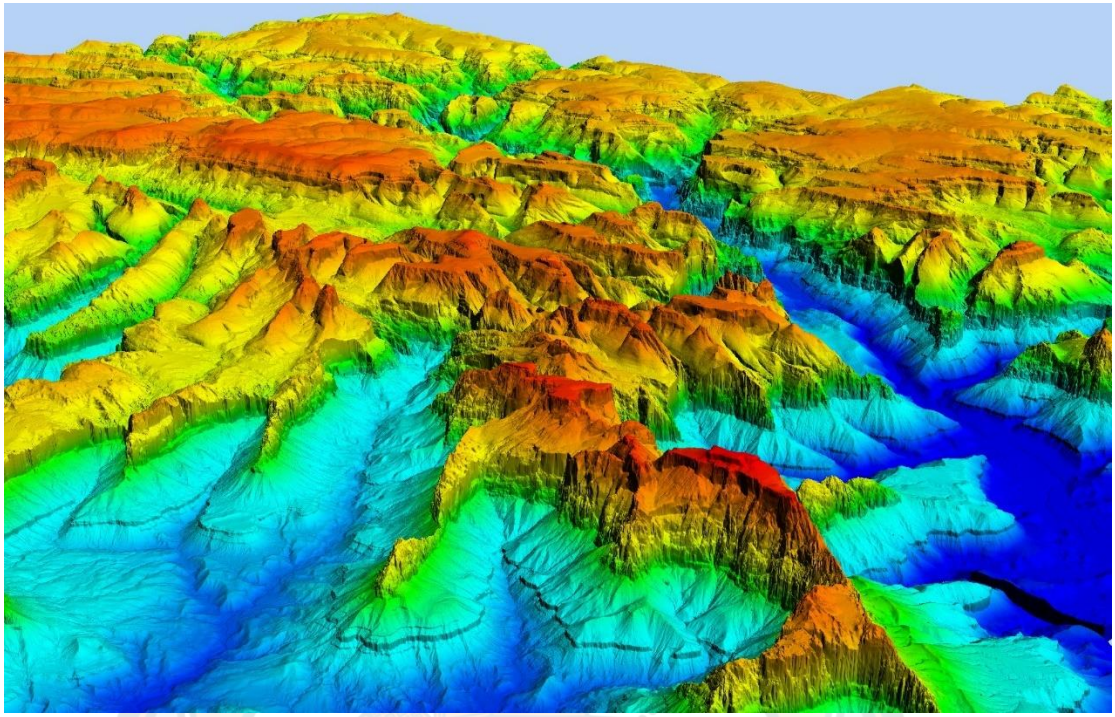

Figure 9 Digital Elevation Model, Source: USGS from computerized data, 2018

Credit: Jason Stoker, USGS. Public domain

4. Flood MODIS

MODIS (Moderate Resolution Imaging Spectroradiometer) is a key instrument aboard the Terra (originally known as EOS AM-1) and Aqua (originally known as EOS PM-1) satellites. Terra's orbit around the Earth is timed so that it passes from north to south across the equator in the morning, while Aqua passes south to north over the equator in the afternoon. Terra MODIS and Aqua MODIS are viewing the entire Earth's surface every 1 to 2 days, acquiring data in 36 spectral bands, or groups of wavelengths (see MODIS Technical Specifications). These data help to improve our understanding of global dynamics and processes occurring on the land, in the oceans, and the lower atmosphere. MODIS is playing a vital role in the development of validated, global, interactive Earth system models able to predict global change accurately enough to assist policymakers in making sound decisions concerning the protection of our environment https://modis.gsfc.nasa.gov/about/. The Moderate Resolution Imaging Spectroradiometer (MODIS) instrument is used to

detect water extent in support of flood response and recovery. The MODIS Near Real-Time Global Flood Mapping Project produces global daily surface and flood water maps at approximately 250 m resolution, in 10×10 degree tiles (https://floodmap.modaps.eosdis.nasa.gov/). MODIS provides natural-color images of tropical cyclones to help track storms and analyze their intensity as they move toward land. MODIS is used to detect wildfires and smoke plumes in support of fire response and recovery. MODIS data helps to power Fire Information for Resource Management Systems (FIRMS) (https://firms.modaps.eosdis.nasa.gov/map). This study uses flood MODIS provided by NASA's international organization to monitor flood areas using model simulation techniques.

5. HEC-RAS Modeling

The hydraulic model is inextricable components in the context of flood modeling and prediction purposes (USACE, 2018). The hydraulic models can be termed as to utilize discharge computed by the hydrologic models to simulate the movement of floodwater along waterways, storage elements, and hydraulic structures (Mihu-Pintilie et al., 2019; Talisay et al., 2019). The hydraulic model is proficient in simulating flood levels and flow patterns and can also model the complex effects of backwater or tidal intrusion, overtopping of embankments, waterways confluences and diversions, bridge constructions, weirs, culverts, and pumps and other obstructions on the flow in the river system (Şen, 2018; Xinjiang & Minghui, 2018; Mihu-Pintilie et al., 2019). They can be directly linked to hydrological models and river models to provide flood hazard mapping, flood risk mapping, flood forecasting, and scenario analysis. The 1-D versions are computationally efficient, but they suffer from several drawbacks including the inability to simulate lateral diffusion of the flood wave, the discretization of topography as cross-sections rather than as a continuous surface and the subjectivity of cross-section location and orientation. The 2-D versions that solve full shallow-water equations have been reported to be able to simulate the timing and duration of inundation with high accuracy (Teng et al., 2017; Maskong, 2019).

Hydraulic models are undergoing rapid development which has led to improvements in both accuracy and computational efficiency (Ahmed et al., 2014).

Apart from advances in individual models deliberated below, the combining of models is also receiving wider recognition as it allows almost limitless possibilities for maximizing the benefits of 1-D, 2-D and 3-D modeling approaches (Teng et al., 2017). The HEC-RAS is a well-known hydrodynamic model for rivers and reservoirs. This program was designed at the Hydrologic Engineering Center (HEC). The second term in the name defines its application: River Analysis System (RAS). The concepts applied in the package are well described by (Brunner, 2016; Dysarz et al., 2019). The Hydrological Engineering Centre River Analysis System (HEC-RAS) version 5.0.7 is a 1-D steady and unsteady flow hydraulic model developed and designed by the U.S. Army Corps of Engineers to aid hydraulic engineers in channel flow analysis and floodplain modeling. The results from the model can be applied in floodplain management and flood insurance studies (Logah et al., 2017). A 1-D hydraulic model was selected for this study due to its extensive application in floodplain analysis, particularly in the USA and free accessibility on the internet. The HEC-RAS model solves the Saint-Venant equations formulated for natural channels (Kheradmand et al., 2018; USACE, 2018).

The discharge values along the river with Digital Elevation Model (DEM) were used to predict flood hazard areas using HEC-RAS models alongside the flood plains in the lower Mekong basin, Cambodia. The result helped the government agencies and disaster relief NGO’s directing efforts to relocate human settlements, high-value crops, place emergency response systems and to increase people's awareness. Another study involved modeling the flooding of the Mekong River basin using the Hydrologic Engineering Center-Hydrologic Modeling System (HEC-HMS) and HEC-RAS to determine the effects of increasing urbanization on peak flood runoff over future periods by MRC, 2011.

6. Mathematic HEC-RAS Modeling

HEC-RAS is a modeling program developed by the US Army Corps of Engineers. It allows two different approaches to be adopted, i.e. (i) steady flow calculations, and (ii) unsteady flow simulation. The unsteady flow simulation has been used in this study to simulate flood inundation. The HEC-RAS modeling package uses the 1-D Saint-Venant equation to calculate open channel flow. In the

unsteady flow simulation, the horizontal exchange of water between channel and floodplain was assumed to be insignificant, and the water discharge is distributed according to the conveyance. The flow in the channel can be presented as:

$$Q_c = \phi Q \quad (1)$$

While Qc has flowed in the channel and Q is total flow. Here, ϕ determines how the flow is partitioned between the floodplain and channel, based on the conveyance of Kc and Kf. Where ϕ is calculated as:

$$\phi = \frac{K_c}{K_c + K_f} \quad (2)$$

While Kc is representing a conveyance in the channel and K_f is floodplain. Conveyance is defined as

$$K = \frac{A^{5/3}}{nP^{2/3}} \quad (3)$$

Where P is the wetted perimeter, A is cross-section area and n represents Manning′s n roughness coefficient. From the above equation, the 1-D equation can be written as follows:

$$\frac{\partial A}{\partial t} + \frac{\partial \phi Q}{\partial x_c} + \frac{\partial (1-\phi) Q}{\partial x_f} = 0 \quad (4)$$

$$\frac{\partial Q}{\partial t} + \frac{\partial}{\partial x_c}\left(\frac{\phi^2 Q^2}{A_c}\right) + \frac{\partial}{\partial x_f}\left(\frac{(1-\phi)^2 Q^2}{A_f}\right) + gA_c\left(\frac{\partial z}{\partial x_c} + S_c\right) + gA_f\left(\frac{\partial z}{\partial x_f} + S_f\right) = 0 \quad (5)$$

Where:

$$S_c = \frac{\phi^2 Q^2 {n_c}^2}{R_c^{4/3}} \; and \; S_f = \frac{(1-\phi)^2 Q^2 n_f^2}{R_f^{4/3} A_f^2} \quad (6)$$

Where A_c and A_f is the cross-sectional area of the flow of the channel and floodplain, x_c and x_f are the distances along the channel and floodplain, R is the hydraulic radius (A/P) and S is the friction slope. The finite difference method was utilized for the discretion of equations **4 and 5** and solved using a four-point implicit method.

7. Generating GIS and HEC-RAS Modeling

The GIS method is an important means to calculate and generate flood hazard maps and river studies (Abdelkarim et al., 2019). Other researchers have studied flood hazard susceptibility mapping using RS data and GIS techniques with the help of statistical, probabilistic, hydrologic, and stochastic neural networks and fuzzy logic (Hong et al., 2018). Recent papers (e.g.Chen et al., 2019; Jodar-Abellan et al., 2019), have indicated that hydrologic assessment using geospatial techniques could be conducted to identify different hydrologic components, prepare hydrologic designs, and develop possible scenarios to overcome the hazards from river flooding. Further, Geographic Information Systems (GIS) have become effective tools for the analysis of spatial management and data manipulation because of their ability to handle large amounts of spatial data (Criado et al., 2018). The combination of statistical and probabilistic models with Remote Sensing (RS) and GIS has often been used by a variety of researchers (Mosquera-Machado & Ahmad, 2007; Nor et al., 2014; Ezz, 2018). There are two main methods in flood hazard mapping called qualitative or quantitative. In recent years, statistical and probabilistic models have been very popular in the quantitative method. For example, some of the statistical and probabilistic models include frequency ratio (FR) and logistic regression (LR). The hydraulic model was used mostly to generate with GIS spatial analysis for identifying possible flood occurrences (Criado et al., 2018; Chen et al., 2019; Dysarz et al., 2019).

GIS is a system designed to capture, store, manipulate, analyze, manage and present all types of geographically referenced data. Recently, GIS has become an essential tool in hydrological modeling because of its capability in handling a large amount of spatial and attributable data. It has a lot of great features such as map overlay and analysis, which help to derive and aggregating hydrologic parameters from different sources such as soil, land cover, and rainfall data if available (Ezz, 2018) cited from (Cheng et al., 2006; de Winnaar et al.,2007). The GIS environment can extract hydrological variables needed from good quality digital elevation models (DEMs), such as catchments shapes, flow directions, slopes, path lengths, and watershed delineation (Ezz, 2018) cited from (Jenson and Domingue, 1988; Wilson

and Gallant, 2000). Likewise, Hong et al. (2018) developed a flood susceptibility assessment that uses intelligent techniques and GIS basic methods. But (Criado et al., 2018) established guidelines to assess the hazard, exposure, and vulnerability, of the population and its property to flood events using the HEC-RAS model for the simulation of the river and ArcGIS to treat geographic information and prepare the relevant maps. Flood modeling has greatly improved in recent years with the advent of geomantic tools and especially Geographic Information Systems (Azouagh et al., 2018; Echogdali et al., 2018). In this study, the combination of HEC-RAS modeling and GIS are used to delineate the flood hazard area. The specificity of this work is to share data with the GIS and HEC-RAS interfaces. Flood management should be considered a spatial problem because of flood intensities and characteristics with the geographic location. As newer GIS software was developed that improved geospatial visualization and computational efficiency, newer versions of HEC-RAS have been developed (Ben Khalfallah & Saidi, 2018).

Coupling GIS and HEC-RAS models were found to give a good performance where the simulated results for both studies showed a close agreement with observed water surfaces. Several other applications of GIS and the HEC-RAS model can be observed in the main literature review in **Table 4.**

Summaries of Literature Review

Table 4 Summaries of Literature Review

Tittle Relevant	Objective	Study Area	Methods	Outcome of Study	Gaps of Study
Delineation of flood-prone areas using the geomorphological approach in the Mekong River Basin (Try et al., 2019)	To delineate flood-prone areas in the Mekong River Basin from geomorphological features by using linear binary classifiers and receiver operating characteristics (ROC) analysis.	Cambodia	The method investigates the performance of five single features and six composite indices associated with flood hazards.	-The outcomes of this study can provide useful information for identifying areas that are prone to flooding.	Landsat 7 based on GIS technique to identifies flood characteristic.
Flood Hazard Mapping and Assessment on the Angkor World Heritage Site (Liu et al., 2019)	To develop a flood hazard index (FHI) model based on a GIS and used synthetic aperture radar (SAR) data to extract historical floods at Angkor from 2007 to 2013.	Cambodia	GIS technique and Analytic Hierarchy Process (AHP) and the Delphi method.	The results show that 9 monuments are at risk by potential floods among the 52 components of the Angkor monuments.	-Used AHP and GIS techniques. -Applied on a land view.
MODIS-Based Investigation of Flood Areas in Southern Cambodia from 2002–2013 (Vichet et al., 2019)	To investigate Spatio-temporal flood inundation and land cover change from 2002 to 2013 in the southern part of Cambodia using Terra satellite on-board Moderate Resolution Imaging Spectro-radio meter (MODIS) images.	Cambodia	-Using Landsat images in GIS techniques to identify flood inundation.	This was a result of increased agricultural productivity. However, water shortages was the major obstacle to increasing agricultural productivity, and it also had a negative impact on aquatic ecologies, such as fish spawning grounds.	Observed flood based on satellite and analyses on GIS technique.

Table 4 (cont.)

Tittle Relevant	Objective	Study Area	Methods	Outcome of Study	Gaps of Study
Flood hazard mapping in four provinces of Cambodia along the Mekong river basin (Hazarika et al., 2007)	To simulate the 1D flood model HEC-RAS for the Mekong River and to estimate the flood depth and extent for the year 2000 flood event in the four provinces of Cambodia.	Cambodia	-HEC-RAS only 1D steady flow -Data flow from 1991 to 2002 -Prepare with SAR Data	-Results show that the flood depth varies from 0 to 9.5 meters in the flood plain. -It was found that the flood-affected 2,286 km of roads and a total of 449 schools.	-2007 previous study -Just identify flood history 2000
Flood Mapping along the Lower Mekong River in Cambodia (Sarann et al., 2018)	To simulate the flood inundation area by using HEC-RAS software. HEC-RAS is a hydraulic model software capable of calculating any hydraulic river study including flood.	Lower Mekong River, Cambodia.	HEC-RAS 1D Steady flow and delineate flood map from 2000 until 2013	The results show that flooding varied from year to year; however, the greatest flood was during 2000 and again in 2011. The simulated flood maps were compared with observed data to figure out that the model was accurate for flood mapping.	Relevant to the studying
Analysis of extreme flow uncertainty impact the size of flood hazard zones for the Wronki gauge station in the Warta river (Dysarz et al., 2019).	To estimate the uncertainty of the maximum flow evaluation and its impact on the uncertainty of the flood hazard zone determination.	Poland	(1) hydrologic data for the Wronki gauge station, (2) a digital elevation model (DEM) for the area surrounding modeled reach, (3) the measurements of the channel cross-sections and structures, (4) additional GIS layers support	The number of uncertainty sources is huge in the case of flood modeling, the length of the data series and the method for evaluation of extreme flows are among the most important.	Relevant to the studying

Table 4 (cont.)

Tittle Relevant	Objective	Study Area	Methods	Outcome of Study	Gaps of Study
Flood hazard mapping in an urban area using combined hydrologic hydraulic models and geospatial technology (Talisay et al., 2019).	Flood hazard map generation of 2, 5, 10, 25, 50 and 100-year return periods was conducted and the number of flooded buildings in each flood hazard level and different return periods was determined.	Valencia City, Bukidnon, the Philippines in 2017	A combination of HEC-HMS and River Analysis System (RAS) models were applied in flood hazard mapping of the Malingon River Basin.	-The output of the study served as an important basis for a more informed decision and science-based recommendations in formulating local and regional policies for more effective and cost-efficient strategies relative to flood hazards.	Combined two modeling's such as HMS and HEC-RAS Modeling
Flood inundation mapping in small and ungauged basins (Vojtek et al., 2019)	To investigate the flood mapping sensitivity concerning the following EBA4SUB input parameters. To investigate the flood mapping sensitivity concerning 1-D HEC-RAS.	Korytarka basin, Slovakia	Sensitivity analysis using the EBA4SUB and HEC-RAS modeling approach.	This finding highlights the importance of the correct estimation of soil and land use properties which affect the excess rainfall estimation.	-1-D steady and unsteady flow analysis -Used simulated flood area (FA) and volume (FV) to identify flow.
Floodplain delineation using the HEC-RAS Model (Patel & Gundaliya, 2016).	Flood inundation mapping and flood return period for 25 and 32 years.	India	To describe the application of the HEC-RAS model with the integration of GIS for delineation of the flood plain.	One of the most important lessons learned from the study is that the use of GIS for the undertaking of flood simulation can improve accuracy and can also prove cost-saving of flood.	Relevant to the studying
Cartography of Flood Hazard in Semi-Arid Climate (Echogdali et al., 2018)	-Conducting a flood hazard map using HEC-RAS modeling. -Four flood maps for return periods of 20, 50, 100 and 500 years are generated.	South-East of Morocco	-HEC-RAS modeling -GIS technique -Discharge Data	Through lateral flood zoning maps, areas that are vulnerable to flood hazards have been identified. This information is useful in defining the minimum height of flood protection.	Relevant to the study.

Table 4 (cont.)

Tittle Relevant	Objective	Study Area	Methods	Outcome of Study	Gaps of Study
Flood hazard maps in the city of Batna (Algeria) by the Hydraulic Modeling Approach (Sami et al., 2016)	To map the flood hazard using a hydraulic modeling method.	Batna at Oued El Gourzi River	GIS, HEC-RAS Modeling and flow date 1-D steady flow analysis	Flood hazard and flood Scenario.	Use only steady flow
Flood Hazard Mapping using Hydraulic Model and GIS (Sein, 2016)	Flood hazard map of different return periods in Ayeyarwady River at Mandaly city.	Myanmar	flood frequency analysis integrates with the 1-D Hydraulic model (HEC-RAS) and Geographic Information System (GIS)	The predicted flood depth ranges vary from greater than 0 to 24 m in the flood plains and on the river. The range between 3 to 5 m was identified in the urban area of Chanayetharzan, Patheingyi, and Amarapua Townships.	Use only 1-D in HEC-RAS Modeling Use only flood frequency analysis distribution to identify flood return period
Flood hazard and flood risk assessment at the local spatial scale (Vojtek & Vojtekova, 2016)	To determine flood hazards in the model area, which has 3.23 km^2, the estimation of maximum flood discharges using HEC-RAS	Slovakia	GIS, RS, HEC-RAS Modeling	Water depth and flow velocity raster were identified as flood hazard and flood risk	-Used only 1-D hydraulic -High expected
Assessing flood inundation mapping through estimated discharge using GIS and the HEC-RAS model (Mokhtar et al., 2018)	To investigate the uncertainties of the hydraulic Model. To examine the influence of estimated discharge on water extent and flood depth.	Malaysia	GIS, R.S and HEC-RAS modeling.	For improved accuracy in flood mapping, factors such as the diverse range of land use surface roughness, topography, and river geometry uncertainties should be considered in the modeling. Finally, flood modeling can be precisely carried out if satellite images during peak flow are available.	-Prepare DEM for input into the model

Table 4 (cont.)

Tittle Relevant	Objective	Study Area	Methods	Outcome of Study	Gaps of Study
Flood hazard assessment under climate change scenarios in the Yang River Basin (Shrestha & Lohpaisankrit, 2017).	To assess the flood hazard potential under climate change scenarios in the Yang River Basin	Thailand	A physically-based distributed hydrological model, Block-wise use of TOPMODEL using Muskingum-Cunge flow routing (BTOPMC) and hydraulic model, HEC-RAS	Inundation maps of return period 25, 50 and 100-year and food scenario.	Sep scenario CC Generate HEC-RAS Used return period 25, 50, 100 -year.
Flood Risk Management in Remote and Impoverished Areas (Heimhuber et al., 2015)	Flood Hazard zoning, Flood Protection Masseurs Framework	Onaville, Haiti	HEC-HMS and HEC-RAS Model	The results of the hydrologic and hydraulic modeling were incorporated into a flood hazard map which formed the basis for flood risk management.	Apply two models (Hydrology and hydraulic)
Flood hazard under CC and HEC-RAS (Shrestha & Lohpaisankrit, 2017)	To assess the flood hazard potential under climate change scenarios in the Yang River Basin of Thailand.	Thailand	Muskingum-Cunge low routing (BTOPMC) and hydraulic model, HEC-RAS	To indicates the severity of flood in the region but also indicate potential damage to food production and negative effects on the livelihoods of local people.	Methodology is relevant to the study.
Flood hazard assessment and the mapping of River Swat using HEC-RAS 2-D model and high-resolution 12-m Tan DEM-X DEM (World DEM) (Farooq et al., 2019)	Flood Hazard Map Flood Hazard Assessment for the river.	Pakistan	HEC-RAS 1-D 2-D model combined 1-D/2-D unsteady flow routing and high-resolution 12 m World DEM.	Flood model and associated hazard maps will help disaster managers to mitigate the flood vulnerability in the study area. It is recommended that the HEC-RAS 1-D/2-D couple model may be tested in future studies once river cross-sections are available for study.	Relevant to the studying.

As the literature review of floods in previously relatively unaffected inhabited areas is constantly growing, according to the data from monitoring studies, it is necessary to progress methodology for flood prediction and prevention in those areas. Hydraulic modeling is a useful, efficient instrument to determine flooded areas and produce flood return periods of spatially distributed variables such as rapidity, depth, characteristics and the water extent of flood inundation areas. The consequences of modeling typically indicate a series of actions that have to be carried out to prevent floods and where possible, eliminate them. 1-D and 2-D hydraulic models are mostly used to evaluate possible flooding. The researchers' presentation involves the use of hydraulic modeling and GIS techniques to develop flood hazard maps and flood return periods (flood inundation areas and flood depth). Flood hazard analysis is a critical first step towards effective flood-risk management and constitutes the basis for taking preventive risks, thus contributing to the sustainable development of river sites.

CHAPTER III

RESEARCH METHODOLOGY

This research is coupling the efficiency of GIS and hydraulic modeling to identify flood hazard maps. This study is coupling the efficiency of GIS and hydraulic modeling to create flood hazard maps. In this section, the study areas, data collection, study processing, and methods of analysis are indicated in **Figure 10.**

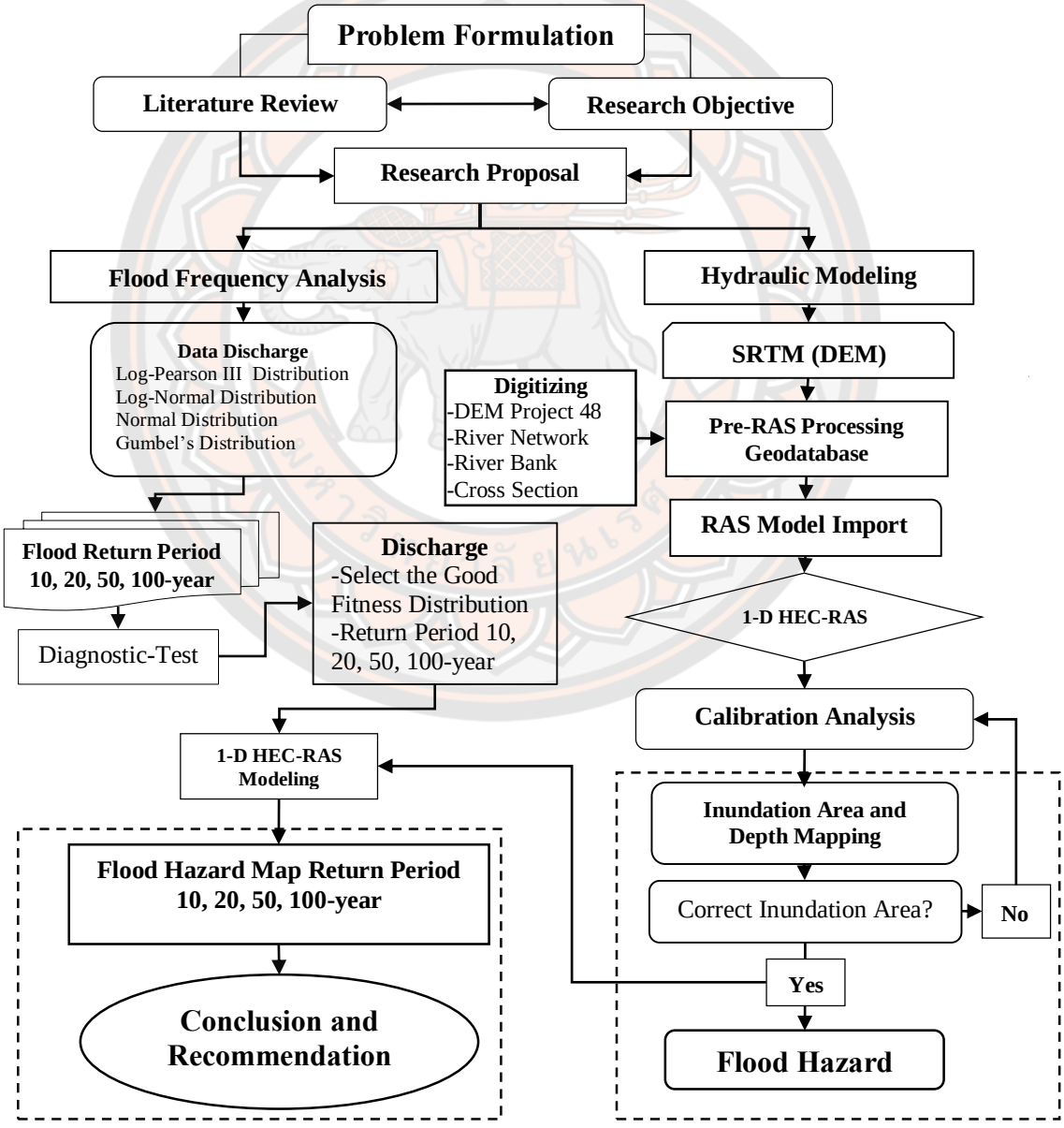

Figure 10 Research Framework

Study Area

Cambodia is one of the countries in South-East Asia which is located from 102.350 to 107.620 longitude and from 9.910 to 14.690 latitude, with an area of 181 035 km^2. Of the land area, 97.5 percent is land while 2.5 percent consists of water (CFE-DM, 2017). The Mekong River is one of the world's great river systems, flowing 4,909 km it influences a vast area of 795,000 km^2 and supports a population of approximately 70 million people. The River flows across six countries: China, Myanmar, Thailand, Lao PDR, Cambodia, and Vietnam. It has a mean annual discharge of 14,500 m^3/s (475 km^3/ year (MRC, 2018). There is a very large difference in the flows during the wet (June to October) months and the dry months (November to May) (MRC, 2018; Sarann et al., 2018; Vichet et al., 2019).

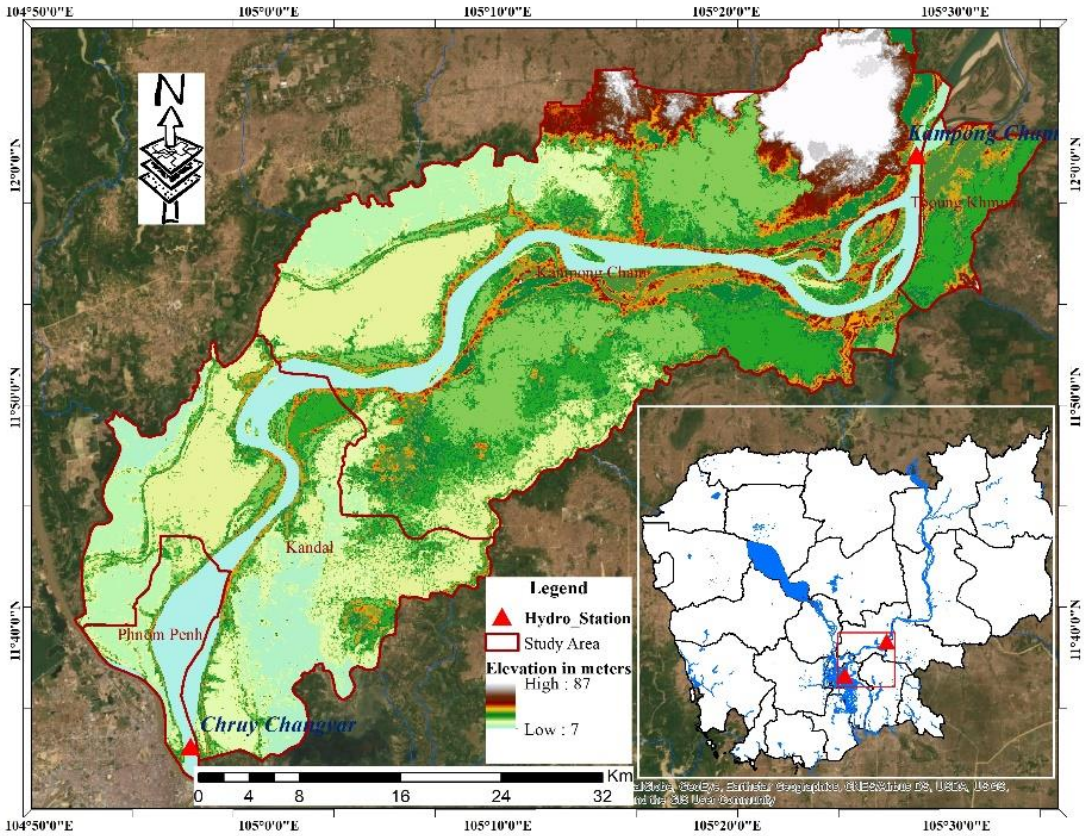

Figure 11 The Study Area of Lower Mekong River, Cambodia

Cambodia flows southward from the Cambodia and Laos border through six provinces and one city such as Stung Treng, Kratie, Kampong Cham, Kboung Khmum, Kandal, and Prey Veng province and Phnom Penh city. The study has assessed the hydraulic process in the Lower Mekong River and focused mainly on flood inundation in the downstream region where Kampong Cham station reaches Chruy Changvar station in Phnom Penh City. The key aim is to develop flood hazard maps based on multi return periods using GIS and HEC-RAS modeling at a part of Kampong Cham, Tboung Khmum (87 km^2), and Kandal (518 km^2) province and Phnom Penh (85 km^2) city and starts from the upstream Kampong Cham station to downstream Chruy Changvar station (Phnom Penh City) area 1948 km^2 and length 103.53 km in Cambodia.

Hydrological Data

Cambodia has a humid tropical climate. The country has two seasons which include a rainy season (May to October) and a dry season (November to April) (MoE, 2019). The average temperature is from 21^oC to 30^oC. The months with the lowest temperature are December and January while the months with the highest temperatures are April and May (CFE-DM, 2017). Especially, the flow Mekong river meets the Tonle Sap system 300 km downstream from Stung Treng province at the Cambodian capital, Phnom Penh (Yu et al., 2019). From October to May, water flows from the Tonle Sap to the Mekong river at a maximum daily discharge rate of 8300 m^3/s, when the wet monsoon reaches the basin in May, the Mekong River rises to a higher level than the Tonle Sap, forcing the latter to reverse its flow towards its lake (Cochrane et al., 2014). This phenomenon creates a floodplain that extends over 15,000 km^2 and stores up to 76.1 km^2 of Mekong's annual flood (MRC, 2018).

The important data of HEC-RAS hydraulic modeling consists of the maximum annual discharge ever recorded in the upstream simulation at Kampong Cham gauging station and the simulation is calibrated with the downstream flow at the Chruy Changvar gauging station. These water discharge recording are using 30 years that available since 1989 to 2018 provided by the ministry of water resource and meteorology in Cambodia (http://www.mowram-nffc.org/index.php/wl/mainstream).

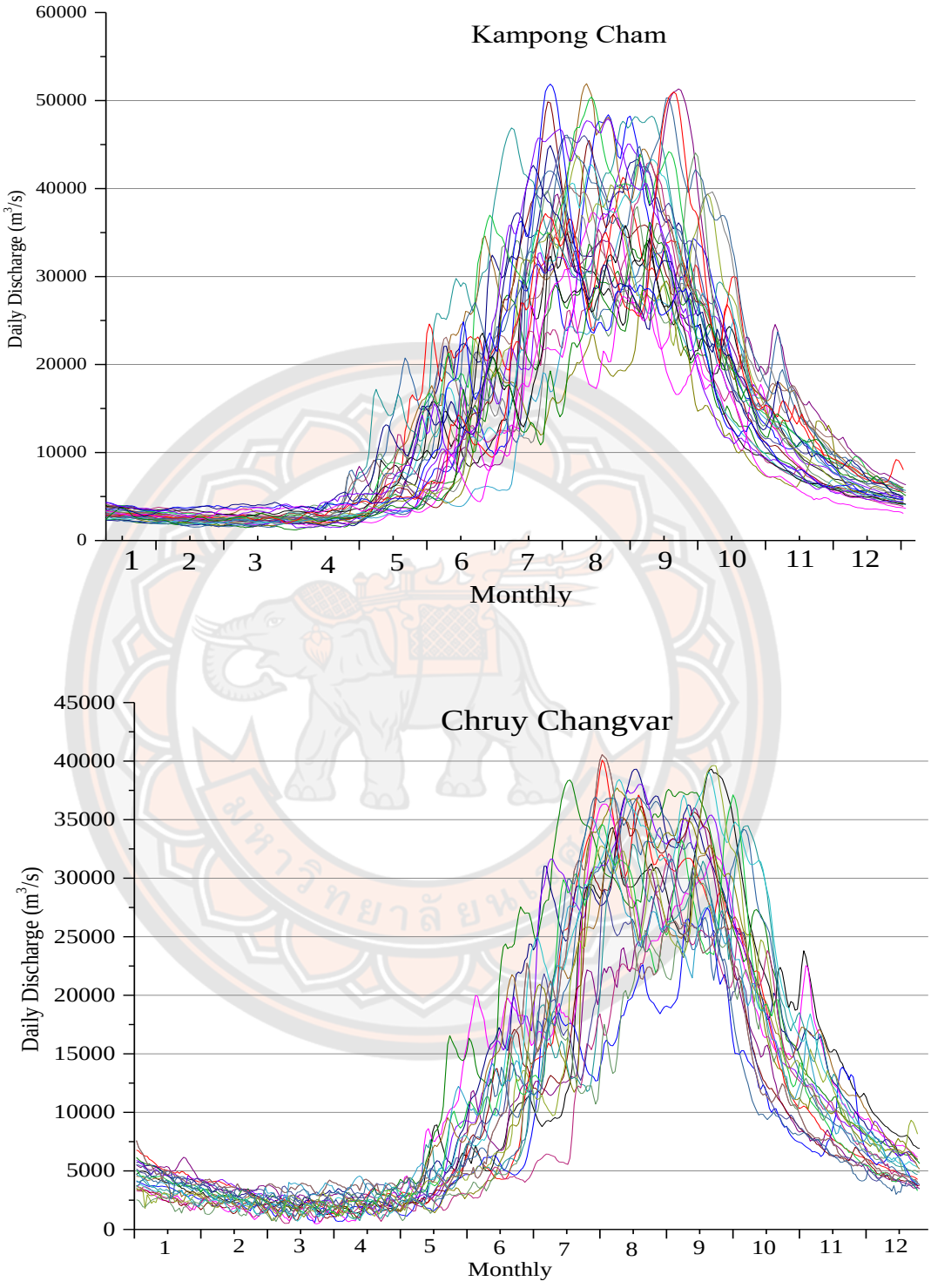

Figure 12 Situation of river flow at Kampong Chan and Chruy Changvar

Source: http://www.mowram-nffc.org/index.php/wl/mainstream

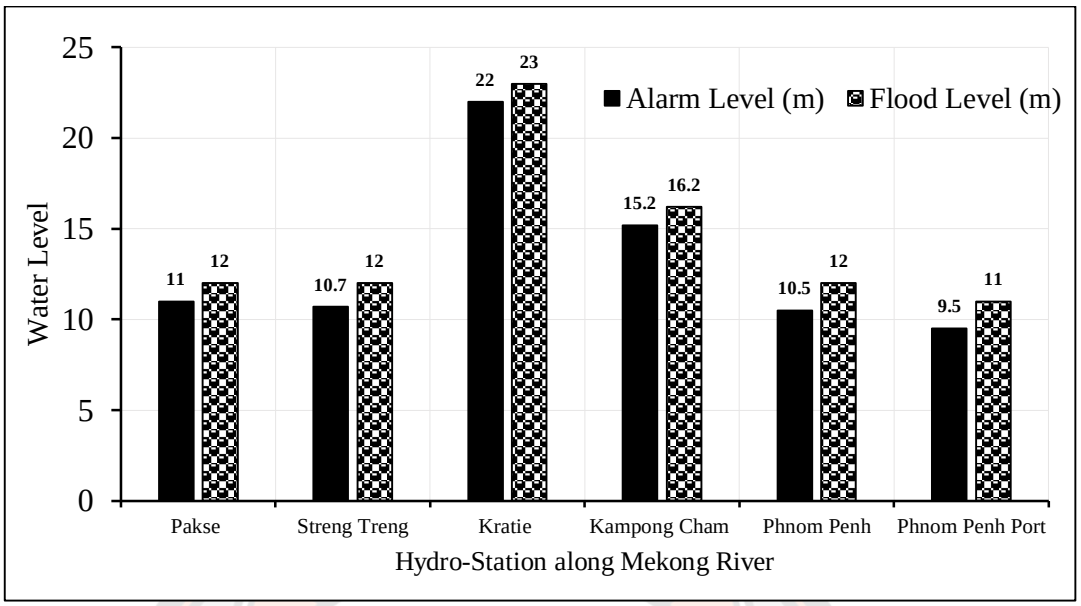

Figure 13 Standard of flood EWS along the Mekong River in Cambodia

Source: Mekong River Commission, 2018

Description of Implements Research

The methodology applying for this studying such as ArcGIS version 10.5, HEC-RAS hydraulic modeling version 5.0.7 (Free License) stand independent software, Easyfit software, and Microsoft office version 2019 generation.

Process Analysis

1. Flood Frequency Analysis

Flood frequency analysis is a method used by hydrologists to predict flow values corresponding to specific return periods or probabilities along the river (Farooq et al., 2018; Bhat et al., 2019). There are several methods of frequency distributions which could be used to carry out the statistical analysis to predict the magnitude of potential flooding. The Log-Pearson Type III (LP3) distribution, Log-Normal distribution, Normal distribution, and Gumbel's distribution methods were

used to predict extreme levels of different return periods of 10, 20, 50 and 100 years using observed discharge data like with the previous study such as Orsini-Zegada and Escalante-Sandoval (2016), Farooq et al. (2018), and Bhat et al. (2019). The methods variety Q (flood peak discharge) with a recurrence interval t is given by (Chow et al., 1988; Ramachandra & Hamed, 2000). Calculating the different return periods of 10, 20, 50 and 100-year, the above distributions are checked with the best fittest by Easyfit software.

1.1 LP3, Log-Normal, Normal, and Gumbel's Distribution

Table 5 PDFs with flood quantile estimators (Q_t)

Distribution	Quantile Function (Q_t)	Description of Factors
L-P type 3	$\log x = \overline{\log x} + K\sigma_{\log x}$ $\overline{\log x} = \frac{\sum(\log x_i)}{n}$ $\sigma_{\log x} = \sqrt{\frac{\sum(\log x - \overline{\log x})^2}{n-1}}$	$\overline{\log x}$, is the average of the log x discharge values. K is a frequency factor. σ, is the standard deviation of the log x values.
Log-N	$x_t = \mu + K_t\sigma$	$K_t = (\frac{1}{C_v})[\exp\{Z(\log(1+C_v^2))^{1/2} - 0.5(\log(1+C_v^2))\} - 1$ Z is a standard normal deviate and C_v is the coefficient of variation $C_v = \frac{\mu}{\sigma}$
Normal	$x_T = \overline{x} + z_T s$ $Z_T = Y_T = -\frac{\sqrt{6}}{\pi}\{0.5772 + \ln[\ln(\frac{T}{T-1})]\}$	X_T = Maximum flood peak discharge $\bar{x}$ = Average value of peak discharge Z_T = Frequency factor for the normal S = Standard deviation of sample size
Gumbel	$Q_T = \overline{Q} + K\sigma_{n-1}$ (1) $\sigma_{n-1} = \sqrt{\frac{\sum(Q-\overline{Q})^2}{N-1}}$ (2) $K = \frac{y_T - \overline{y_n}}{S_n}$ $y_T = -\lvert \ln.\ln\frac{T}{T-1} \rvert$	Q_T = maximum flood peak discharge $\overline{Q}$ = Average value of Q σ_{n-1} = Standard deviation of sample size N $\overline{y}_n$ = Reduce mean, of sample size N S_n= Reduce standard deviation, of sample N

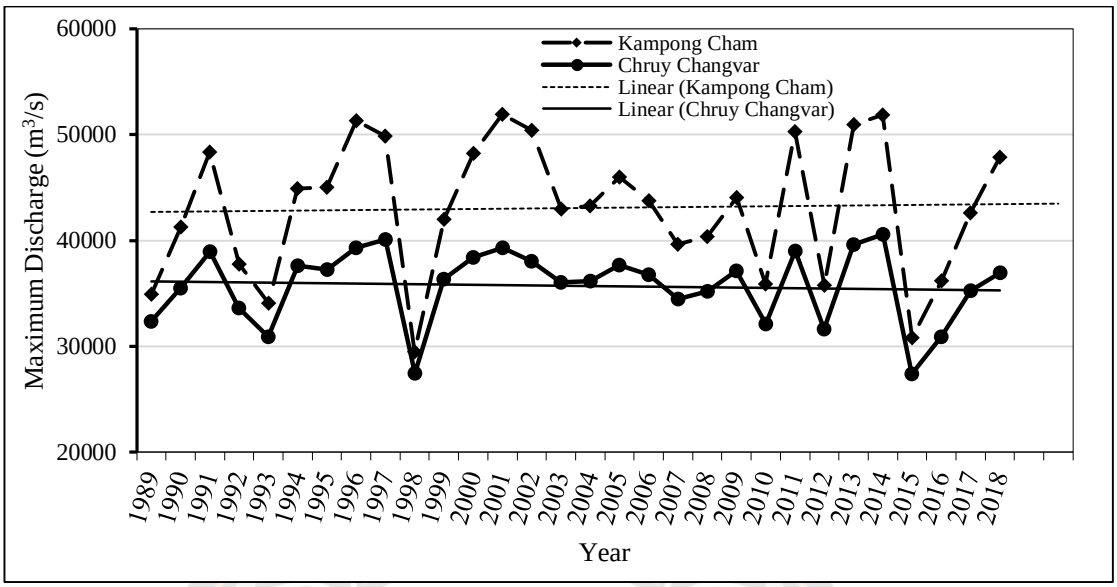

Figure 14 Annual peak discharge in gauging station of LMR (1989-2018)

1.2 Goodness of Fit Test

The applicability of the distributions for the investigation could be tested using various appropriate statistical algorithms such as goodness of fit statistical tests. The goodness of fit test can be used in flood frequency analysis to aid in the selection of a comparatively better probability distribution method rather than reject the other distributions being tested. To measure how well the observed data corresponds to the fitted model, we applied three goodness of fit tests (Kolmogorov-Smirnov Test, Anderson-Darling Test, and Chi-Square Test) equation in Easyfit software.

2. 1-D Hydraulic Model

HEC-RAS is used the main software to designed flood hazards by 1-D calculations on river channels either natural or man constructed. It allows steady flow and unsteady flow. HEC-RAS modeling is used to analyses important elements of free-surface fluid flow such as for flood return period and producing efficiency flood hazard map. This research is used HEC-RAS modeling to simulate inundated areas. Furthermore, steady-flow and unsteady-flow simulations were conducted using version 5.0.7 on the HEC-RAS model, developed by the US Army Corps of Engineers (HEC, 2019). HEC-RAS version 5.0.7 is the hydraulic model that is designed to

perform 1-D hydraulic calculations and combinations for a full network of the study and constructed and cross-section channels. Furthermore, HEC-RAS modeling is used for steady and unsteady flow water surface profiles, using the energy equation with an iterative procedure called the standard step method.

$$Z_2 + Y_2 + \frac{a_2 V_2^2}{2g} = Z_1 + Y_1 + \frac{a_1 V_2^2}{2g} + h_e$$

where: Z_1, Z_2 are the elevations of the main channel inverts, Y_1, Y_2 is the depths of water at cross-sections, V_1, V_2 are the average velocities (total discharges/total flow area), a_1, a_2 are the velocity weighting coefficients, that account for non-uniformity of the velocity distribution over the cross-section, g: gravitational acceleration, and h_e: is the energy head loss. A steady flow is a condition in which depth and velocity at a given channel location do not change with time. Therefore, gradually varied flow is characterized by minor changes in water depth and velocity from one cross-section to another. The cross-section sub-division for the water conveyance is calculated within each reach using the following equations:

$$Q = KS_f^{1,2}, while\ K = \frac{1.486}{n} AR^{2/3}$$

where: K = conveyance for subdivision, n = Manning roughness coefficient, A = flow area subdivision, R = hydraulic radius for subdivision (wetted area/wetted perimeter) and S_f = friction slope.

3. Development DEM and Cross Section

3.1 Developing DEM (Digital Elevation Model)

A Digital Elevation Model (DEM) is a specialized database that represents the relief of a surface between points of known elevation. By interpolating known elevation data from sources such as ground surveys and photogrammetric data capture, a rectangular digital elevation model grid can be created (Carrara, 1995; Shamsi, 2005). DEM extracts the elevation value of each point that helps to predict the probable submergence depth of respective points/areas within the boundary. NASA only needed 11 days to capture Shuttle Radar Topography Mission (SRTM) 30-meter digital elevation model. Back in February 2000, the Space Shuttle

Endeavour launched with the SRTM payload. Using two radar antennas and a single pass, it collected sufficient data to generate a digital elevation model using a technique known as interferometric synthetic aperture radar (InSAR) (Brimicombe, 2010). C-Band penetrated canopy cover to the ground better but SRTM still struggled in sloping regions with foreshortening, layover, and shadow.

SRTM DEM data is being housed on the USGS Earth Explorer. To download, select your area of interest. Under the data sets tab, select Digital Elevation > SRTM > SRTM 1-ArcSecond Global. DEM was used to extract the geometry of the river in the study area. The DEM was projected in the projection coordinate system of WGS_1984 UTM zone 48N. The DEM file used in this study was downloaded from the U.S. Geological Survey (USGS).

3.2 Developing Cross Section

The DEM is a 30 × 30 m spatial resolution project coordinate system WGS_1984_UTM_Zone_48N. The preparing DEM is input to RAS Mapper to conduct a triangular irregular network (TIN) which represents the topography to identify river network, riverbank, and 100 cross-sections as the result **Figure15**.

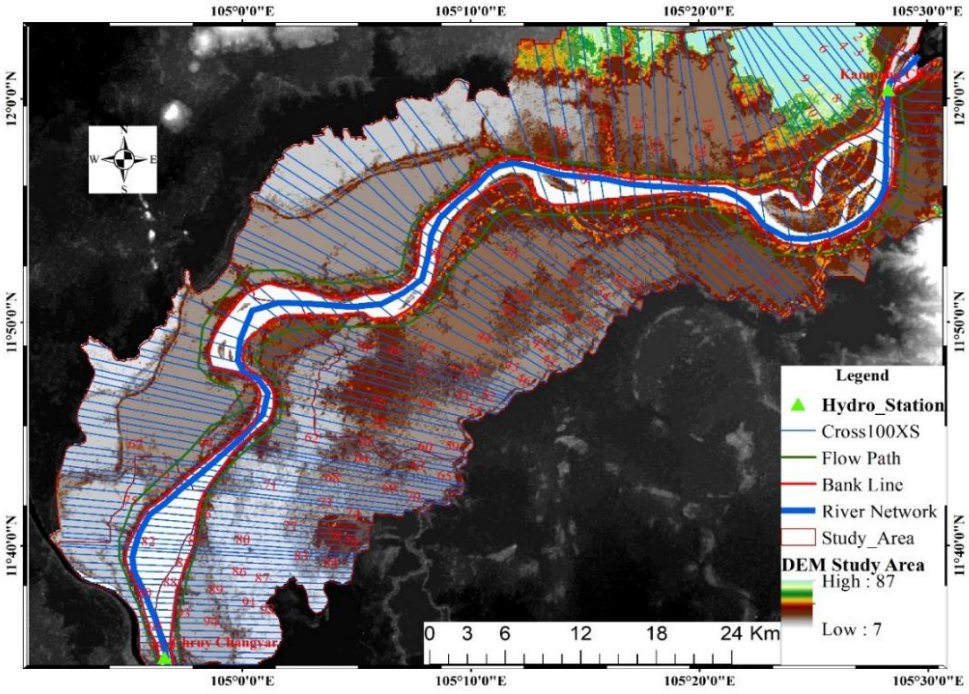

Figure 15 Cross-section and DEM coordinate system UTM_Zone_48N

Preparing water surface elevation data as read in a scatter point data set with stream stage values which are derived from the HEC-RAS model and subsequently read in the RAS map. Water elevation data consist of a series of surface water elevation points defined as x, y, z (where z is the elevation of the water surface). Some parameters required for the hydraulics model in HEC-RAS are stream centerline, main channel banks, cross-section lines, and material zones which are called channel geometry. The geometric data were derived based on the existing satellite imagery from Google Earth. A total of 100 cross-sections were taken over the single reach model. A great number of cross-sections were chosen for more detailed flood maps. Reducing the number of cross-sections results in poorer inundation maps. An example of the water surface elevation is given in cross-section of Roughness coefficients (Manning's n) used in the study area was 0.035 for river area, 0.05 for right bank and left bank area.

2.2 One-Dimensional Unsteady Flow

Unsteady flow data is then imported into HEC-RAS as a boundary condition to model the real historical event. In this study, recorded upstream stream flow data at Kampong Cham station for 2011, 2013, and 2018 flood events were assigned as the upstream boundary condition to the river model and normal depth was set as the downstream boundary condition. Simulation time in HEC-RAS must be synchronized with the flow data. At this stage, HEC-RAS had acquired everything the model needed to perform the hydrodynamic modeling.

The final simulation process is to compute the unsteady flow model in the 'Run' windows. During the computation, the 1-D model HEC-RAS characterized the flow as unsteady, with the flow moving in a downstream direction (1-D) and the provided cross-section as the whole characterization of the river environment. Two extreme high discharge event simulations were performed in this study and the outputs were analyzed. Calculated flow discharges at the downstream boundary for both events were fitted to the observed discharge to validate the simulation.

A high discrepancy result would suggest that the base model parameter should be fixed using sensitivity analysis where the simulated discharge is fitted to the observed discharge by optimization of Manning's **n**. In this study, the calibration values of **n** that gave the best agreement between observed and simulated results are equal to 0.035 for the main channel and 0.05 for the floodplain.

2.3 One-Dimensional Steady Flow

The Hydrologic Engineering Centre's River Analysis System (HEC-RAS, version 5.0.7), a 1-D hydraulic-flow model developed by the U.S. Army Corps of Engineers (USACE), is used for the study. HEC-RAS uses several input parameters for the hydraulic analysis of the stream channel geometry and water flow. These parameters are used to establish a series of cross-sections along the stream. In each cross-section, the locations of the stream banks are identified and used to divide into segments the left floodway, main channel, and the right floodway. At each cross-section, HEC-RAS uses several input parameters to describe the shape, elevation, and relative location along the stream such as:

1) River station (cross-section) number.
2) Lateral and elevation coordinates for each terrain point.
3) Left and right bank station locations.
4) Reach lengths between the left floodway, stream centerline, and right floodway of adjacent cross-sections.
5) Manning's roughness coefficients.
6) Channel contraction and expansion coefficients.
7) Geometric description of any hydraulic structures

HEC-RAS assumes that the energy head is constant across the cross-section and the velocity vector is perpendicular to the cross-section. After defining the stream geometry and the flow values for each reach within the river system, the channel geometric description and flow rate values are the primary model inputs for the hydraulic computations (USACE, 2018). The basic computational procedure is based on the iterative solution of the energy equation. Given the flow and water surface elevation at one cross-section, the goal of the standard step method is to

compute the water surface elevation at the adjacent cross-section (Hicks & Peacock, 2005).

Post-Processing of HEC-RAS Modeling

The cross-sections are computed to the terrain developed by DEM using RAS mapper and then imported into HEC-RAS software version 5.0.7. Moreover, the cross-sectional quality was checked on the geometric data to make sure that no erroneous information was imported. Some of the cross-sections are edited, where found necessary, using graphical cross-section editor. This value has been calibrated through a comparison of the HEC-RAS water level for different discharge values against the available rating curve data. Therefore, according to the previous studies and available data (data from hydrometric stations), the HEC-RAS model is calibrated. Below is described flow processing of the evaluating step.

Stream Network, Cross Section, and Bounding Polygon Generation: After completing "Theme Setup" and "Read RAS GIS Export File", it will read the results from the export file and create initial datasets. The stream network, cross-section data, bank station data, and bounding polygon data will be read, and shapefiles will automatically be generated.

Water Surface Generation: Based on water surface elevations of the cross-sectional cut lines and bounding polygon theme, the water surface was generated for each water surface profiles.

Floodplain Delineation: After the generation of water surface, the next step is the delineation of the floodplain. The floodplain delineation will create a poly-line theme identifying the floodplain and a depth grid. The water depth grid is created by the subtraction of the rasterized water surface from the DEM.

The different return periods of flood peak were obtained from the goodness distribution and used as an input to the HEC-RAS model in order to simulate results for each cross-section. At the same time, water surface profiles were running in the model for 10, 20, 50, and 100-years. After running input data in the HEC-RAS model, the result outputs were exported to ArcGIS in the format of the raster export file. The RAS-Mapper export file is imported into ArcGIS after generating water surface and flood plain delineation. ArcGIS is used to generate flood depth and flood inundation for different return periods.

4. 1-D Hydraulic Model Calibration

Statistics were used to quantify model performance compared to observations. Statistics include Nash-Sutcliffe Efficiency (NSE), Observed Standard Deviation Ratio (RSR), coefficient of determination (R^2), and percent bias (PBIAS) were computed using daily average flow. NSE measures the relative magnitude of the residual variance compared to the measured data variance. NSE ranges between -∞ and 1.0, where NSE equal to one is optimal. Values of NSE less than 0.0 indicate the mean observed value is a better predictor than the simulated value, meaning that the performance is unacceptable (USACE, 2018). NSE is computed using Equation 1.

$$\mathrm{NSE} = 1 - \left[\frac{\sum_i^n \left(\mathrm{Q_{obs_i}} - \mathrm{Q_{sim_i}}\right)^2}{\sum_i^n \left(\mathrm{Q_{obs_i}} - \overline{Q_{obs_1}}\right)^2}\right] \qquad (1)$$

RSR normalizes the Root Mean Square Error (RMSE) by using the standard deviation of the observations, incorporating the benefits of error index statistics so that the resulting statistic can be applied to various constituents. The RSR is computed using **Equation 2**.

$$\mathrm{RSR} = \frac{\mathrm{RMSE}}{\mathrm{STDEV_{obs}}} = \frac{\sqrt{\sum_{i=1}^{n} (\mathrm{Q_{obs_i}} - \mathrm{Q_{sim_i}})^2}}{\sqrt{\sum_{i=1}^{n} (\mathrm{Q_{obs_i}} - \mathrm{Q_{obs_{mean}}})^2}} \qquad (2)$$

R^2 describes the degree of collinearity between simulated and observed data and describes the proportion of the variance in measured data explained by the model. R^2 is oversensitive to outliers and insensitive to additive and proportional differences between model predictions and measured data. R2 is computed using Equation 3.

$$R^2 = \left[\frac{\sum_{i=1}^{n} (\mathrm{Q_{sim_i}} - \overline{\mathrm{Q_{sim}}})(\mathrm{Q_{obs_i}} - \overline{\mathrm{Q_{obs}}})}{\sqrt{\sum_{i=1}^{n} (\mathrm{Q_{sim_i}} - \overline{\mathrm{Q_{sim}}})^2} \sqrt{\sum_{i=1}^{n} (\mathrm{Q_{obs_i}} - \overline{\mathrm{Q_{obs}}})^2}}\right]^2 \qquad (3)$$

PBIAS measures the average tendency of the simulated data to be larger or smaller than the observed data. The optimal value for PBIAS is zero (0.0), with low absolute percent bias indicating accurate model simulation. Positive values mean the model's underestimation bias when compared to the observed, whereas negative values indicate the model's overestimation bias. PBIAS is computed using Equation 4.

$$\text{PBIAS} = \frac{\sum_{i=1}^{n}(Q_{obs_i} - Q_{sim_i}) \times 100}{\sum_{i=1}^{n}(Q_{obs_i})} \qquad (4)$$

Where:
Q_{obs} is the observation water level
Q_{sim} is the water discharge that got from simulation
n is the total number of observations and simulated data.

Table 6 HEC-RAS model performance evaluation calibration

Remarks	Statistical Criterion			
	NSE	RSR	R^2	PBIAS
Very Good	0.65<NSE≤1.00	0.00<RSR≤0.60	0.65<R^2≤1.00	PBIAS<±15
Good	0.55<NSE≤0.65	0.60<RSR≤0.70	0.55<R^2≤0.65	±15≤PBIAS<±20
Satisfactory	0.40<NSE≤0.55	0.70<RSR≤0.80	0.40< R2≤0.55	±20≤ PBIAS<±30
Unsatisfactory	NSE≤0.40	RSR>0.80	R^2 ≤0.40	PBIAS≥±30

Note:
NSE = Nash-Sutcliffe efficiency
RSR = Observed Standard Deviation Ratio
R^2 = Coefficient of Determination
PBIAS = Percent bias

5. Data on Flood MODIS Observation

This study used the following Project Summary MODIS Product README (https://floodmap.modaps.eosdis.nasa.gov). MODIS products flood extent the best surface spectral-reflectance data over 14 days, with the least effects from

atmospheric water vapor (NASA organization). This study involved an analysis of MODIS14-day composite data acquired modified such as 2011 Aug 28, 2013, Oct 26, 2017, Aug 14, and 2018 Aug, 31. The spatial distribution of the start dates varied year by year. Although there is a limitation that spatial resolution becomes coarser than Landsat, the time series MODIS data could be used to determine these dates to the nearest week and to map the spatial extent of a flood. The MODIS flood product is supplied annually, and it covers land areas with a 500 m spatial resolution. The default projection of original MODIS data is a MODIS sinusoidal tiling system. The default projection of original MODIS data is a MODIS sinusoidal tiling system as like Ahamed and Bolten (2017) and Vichet et al. (2019).

With the ArcGIS Spatial Analyst extension, the Multivariate toolset provides tools for both supervised and unsupervised classification. The Image Classification toolbar provides a user-friendly environment for creating training samples and signature files used in supervised classification. The Maximum Likelihood Classification Tool is the main classification method. A signature file, which identifies the classes and their statistics, is a required input to this tool.

6. Flood Modeling and Hazard Mapping

Water discharge relationships were used as boundary conditions downstream and upstream of the model (determined using the reference model). To avoid boundary condition influences, the section of the reach considered for the construction of the different return periods was much longer than the area of interest. Once satisfactory calibration data is seldom available for inundation models, the different return periods here were calibration by using measurements at a single point which is the normal practice. Finally, we performed, for each modeling flood return period, steady-flow simulations four hypothetical flood events: 10, 20, 50, and 100-year return period flood events. The HEC-RAS Mapper floodplain delineation capabilities (HEC, 2018) were used to construct flood hazard maps issues of the HEC-RAS 1-D simulation. The available DEM was used for the interpolation of the calculated flood-stage. We used ArcGIS 10.5 to process the results of the simulations performed with resolution 30 meters.

Data Usage for Applies to this Research

Flood frequency analysis of 10, 20 50, 100 years return period was calculated by the model input type of methods. This program intended to assist in the frequency analysis of discharge data. The procedures used are based on semi-graphical methods. Similarly, floods of different return periods were calculated using the GIS method. Software ArcGIS 10.5 is used for analysis and clarification of GIS data. All the statistical data was entered and analyzed using Microsoft Excel 2019 and Easyfit software.

Table 7 Data usage in the research study

Data	Detail	Sources
DEM	Resolution 30m x 30m	USGS Earth Explorer
Water Discharge	30 years (1989-2018)	Ministry of Water Resource and Meteorology
Water bodies	09/08/2016	Open Development Cambodia
MODIS Observed	2011, 2013, 2017, and 2018	https://floodmap.modaps.eosdis.nasa.gov
Water Level	10 years (2008–2017)	Mekong River Commission (MRC)
Google Satellite	The year 2019	Map Layer RAS-Mapper Version 5.0.7
Cross Section (100XS)	KC (Upstream) to CC (Downstream)	RAS-Mapper Version 5.0.7

CHAPTER IV

RESULTS AND DISCUSSION

Flood Frequency Analysis

Flood frequency analysis is a statistical measure for sympathetic the hydrological behavior of rivers and the most common technique used for estimation of flood magnitude (Farooq et al., 2018; Bhat et al., 2019). The study involves exploring the annual peak discharge to calculate statistical information such as average values, median standard deviation (SD), kurtosis, skewness minimum (Min.), and maximum (Max.). The statistical attributes are then used to construct frequency distributions, revealing the probability of various discharges as a function of recurrence interval or exceedance probability. The calculation of data for the derivation of expected water discharge for all floods with various return periods (10, 20, 50, and 100-year) are shown in **Tables 9 and 10**. The flood frequency analysis and corresponding water discharge magnitudes of various floods derived through Log-Pearson type III, Log-Normal, Normal, and Gumbel distribution for both gauging stations (Kampong Cam and Chruy Changvar) are comprehended in **Figure 17 and 18**. As the results indicated that all flood frequency analysis used for this study are increasing order 10, 20, 50, and 100-year return period. According to (Gao et al., 2017; Kasiviswanathan et al., 2017), increasing water discharge events are importance to studies characterizing of floods. For example, flood frequency analysis (FFA) shows a critical to design of large hydraulic structures (e.g., dams, reservoirs, and levees) and civil structures across streams (e.g., highways, culverts, and bridges). FFA is an important tool for water resources management and water structure design.

1. Estimation of MFD by Four Probability Distributions

The discharge averages of the calculated data are 43069 and 35733, standard deviation (6482 and 3538), kurtosis (-0.77 and 0.16), and skewness (-0.40 and -0.88) for Kampong Cham and Chruy Changvar gauging stations respectively show details in **Table 8,** below.

Table 8 Descriptive data at Kampong Cam and Chruy Changvar station

Station	Average	Median	SD	Kurtosis	Skewness	Min.	Max.
KC	43069	43520	6482	-0.77	-0.400	29491	51919
CC	35733	36542	3538	0.164	-0.887	27402	40556

Flood hazard maps for the different return periods of 10, 20, 50, and 100-year are produced using the peak water discharge over the last 30 years (1989-2018). The peak water discharges of upstream and downstream in a multi return period are obtained using four technical analyses: Log-Pearson type III, Log-Normal, Normal, and the Gumbel distribution. The calculation of parameters for the derivation of expected discharge for all floods with various return periods (10, 20, 50, and 100-years) are presented in **Table 10** (Kampong Cham upstream) and **Table 11** (Chruy Changvar downstream).

Table 9 Flood frequency analysis of upstream Kampong Cham station

Return Period (Years)	Peak Discharge in Deference Distribution at KC Station (m^3/s)			
	Log-Pearson III	Log-Normal	Normal	Gumbel
10	52208	50701	50242	51523
20	54990	55158	53698	55160
50	59381	57459	55376	59869
100	62194	61510	58171	63397

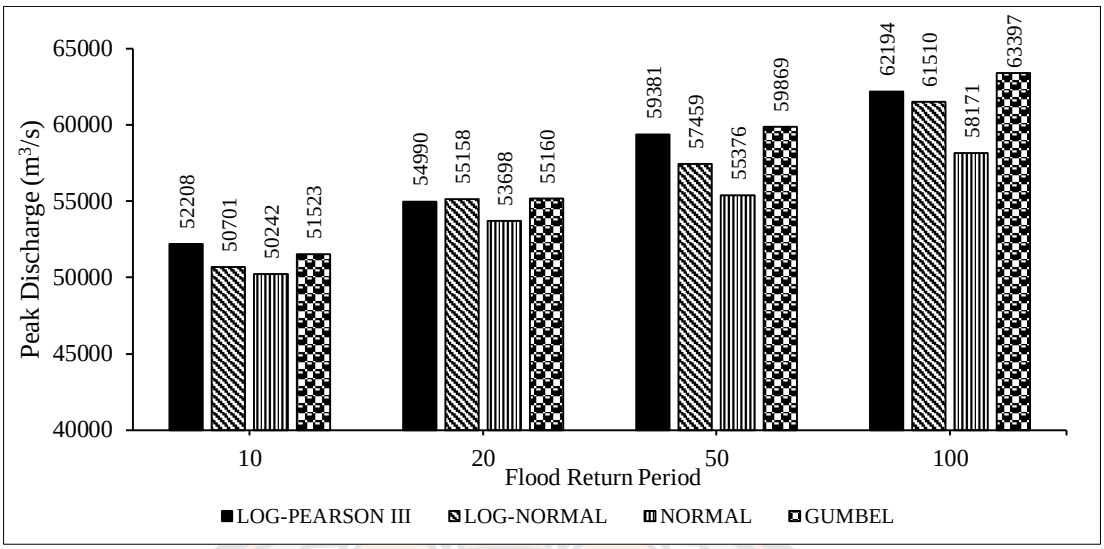

Figure 16 Plots MFD estimates for different return periods at KC station

Table 10 Flood frequency analysis of downstream Chrung Changvar station

Return Period (Years)	Peak discharge of deference distribution at CC Station (m^3/s)			
	Log-Pearson III	Log-Normal	Normal	Gumbel
10	40681	39902	39648	40348
25	42100	42185	41535	42333
50	44292	43340	42451	44904
100	45666	45334	43977	46830

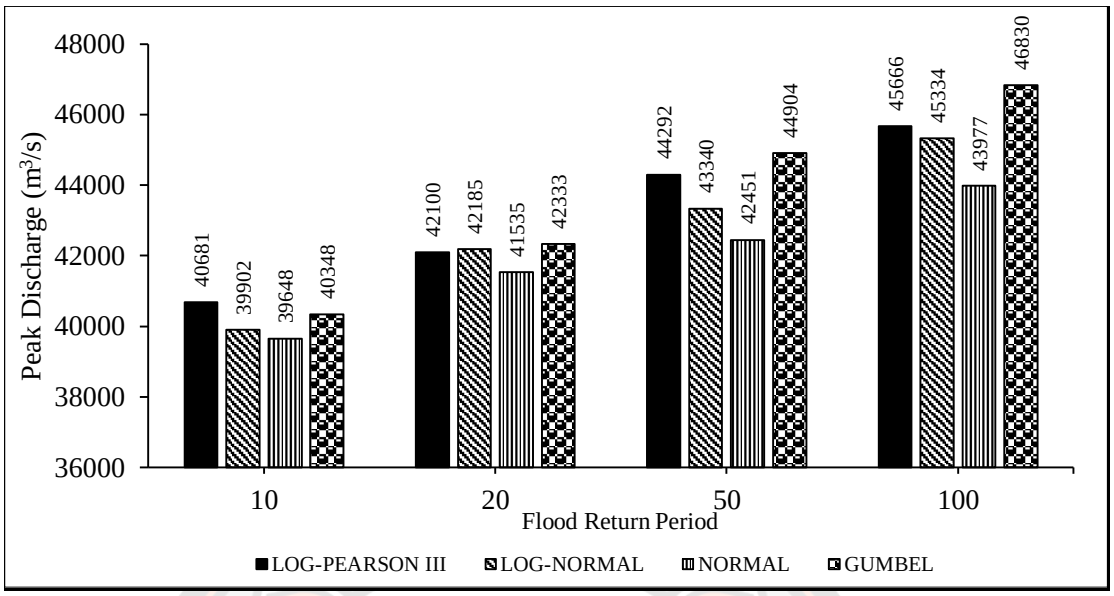

Figure 17 Plots MFD estimates for different return periods for CC station

Flood frequency analysis is important for flood-prone rivers like at the Mekong River in Cambodia. Hence, the estimation of peak flood discharge at the desired location is essential for planning, design, and management of hydraulic structures (Vivekanandan, 2015). Historical reports reveal that the Lower Mekong River witnessed a series of floods over centuries and many among them have resulted in widespread destruction. Flooding has been a recurrent phenomenon in the Lower Mekong River. In the literature review, a few notable flood events of the recent past are those of 1978, 1991, 1994, 1996, 2000, 2001, 2002, 2011, and 2013 (CFE-DM, 2017; MRC, 2018). In Cambodia, floods are among the most devastating of the recurring natural hazards. Flood hazard assessment requires flood event magnitude and the probability of occurrence. Flood frequency analysis is the most common technique used for the at-site estimation of flood recurrence magnitude.

2. The Goodness of Fit by Easyfit Software

Flood frequency analysis based on Easyfit Software is for the selection of the best distribution to estimate the magnitude of water discharge. The goodness of fit tests can be used in flood frequency analysis to compare different methods to assess the probability distribution technique (Orsini-Zegada & Escalante-Sandoval, 2016; Farooq et al., 2018).

Table 11 Distribution fitting parameters for LP3, LN, Normal and Gumbel

N°	Distribution	Kampong Cham (Upstream)		Chruy Changvar (Downstream)	
1	Log-Pearson III	a=9.1078, b=-0.0523, g=11.14		a=3.3471, b=-0.0570, g=10.67	
2	Log-Normal	s=0.1553	m=10.66	s=0.1025	m=10.4787
3	Normal	s=6481.59	m=43068.63	s=3538.25	m=35732.60
4	Gumbel Max	s=5053.68	m=40151.56	s=2758.76	m=34140.19

Table 12 Goodness of Fit for Kampong Cham (Upstream) Station

Distribution	Kolmogorov		Anderson		Chi-Squared	
	Statistic	Rank	Statistic	Rank	Statistic	Rank
Log-Pearson III	0.0933	1	0.3371	1	0.2096	1
Normal	0.1053	2	0.4226	2	0.5162	2
Log-Normal	0.1096	3	0.5972	3	2.0160	3
Gumbel	0.1419	4	1.4984	4	3.6242	4

Table 13 Goodness of fit for Chruy Changvar (Downstream) station

Distribution	Kolmogorov		Anderson		Chi-Squared	
	Statistic	Rank	Statistic	Rank	Statistic	Rank
Log-Pearson III	0.0902	1	0.2656	1	0.8801	1
Normal	0.1391	2	0.7468	2	2.2385	2
Log-Normal	0.1603	3	1.0036	3	5.9584	4
Gumbel	0.2048	4	2.6707	4	2.5205	3

The probability-probability (P-P) plot is a graph of the empirical CDF values plotted against the theoretical CDF values. It is used to determine how well a specific distribution fits the observed data. This plot will be approximately linear if the specified theoretical distribution is the correct model. Probability distribution functions (PDF) and cumulative distribution functions (CDF) of the gauge station are given in **Figure 18**. PDF and CDF of LP3 and Normal distributions fit best with the

observed data while Gumbel Max and Log-Normal distributions fit poorly. Moreover, **Figure 18**. shows that LP3 is the best fit distribution at Kampong Cham and Chruy Changvar gauge station and could be used for flood recurrence calculation. The best fit at Kampong Cham and Chruy Changvar gauge stations followed by LP3 see in **Tables 12 and 13**.

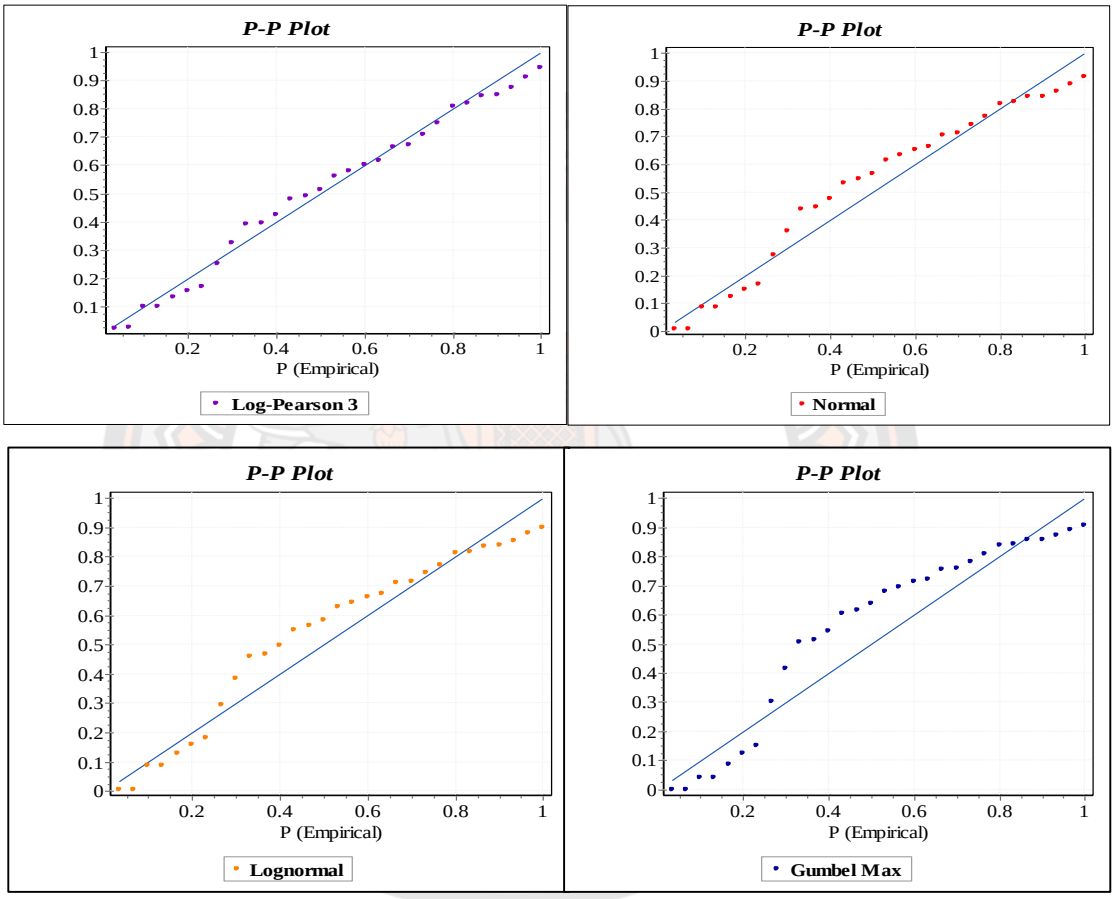

Figure 18 Plot delineation analysis best fit of the difference distribution

Fitting parameters of the LP3, LN, Normal, and Gumbel distributions are giving in **Tables 12 and 13**. Calculated parameters are within the limits of the statistics. For the selection of best-fit distributions, we applied Kolmogorov–Smirnov, Anderson, and Chi-squared tests in Easyfit software. The results are given in **Tables 12 and 13**. Kolmogorov and Anderson goodness-of-fit for the given data of Kampong Cham **(Table 12)** are ranking LP3 value 1, Normal value 2, Log-Normal value 3, and Gumbel value 4. However, the chi-squared test is ranking LP3 and Normal

distributions at 1 and 2, respectively. Likewise, all four goodness-of-fit for the given data of Kampong Cham station **(Table 12)** is ranking LP3 value 1, by Kolmogorov by Anderson–Darling and chi-square. At the Chruy Changvar downstream **(Table 13),** Kolmogorov–Smirnov is ranking LP3 value 1 and Normal value 2 as within Anderson and chi-squared analysis are ranking the same Kampong Cham station.

Overall, flood frequency analysis is an available approach to estimate the long-term flow behavior at the lower Mekong River. On the other hand, the previous research (Wan Deraman et al., 2017; Farooq et al., 2018; Bhat et al., 2019; Wu et al., 2019) are the most commonly apply many distribution analysis. Hence, the resulting study demonstrates that the river discharge can be satisfactorily projected by anyone of the used probability distribution methods; however, as revealed by the goodness-of-fit test, Pearson type III has been found to be the best-fit probability of the four distribution tests as shown by (Bhat et al., 2019) and (Farooq et al., 2018) who used Log-Pearson type III distribution analysis along the river. As the results, best fit distribution, i.e., LP3 was used for calculation of return periods at the Lower Mekong River. Return periods at Kampong Cham gauge station will be used for the simulation of the 1-D flood model and then the flood hazard assessment which will work as a baseline for flood possibility development.

Model and Flood Hazard

The 1-D modeling is performed using the HEC-RAS version 5.0.7 which offered various output possibilities in terms of detailed animation and mapping of flood characteristics within the RAS mapper feature. Model validation told place during the short-term and long-term period for which data are available at downstream. The goodness of fit model simulation is calculated for these combined datasets and are summarized in **Figure 19.** The model calibration plot of observed flood discharge with the downstream model simulation for Chruy Changvar gauging station in **Tables 14 and 15.** According to the accuracy of model simulation, the study is following the calculation of 10, 20, 50, and 100-year return periods along the lower Mekong River, regarding the flood extent, water surface elevation, and flood depth is exported. The study considers both simulations such as short-term and long-term to

achieve model accuracy and model application to determine flood probability and frequency.

1. Short-Term Model Calibration (2011, 2013, 2017, and 2018)

In the study, HEC-RAS 5.0.7 was utilized for hydraulic analysis, and GIS 10.5 is used for mapping. First, the 1-D hydraulic model of the study area is prepared to utilize GIS. Digital Elevation Model (DEM) resolution 30m×30m is produced by USGS (https://earthexplorer.usgs.gov/) and prepared in ArcGIS projected coordination (WGS 1984 UTM Zone 48N). Then, DEM was transferred to RAS Mapper for the cross line along the river study area. Peak discharge at 30 years was used to validate flood frequency distribution and Normal standard Manning roughness coefficient values were entered into the HEC-RAS program for calculating.

The model calibration is carried out using the daily water discharge (downstream) the Chruy Changvar station 2011, 2013, 2017, and 2018, respectively. The daily discharge upstream station is extracted as the input for the boundary condition to simulate the flood inundation performance in the Lower Mekong River. The calibration period uses the annual peak flood recorded 2011, 2013, 2017, and 2018 with discharge available during this period at the downstream locations (Chruy Changvar) as shown in **Figures 19, 21, and 22**. Furthermore, the model calibration is evaluated simulation of the fit goodness using the Nash-Sutcliffe (NSE), RSR normalizes the Root Mean Squared Error (RSR), Correlation coefficient (R^2), and percent bias (PBIAS) equation.

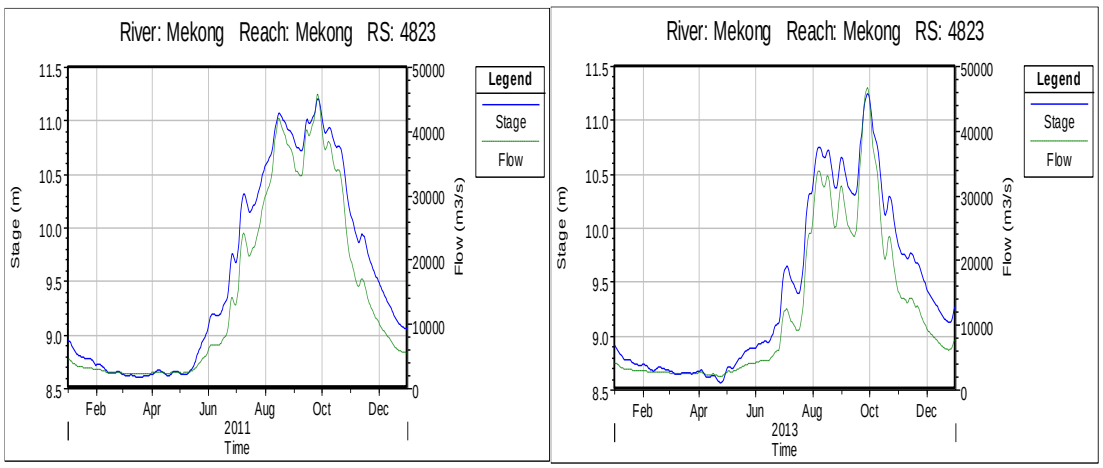

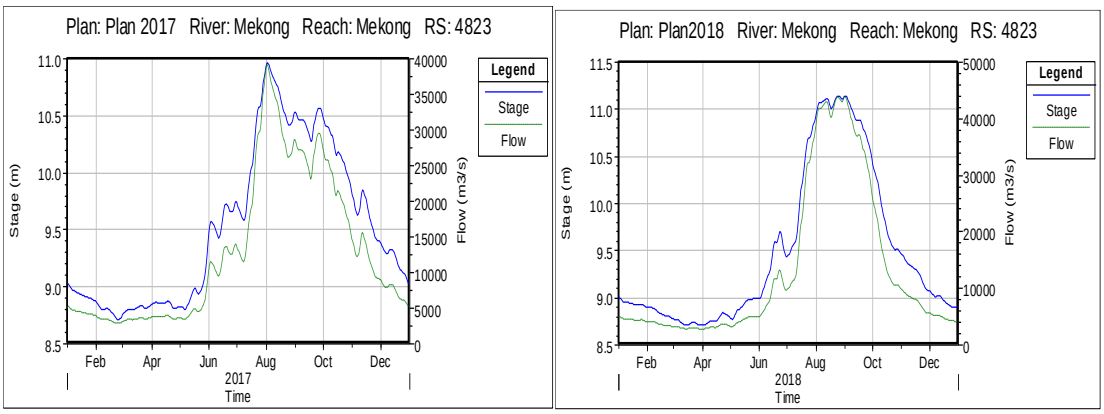

Figure 19 Stage and flow hydrograph plot simulation 2011, 2013, 2017, and 2018

The performance of water discharge simulation and downstream discharge observed is available as the NSE, RSR, R^2, and PBIAS values are 2011 (0.97, 0.16, 0.98, and -12), 2013 (0.96, 0.17, 0.97, and -5), 2017 (0.97, 0.16, 0.98, and -6), and 2018 (0.96, 0.19, 0.98, and -9) respectively (see **Table 14**).

Table 14 The 1-D HEC-RAS Model Calibration Short-Term

Downstream Station	Year Sim.	NSE	RSR	R^2	PBIAS (%)
Short-Term model simulation	2011	0.97	0.16	0.98	-12
	2013	0.96	0.17	0.97	-5
	2017	0.97	0.16	0.98	-6
	2018	0.96	0.19	0.98	-9

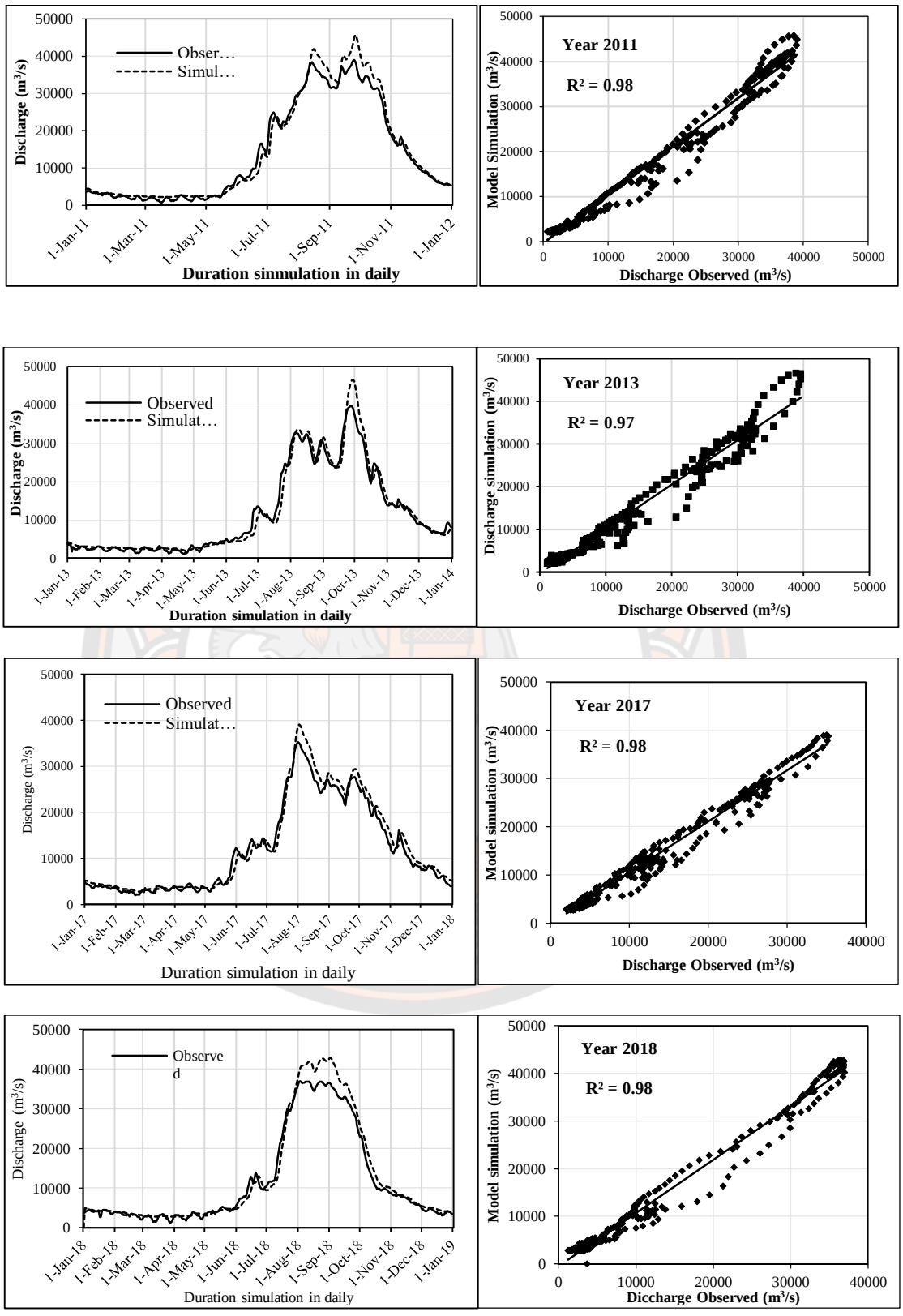

Figure 20 Model simulation at the downstream (2011, 2013, 2017, and 2018)

2. Long-Term Model Calibration (15 and 30 Years)

Accuracy purposes, the 1-D water discharge test simulation is computed to the HEC-RAS model. The data needs for this flow accuracy assessment input consisted of average discharge values at the upstream gauging station for the long-term as 15 years and 30 years see the output in **Figure 21 and Figure 22**. The performance evaluates the fit goodness of simulation as the NSE, RSR, R^2, and PBIAS values are 15 years (0.97, 0.15, 0.97, and -6) and 30 years (0.96, 0.16, 0.97, and -5) respectively show in **Table 15.**

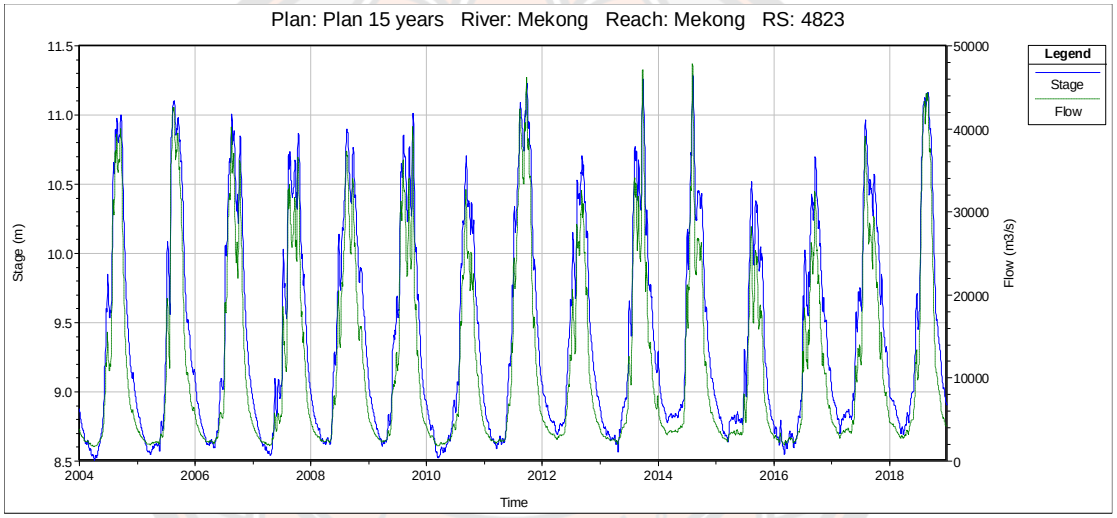

Figure 21 Stage and flow hydrograph plot simulation 15 years (2004 -2018)

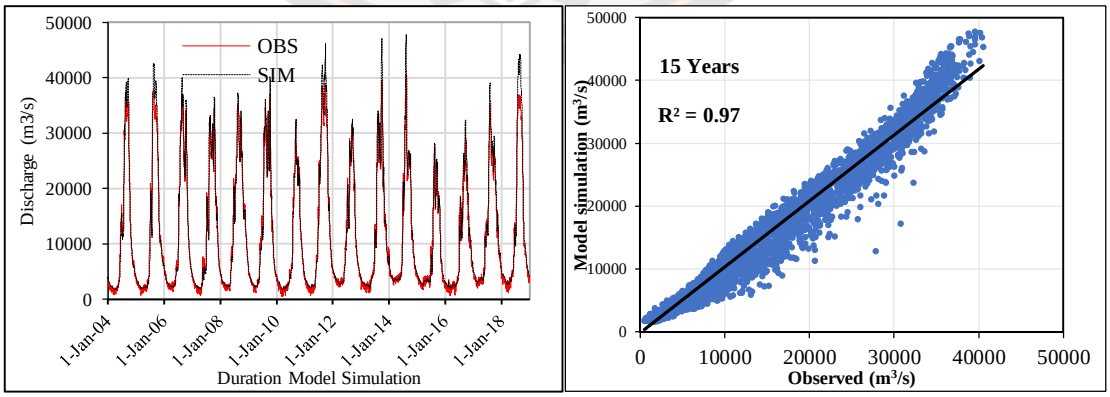

Figure 22 Model calibration and Correlation coefficient (R^2) (2004-2018)

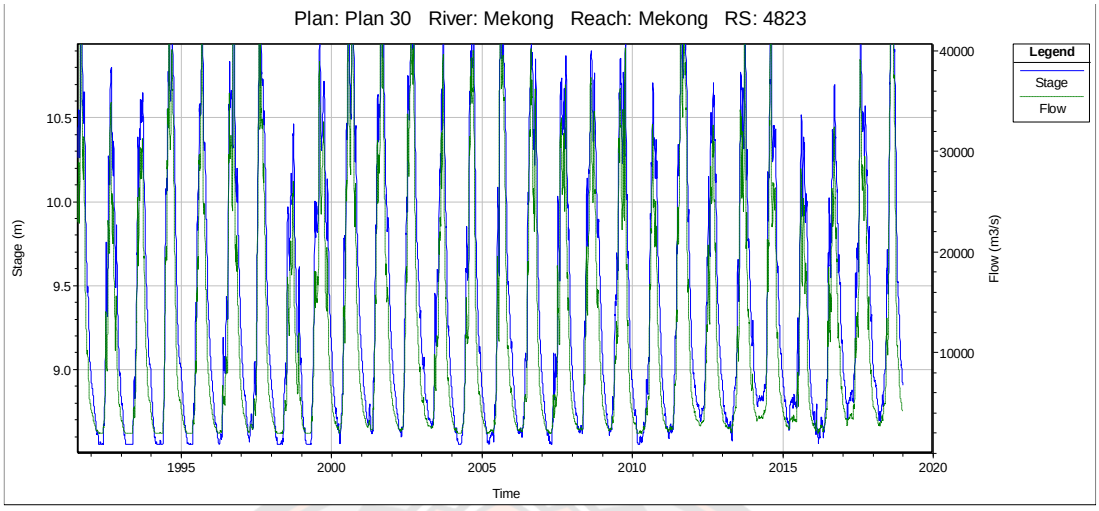

Figure 23 Stage and flow hydrograph plot simulation 30 years (1989-2018)

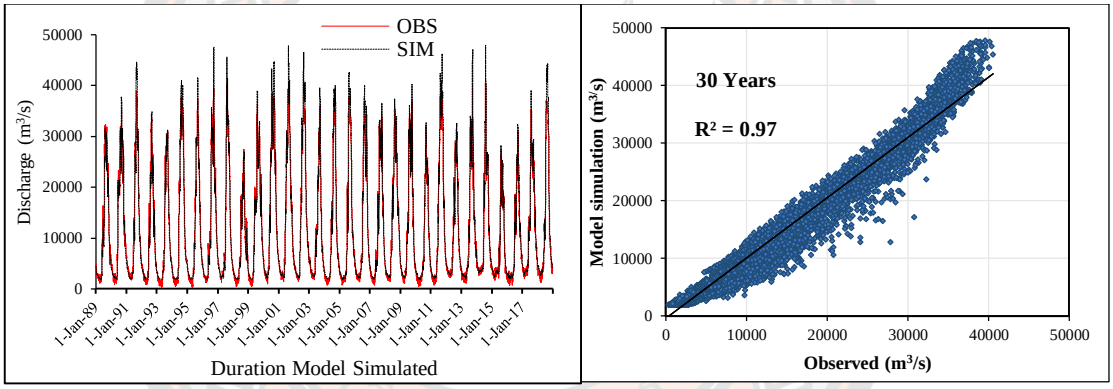

Figure 24 Model calibration and Correlation coefficient (R^2) (2004-2018)

Table 15 Summary statistics for the 1-D HEC-RAS model calibration

Downstream Station	Year Sim.	NSE	RSR	R^2	PBIA (%)
Long-Term Model Simulation	15 Years	0.97	0.15	0.97	-6
	30 Years	0.96	0.16	0.97	-5

The performance rating in the HEC-RAS model, the fit value short-term, and long-term simulation are satisfied respectively. Moreover, the value of RSE, RSR, R^2, and PBIAS gave the value short-term and long-term simulation show in **Tables 15 and 16**. Thus, it evidences that the effectiveness of the HEC-RAS model

can be simulated and provided a satisfying result. As a result, HEC-RAS modeling could give an effective output to both affected area and flood depth.

Table 16 Summary statistic of model simulation (Average, Standard Dev., Max)

Years	Average			Standard Dev.			Maximum		
	OBS.	**SIM.**	**%**	**OBS.**	**SIM.**	**%**	**OBS.**	**SIM.**	**%**
2011	14051	14734	5	12981	14047	8	39023	45673	17
2013	11832	11989	1	11055	11692	6	39612	46583	18
2017	12072	12719	5	9598	10261	7	35243	39084	11
2018	11832	12767	8	11813	13259	12	36928	42844	16
15 year	11061	11427	3	11364	12131	7	36144	40002	11
30 year	11681	11829	1	10784	11408	6	40556	47820	18

Note: % = Percentage difference of Observed **(OBS.)** and Simulation **(SIM.)**

3. Flood Extent of Model Simulation and MODIS Observation

According to Ahamed and Bolten (2017), critical flood events in the lower Mekong River occurred in 2000, 2011, 2013, and 2016 causing common loss of life, significantly damaged property livelihoods. Hence heavy rains starting in October, caused these impressive floods along the Mekong River and the Tonle Sap in Cambodia (Chung et al., 2019). The Moderate Resolution Imaging Spectroradiometer (MODIS) on NASA's Terra satellite captured duration 14 days recorded image such as 2011 (10-24, October), 2013 (12-26, October), 2017 (1-14, August), and 2018 (17-31, August) are available recorded flood extent at the case study area by international satellite (NASA). The annual peak flood extent in the HEC-RAS model simulation during 2011, 2013, 2017 and 2018 are compared with the MODIS flood (NASA) observation dataset **(Figure 27).** According to the performance spatial inundation extent in Table 17, the HEC-RAS model simulated the flood extent with differences of 0.01% in 2011, 0.26% in 2013, 0.14% in 2017, and 0.26% in 2018.

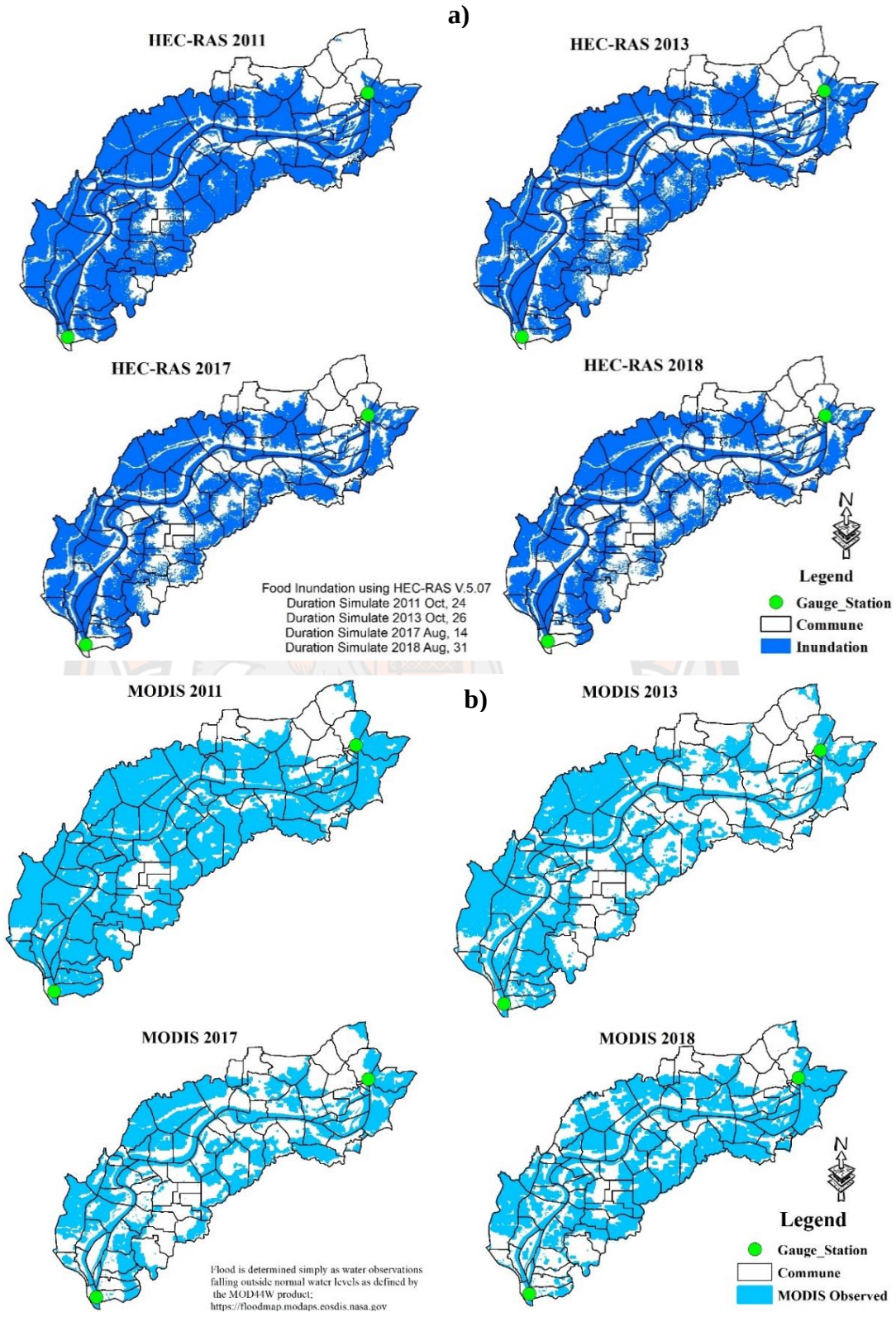

Figure 25 a) Model simulation and b) MODIS flood observed at specifics date

Table 17 Model simulation of flood extent and MODIS flood extent observed

Year	MODIS Flood Extent	Model Simulation	Difference Area (%)
2011	1410 km^2	1420 km^2	0.01
2013	1004 km^2	1262 km^2	0.26
2017	1005 km^2	1145 km^2	0.14
2018	857 km^2	1082 km^2	0.26

Flood Return Period

1. Performance Model Simulation of Flood Return Period

The HEC-RAS hydraulic modeling for the Lower Mekong River is performed using the USACE Hydrologic Engineering Centre's River Analysis System (HEC-RAS) version 5.0.7 for performing 1-D steady flow analysis. Which input cross-section plots generated from upstream to downstream, the available flood return period for 10, 20, 50, and 100-year profiles up to the downstream area as shown in **Figure 26**.

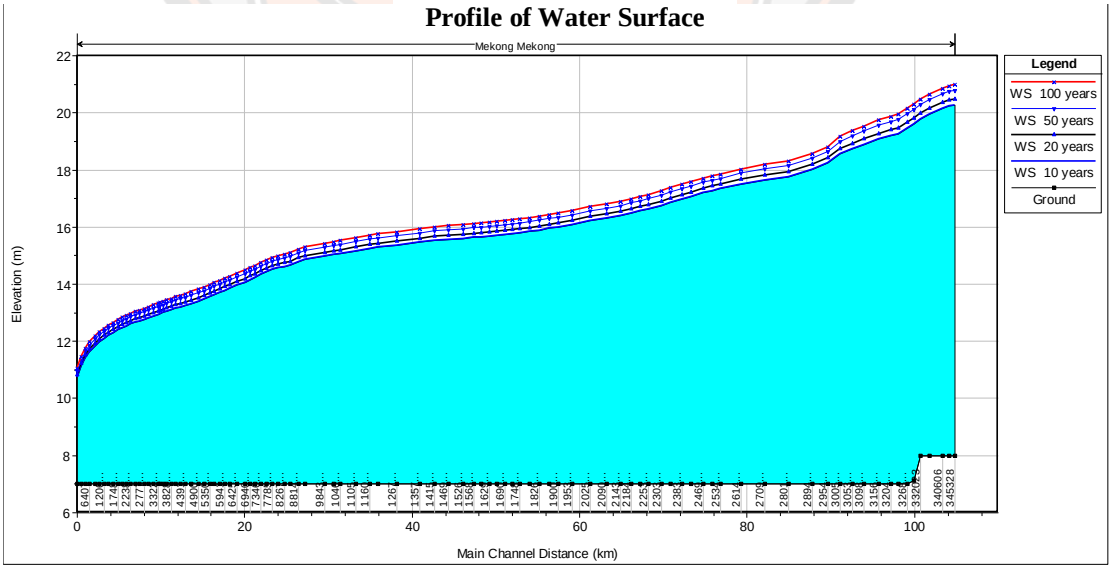

Figure 26 Water surface of flood return period 10, 20, 50, and 100-year

The results of model sensitivity to changes in selected parameters are reported in **Table 3**. To estimate relative sensitivity of roughness coefficients (**Manning's n**) for main channel 0.035 and right 0.06 and left 0.06 banks of floodplains were varied in the **Manning's n** computed values according to the normal standard.

F**igure 27** is presenting the distance discharge along the channel study river.

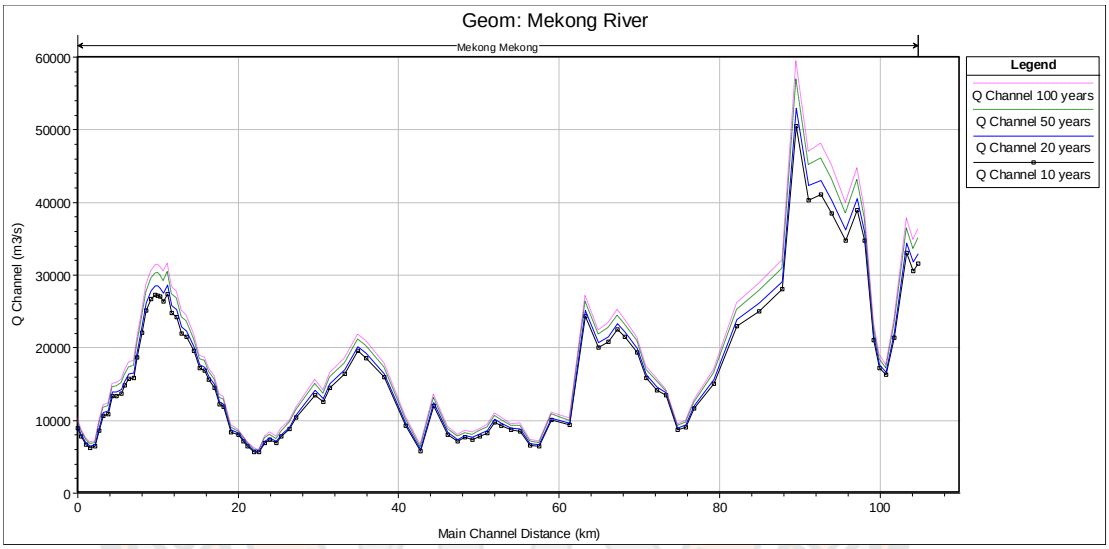

Figure 27 Discharge at the channel of model simulation 10, 20, 50, and 100-year

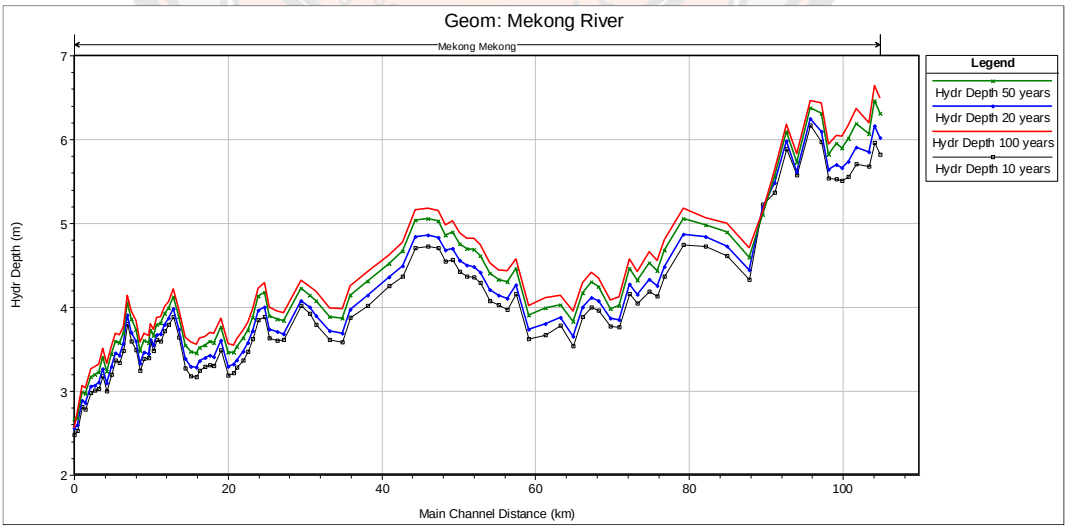

Figure 28 Hydrology depth of model simulation during 10, 20, 50, and 100-year

Overall, the simulation of the HEC-RAR model has indicated the hydrology depth and the water discharge along the channel in order to increase the most difference value. According to the three cross-sections, which are the water surface elevation (W.S.E), water discharge Q (channel, right, and left), and depth of the water in the channel of the river.

Table 18 Results from HEC-RAS showing water depths and water surface

Cross Station	Return Period (year)	W.S Elev. (m)	Q at Channel (m^3/s)	Q at the Right (m^3/s)	Q at the Left (m^3/s)	Channel Depth (m)
RS 345328 (Upstream)	10	20.27	31638.62	5699.64	14869.74	12.27
	20	20.48	32935.66	6113.22	15941.13	12.48
	50	20.80	35048.93	6790.32	17541.75	12.80
	100	20.98	36339.94	7212.68	18641.40	12.98
RS 116083 (Centre)	10	15.25	19571.83	18604.43	14034.73	8.25
	20	15.37	20195.20	19634.23	15160.57	8.37
	50	15.57	21184.49	21286.15	16910.36	8.57
	100	15.70	21807.19	22309.97	18076.85	8.70
RS 4823 (Downstream)	10	11.43	6645.77	3216.24	42346	4.43
	20	11.52	6907.3	3420.36	44662.32	4.52
	50	11.70	7315.70	3749.65	48315.64	4.66
	100	11.80	7563.54	3981.97	50648.69	4.76

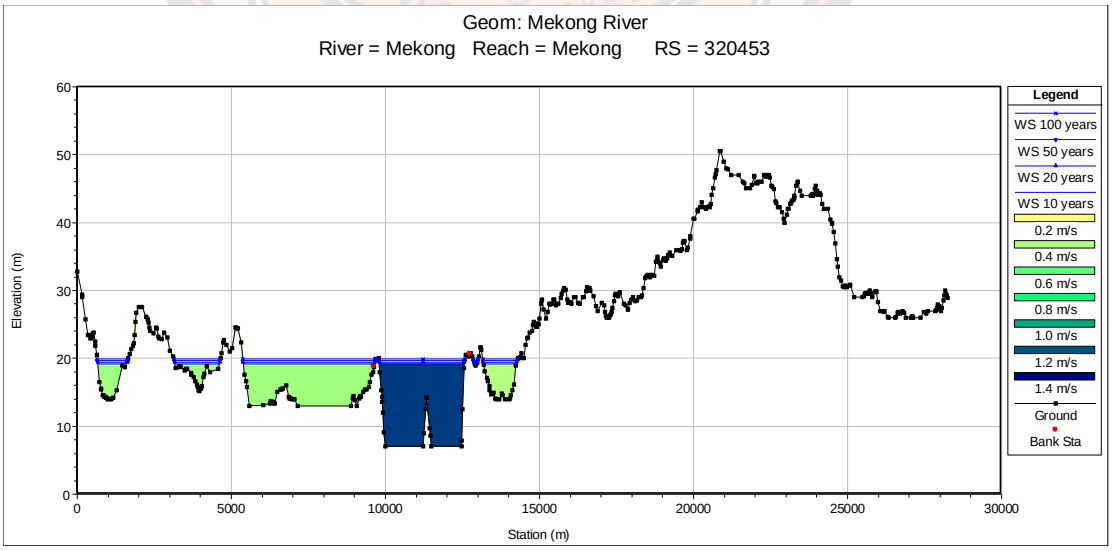

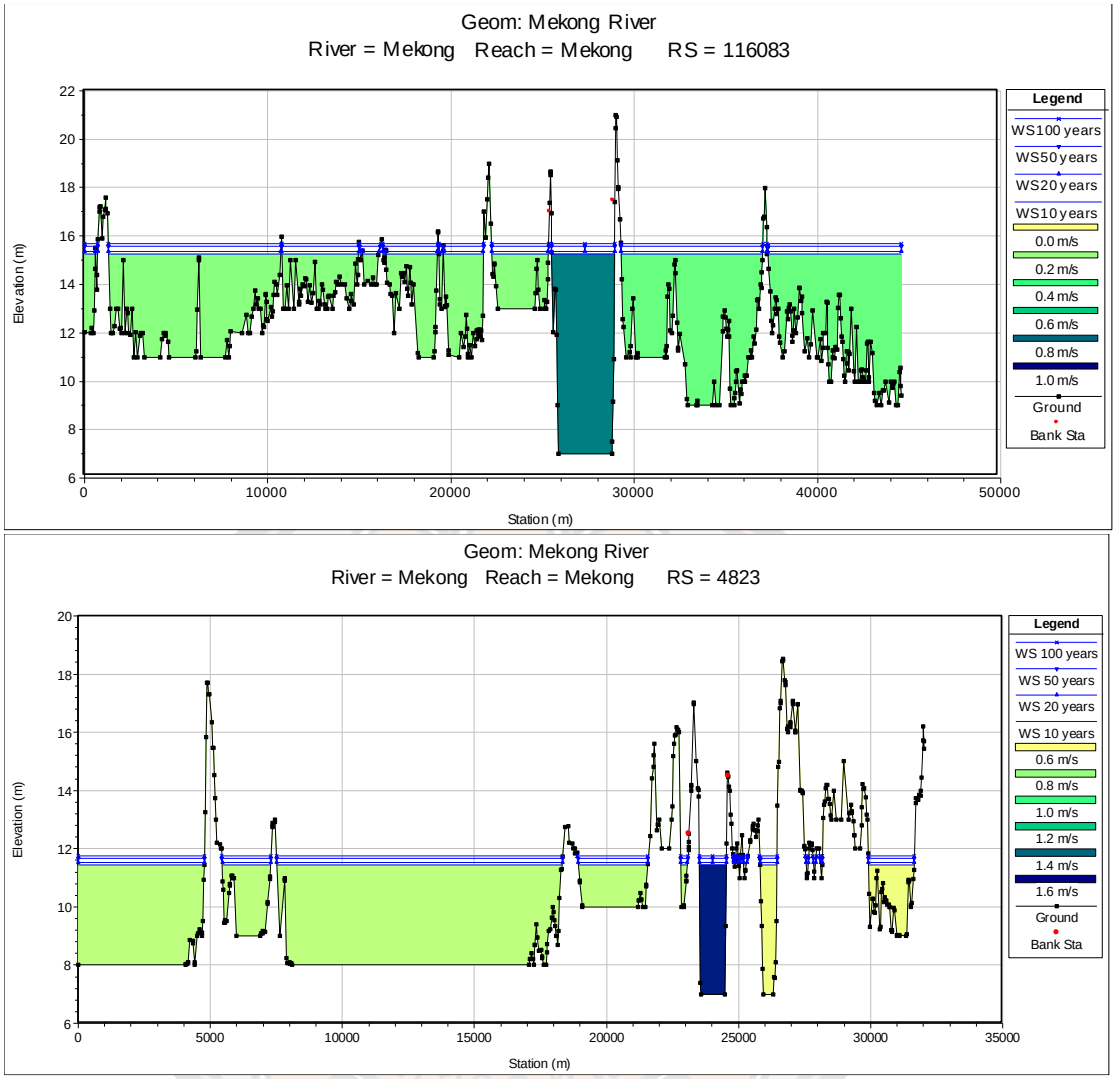

Figure 29 Water surface in cross-section (RS=1515, RS=116083, and RS=4823)

2. Flood Extent

The flood extent layer consists of an inundation boundary shapefile vector layer capturing the areas affected by the flood during the multi-return period of 10, 20, 50, and 100-year. This section discusses the sensitivity of flood mapping results as a function of the applied solution scheme using default model parameters. The result shows the simulated flood inundation maps of the flood event with a return period of 10, 20, 50, and 100-year, and the reference flood inundation map used for evaluation is presented in **Figure 30**. The flood extent layer consists of an inundation Boundary shape file vector layer capturing the areas affected by the flood during the

whole day simulation period. As a result, the model simulation of flood extent in 10, 20, 50, and 100-year return period are showing the total area as 1568 km^2, 1578 km^2, 1591 km^2, and 1599 km^2. Altogether, in the first increase of flood extent return periods (10 and 20-year), the flood extent increases only 10 km^2 and increase 8 km^2 in the last two.

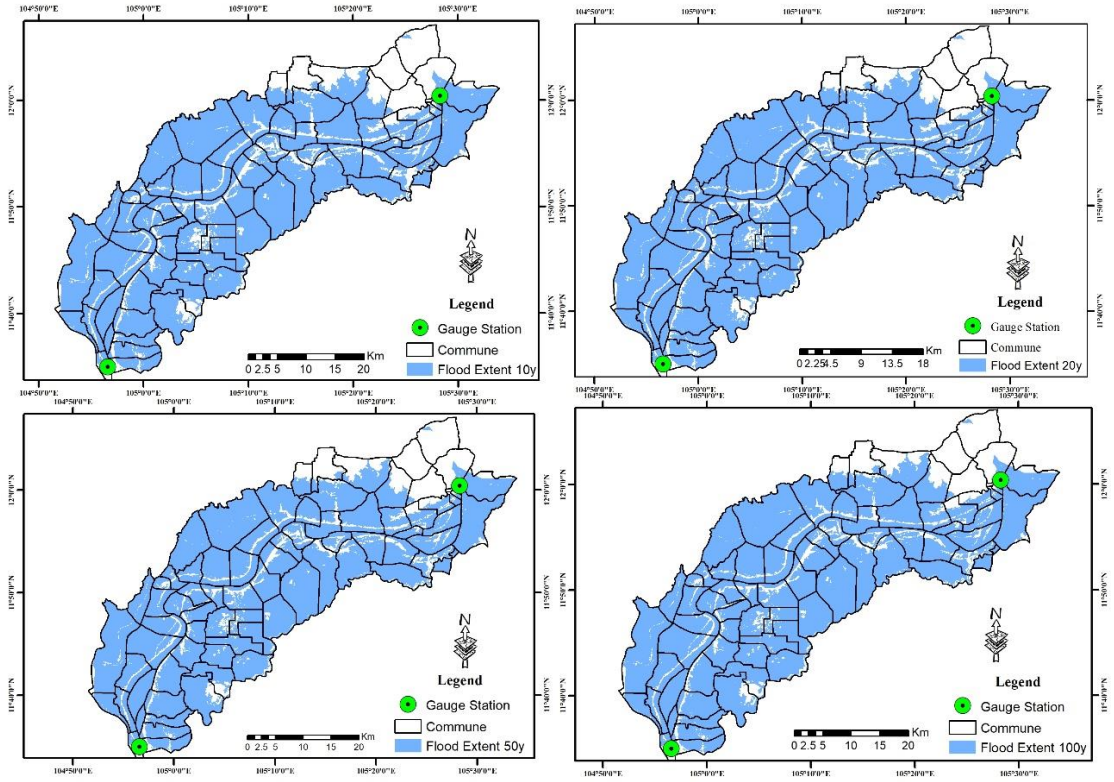

Figure 30 Flood extent of the multi return period 10, 20, 50, and 100-year

3. Flood Depth

The maximum flood depth maps are generated by the 1-D model by taking into consideration the maximum depth for the multi return period. According to the model simulation, the flood return period of 10, 20, 50, 100-year are integrated depth value as 12.86 m, 13.10 m, 13.46 m, and 13.69 m. Based on the flood early warning system along the lower Mekong River remark by MRC shows that the upstream station (Kampong Cham) has been alarmed at 15.2 m and flooding at 16.2 m but the downstream (Chruy Changvar) has been alarmed at 10.5 m and flooding at 12

m, so the results indicated upstream are still stable but the downstream results are affected by the rainy season. According to (Okazumi et al., 2013; CFE-DM, 2017; Sarann et al., 2018) indicated the lower Mekong River in Cambodia, is significantly affecting agriculture and properties at the floodplain area.

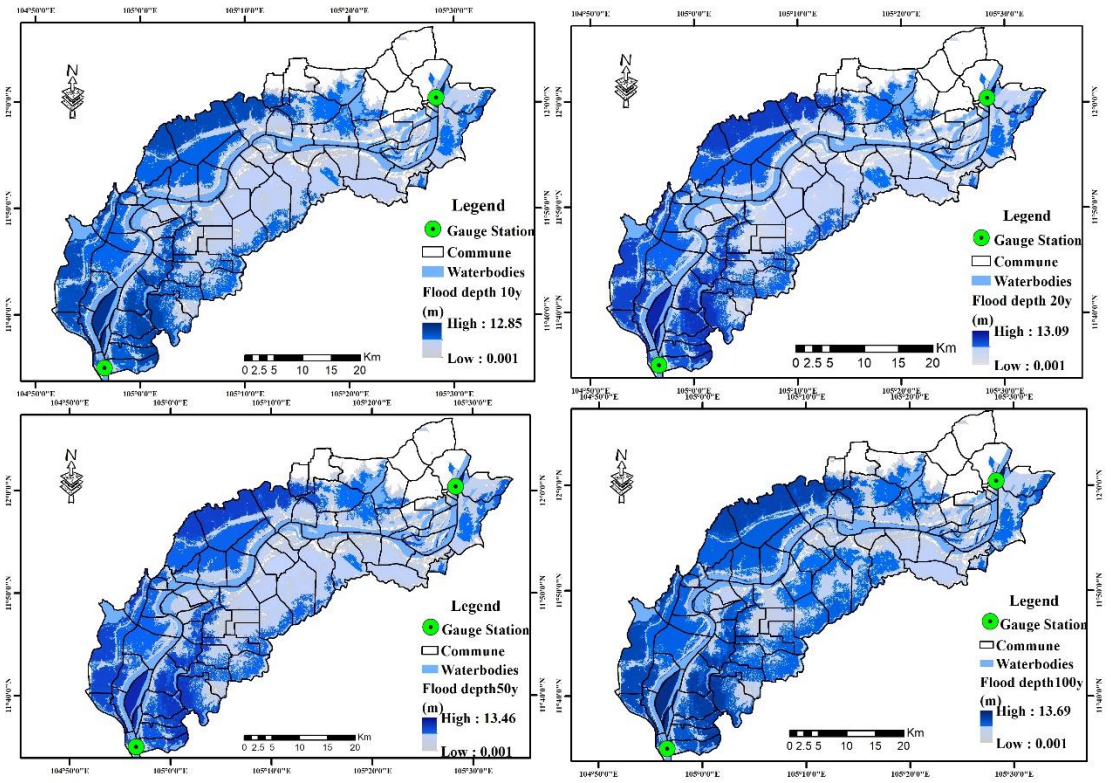

Figure 31 Flood depth of the multi return period 10, 20, 50, and 100-year

Flood Hazard Map

Generally, the flood hazard assessment is based on a quantifiable variable like flood extent, water velocity, or water depth, and indicates the vulnerability of built-up areas to hydrological events with possible destructive impact. In this research, we provided the flood hazard assessment using only the flood extent and flood depth resulting from the four-return period (10, 20, 50, and 100-year) of HEC-RAS 1-D. The generated flood hazard categories of water depth for each flood extent was classified according to the Cambodian criteria of the Ministry of Water Resources and Meteorology as shown in **Figure 32**.

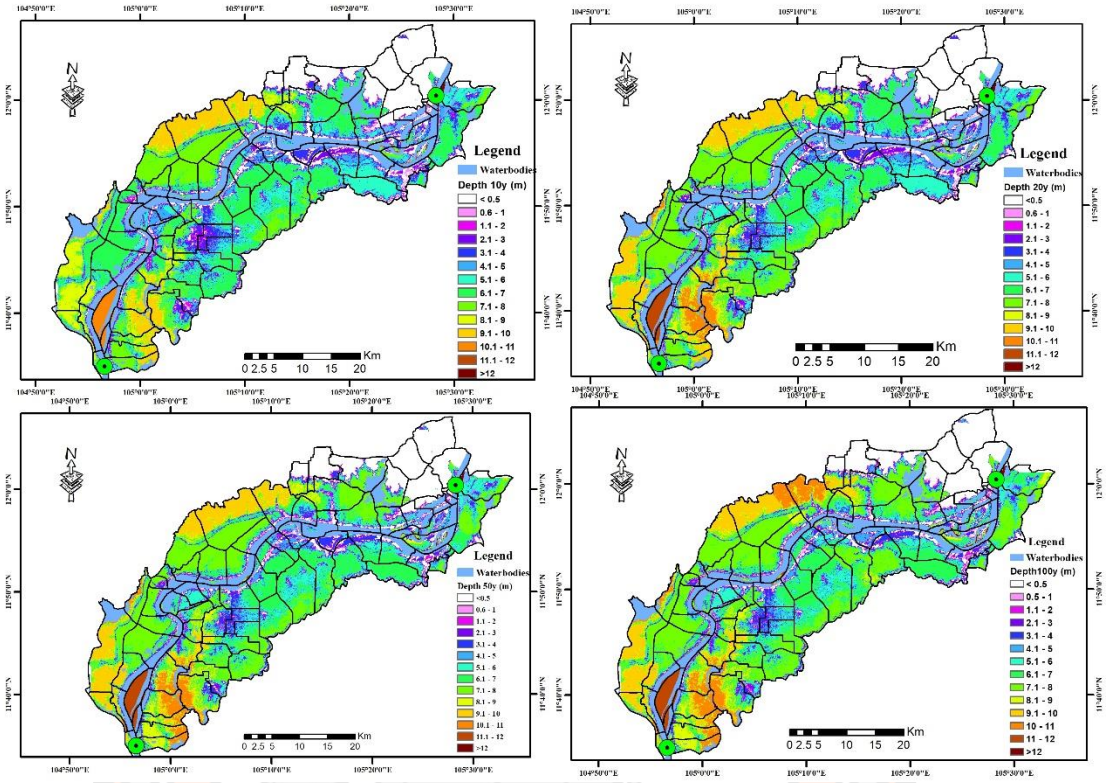

Figure 32 Flood hazard map based on depth classification of the return period

Table 19 Flood depth on the classification of the multi return period

Depth Classify (m)	10-year	20-year	50-year	100-year
<0.5	21	20	14	18
(0.5-1)	20	17	22	19
(1.1-2)	49	42	43	43
(2.1-3)	68	60	53	51
(3.1-4)	92	83	82	74
(4.1-5)	145	124	109	107
(5.1-6)	225	214	184	173
(6.1-7)	417	308	287	267
(7.1-8)	214	337	404	439
(8.1-9)	109	80	93	99

Table 20 (cont.)

Depth Classify (m)	10-year	20-year	50-year	100-year
(9.1-10)	141	165	159	145
(10.1-11)	77	67	69	97
(11.1-12)	77	140	130	108
>12	21	27	45	66

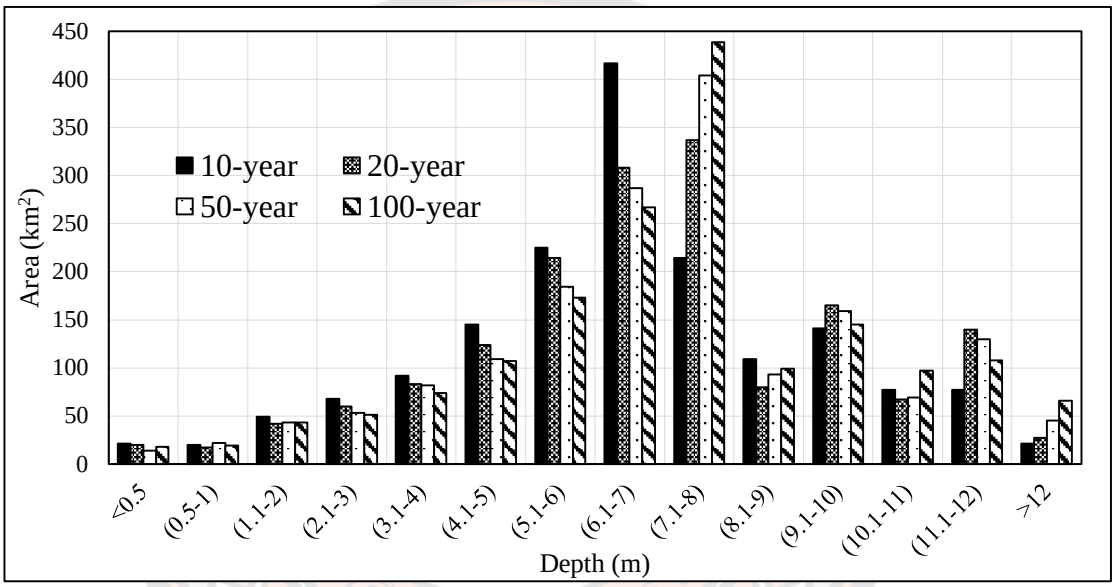

Figure 33 Flood hazard area based on classification depth in the return period

Table 20 Summary of the flood extent and the maximum flood depth

Return Period	Flood area (km^2)	Area difference (%)	Max. flood depth (m)	Depth difference (%)
10-year	1677	_	12.86	_
20-year	1685	0.47	13.10	1.87
50-year	1697	0.71	13.46	2.74
100-year	1707	0.59	13.69	1.71

To calibrate the HEC-RAS hydraulic model, the discharge values for the 10, 20, 50, and 100-year return periods and flood events are entered in the model for

flood hazard mapping. The results of mapping for 10, 20, 50, and 100-year return period flood events are shown in **Figure 31** respectively. The total inundation area and the peak flood depth for each return period flood event are summarized in **Table 20**. It is seen that the difference in the flood area is decreased when the return period is increased while the difference in depth is increased. This implies that the increase of discharge has more effect in the increase of flood depth than the increase of flood extent. This may because of the characteristic of flood area that it was surrounded by mountains so that the flood is limited in a horizontal direction but is not limited in a vertical direction. **Table 20** shows that the area of flood depth extent of around 6 m to 8 m covers most of the study area at flood depths of more than value 8 m and are high risks mostly in the lower Mekong River in Cambodia. Also, (Mohammed et al., 2018) shows that releasing more water from upstream of the Mekong would also affect flood duration and the frequency of flood occurrences downstream and (Oddo et al., 2018) cause direct damage to people, structures, and land cover as assessed using the 2011 Southeast Asian flood as a case in the lower Mekong River area of Cambodia.

Furthermore, most the model applied along Mekong River such as SWAT, IQQM, ISIS models (MRC, 2018) and (Chung et al., 2019) applied rainfall-runoff–inundation (RRI) model was used to simulate flood inundation in the Stung Sen River Basin of Cambodia and (Liu et al., 2019) developed a flood hazard index (FHI) model based on a GIS (Geographic Information System) and used synthetic aperture radar (SAR) data to extract historical floods at Angkor from 2007 to 2013. HEC-RAS hydraulic model should be recommending to use along the river (Shrestha & Lohpaisankrit, 2017; El-Naqa & Jaber, 2018; Abdelkarim et al., 2019; Farooq et al., 2019). Likewise, the study is used this model for conduced flood inundation and flood hazard maps. As the results, the HEC-RAS model can assume that it is able to simulate the flood area from flooding effectively.

CHAPTER V

CONCLUSIONS AND RECOMMENDATIONS

This study provides useful guidance for the application of hydraulic modeling in the Lower Mekong River, Cambodia. The results from this study indicate that the high resolution of DEM and the water discharge upstream gave good performance outcomes when entered into the model. Then, downstream is calibrated to present the accuracy of the model. Furthermore, the LP3 distribution analysis of the return period 10, 20, 50, 100-year is the best fitted with the 52,208 m^3/s, 54,990 m^3/s, 59,381 m^3/s, and 62,194 m^3/s, respectively. Indeed, the LP3 is better analyzed by Easyfit software. In conclude, the study flood frequency analysis are expected to be useful for designing the dimension of hydraulic structures such as bridges, levees, and spillways in along the Lower Mekong River. Moreover, the result of flood frequency analysis can be also used as an essential decision support instrument for land-use regulation and floodplain management of the River.

According to the demonstration of the model simulation during 2011, 2013, 2017, and 2018 (short-term) due to calibration with the cross-section downstream, the output of value NSE, RSR, R2 and PBIAS statistics test as showing 2011 (0.97, 0.16, 0.98, and -12), 2013 (0.96, 0.17, 0.97, and -5), 2017 (0.97, 0.16, 0.98, and -6), and 2018 (0.96, 0.19, 0.98, and -9) respectively showed good accuracy. Likewise, the performance of model simulation in 15 years and 30 years (long-term) as the calibrated results of NSE, RSR, R^2, and PBIAS values are 15 years (0.97, 0.15, 0.97, and -6) and 30 years (0.96, 0.16, 0.97, and -5) respectively very good accuracy.

To construct a flood hazard map for the highest flood-affected area, the implicated model and calibration value of Manning's n **0.035** for simulating 1-D flood depth is needed. The simulated model is based on input flood frequency analysis of the multi return period 10, 20, 50, and 100-year confirmations are 52208 m^3/s, 54990 m^3/s, 59381 m^3/s, and 62194 m^3/s almost identical in the year 2011, 2013, 2017, and 2018 (50295 m^3/s, 50295 m^3/s, 42629 m^3/s, and 47900 m^3/s) observed at peak discharge. Thus, it proves that the productivity of the HEC-RAS model can be

simulated. Moreover, the HEC-RAS model could give a valid output of both the affected area and flood depth. However, the study still has a few assumptions, and errors can occur in flood maps that were produced based on upstream water discharge. Riverbank change and other developments were not accounted for made a field observed. Nevertheless, the coupling between HEC-RAS and ArcGIS provides a capability to flood mapping for the study along the river. The flood hazard map from 10, 20, 50, and 100-year return periods provides satisfactory samples for this process.

In short, this study presents a method for improving the prediction of flood events and flood prevention system. The aims were to reduce damage from floods and providing a better quality of life in along the community river. The coupling GIS and HEC-RAS modeling helps to develop a solution for sustainable flood protection and ensuring a cleaner, safer environment. The relationship between this study and other studies are in proving the necessity of GIS and HEC-RAS hydraulic modeling before flood mitigation measures realization in the territory. These actions could prove the significance of the risk analysis in flood protection by stating the economic value of protected properties endangered by floods. A presented study mentions the successful combination of scientific and practical experiences to show the effectiveness of modeling techniques for engineering practice; exactly it presents a successful real functioning system of flood mitigation measures that increase sustainability and environmental protection of the territory. The outcome of the study served as an essential basis for a more informed decision and science-based recommendations in formulating local and regional river policies for more effective and cost-efficient strategies relative to flood hazards. Research still needs to be done in order to clarify the global role of hydraulic uncertainty on flood hazard evaluations and explore the different criteria that should be considered when producing flood maps for this specific purpose. However, this work highlights the special attention that needs to be given when using existing flood hazard maps or producing simplified hydraulic analyses for community river estimation flood purposes as they may be inaccurate.

1) The HEC-RAS model is an appropriate hydraulic model for use in simulating discharge with an unsteady and steady performance in conducting flood return periods in the Lower Mekong River, Cambodia.

2) Both discharge and cross-section data are significant and are used to estimate peak discharge by flood frequency analysis.
3) Model calibration is needed to conduct for the future study due to provide a confidence decision to choose which hydraulic model be the best choice to conduct research.

Furthermore, the study has limitation in accuracy valuation due to lack of field observation data. It is important and necessary to use observed data to calibrate the hydraulic model in order to interpret. However, accuracy of the results is used data water discharge (i.e. Kampong Cham reach Chruy Changvar gauging station), are playing an important role in the 1-D HEC-RAS model. Furthermore, DEM (Digital Elevation Model) 30×30 resolution is an important cross-section data for model assessment. The calibration of the resulting model requires knowledge of the study area are used Nash-Sutcliffe Efficiency (NSE), Observed Standard Deviation Ratio (RSR), coefficient of determination (R^2), and percent bias (PBIAS) by computed using daily average flow. The study is using four flood frequency analyses (Log-Pearson type III, Normal, Log-Normal, and Gumbel distributions) and applying Easyfit software to evaluate the best goodness of distributions.

RECOMMENDATIONS

The study concludes with several recommendations for improved flood mitigation in the future, from infrastructure to strengthening the early warning system, to building the capacity of disaster committees and local authorities to prepare for disaster management, to scaling up the cooperation between different stakeholders. The study also recommends further modeling and hazard mapping. Cambodians are no strangers to seasonal flooding. The following recommendation indicates some aspects of improving flood inundation modeling for further study:

1) The researcher should include hydrological analyses such as estimations of design flow and groundwater. This research does not consider any discharge from other tributaries along the river reach.
2) To further evaluate the effects of geometric data in 1-D hydraulic modeling, more variability of inclusion and exclusion of cross-sections (e.g. at the

riverbank, a width of cross-sections) should consider. Moreover, the characteristics of the river (e.g. length of the river, slope, and geomorphology) and varying upstream/downstream boundary conditions (e.g. releasing water from a dam, tide level, barrage) might give different results.

3) In this finding, the DEM resolution 30×30 meters use the functions available in ArcGIS software (i.e. Spatial Analysis tools) and modeling. Further study is a recommendation of the good resolution of deference DEM.
4) Further research should be done considering other variables for the calibration and validation process. In this study, only two calibrates were used discharge, which is enough for calibrating the 1-D model. In contrast, it may not be significant in the calibration of the 2-D model.
5) In developing the flood hazard map, accuracy is important. However, it is dependent on the precision of the variables used (estimation of the design flow, data collection techniques of DEMs, hydraulic modeling approach). Concerning uncertain variables, the approach of using the probabilistic hazard map should be deliberate and explored further.
6) Include institutional strengthening and the training of staff at all levels, from the local community to the technical specialist and the decision-maker, in programs of assistance on flood hazard mitigation.

The important that should consider, among nonstructural measures such as; the education and training of local community leaders so that they can better deal with the dangers of floods and flood hazards, the improvement of flood alert systems, the design of alternative types of infrastructure and housing construction that will withstand certain natural hazards, and the relocation of populations and activities situated in areas of unacceptably high risk.

REFERENCES

REFERENCES

Books

Ahmed, N., Taylor, S. W., & Sheng, Z. (2014). *Hydraulics of Wells Design, Construction, Testing, and Maintenance of Water Well Systems*. Virginia: American Society of Civil Engineers.

Brimicombe, A. (2010). *GIS, Environmental Modeling and Engineering.* New York: CRC Press.

Carrara, A., & Guzzedi, F. (1993). *Geographical Information Systems in Assessing Natural Hazards*.

Carrara, A. (1995). *Geographical Information Systems in Assessing Natural Hazards* (F. Guzzetti Ed. Vol. 5). New York: Springer Science & Business Media.

Cfe-Dm. (2017). *Disaster Management Reference Handbook-Cambodia 2017*. Hawaii: Center for Excellence in Disaster Management & Humanitarian Assistance.

Chow, V. T., Maidment, D. R., & Mays, L. W. (1988). *Applied Hydrology*. New York: McGraw-Hill.

Dagli, S., & Ferrarini, B. (2019). *The Growth Impact of Disasters in Developing Asia*. Mandaluyong: ADB.

Doyle, R. (2003). *Flood-Random House UK*. London: Random House.

Iaea. (2003). *Flood Hazard for Nuclear Power Plants on Coastal and River Sites (International Atomic Energy Agency)*. Vienna: International Atomic Energy Agency.

Lunetta, R. S., & Lyon, J. G. (2000). *Remote Sensing and GIS Accuracy Assessment.* Washington, D.C.: CRC PRESS.

Micah, M. M. (2016). *Flood Hazard Mapping _ Uncertainty and its Value in the Decision-Making Process.* EH Leiden: CRC Press.

Miller, J. J., & French, R. H. (2012). *Flood Hazard Identification And Mitigation In Semi- And Arid Environments*. Singapore: World Scientific.

Oecd. (2016). *Financial Management of Flood Risk.* Paris: OECD Publishing.

Proverbs, D., & Soetanto, R. (2004). *Flood Damaged Property A Guide to Repair*: Blackwell Publishing Ltd.

Ramachandra, R. A., & Hamed, K. H. (2000). *Flood Frequency Analysis*. United State: CRC Press.

Şen, Z. (2018). *Flood Modeling, Prediction and Mitigation*. Cham, Switzerland: Springer Nature.

Shamsi, U. M. (2005). *GIS Applications for Water, Wastewater, and Stormwater Systems*. Florida: CRC Pres.

Smith, K., & Petley, D. N. (1991). *Environmental Hazard*. New York: Routledge.

Systems, B., Dyhouse, G., Hatchett, J., & Benn, J. (2007). *Floodplain modeling using HEC-RAS.* (C. Totz Ed.). Pennsylvania: Haestad Press.

Tomaszewski, B. (2015). *Geographic Information Systems (GIS) for Disaster Management*.

Usace. (2018). *Analyzing Flood Risk for Forecast Informed Reservoir Operations in the Russian River Watershed Using HEC-WAT*. Institute for Water Resources Hydrologic Engineering Center: Institute for Water Resources Hydrologic Engineering Center.

Weng, Q. (2010). *Remote Sensing And GIS Integration.* New York: McGraw-Hil.

Xinjiang, L., & Minghui, H. (2018). *Modeling, Analysis and Control of Hydraulic Actuator for Forging*. Singapore: Springer Nature.

Journals

Abdelkarim, A., Gaber, A. F. D., Youssef, A. M., & Pradhan, B. (2019). Flood Hazard Assessment of the Urban Area of Tabuk City, Kingdom of Saudi Arabia by Integrating Spatial-Based Hydrologic and Hydrodynamic Modeling. *Sensors, 19*(5), 1-23. doi: 10.3390/s19051024

Abdulrazzak, M., Elfeki, A., Kamis, A., Kassab, M., Alamri, N., Chaabani, A., & Noor, K. (2019). Flash flood risk assessment in urban arid environment: case study of Taibah and Islamic universities' campuses, Medina, Kingdom of Saudi Arabia. *Geomatics, Natural Hazards and Risk, 10*(1), 780-796. doi: 10.1080/19475705.2018.1545705

Abebe, Y. A., Ghorbani, A., Nikolic, I., Vojinovic, Z., & Sanchez, A. (2019a). A coupled flood-agent-institution modelling (CLAIM) framework for urban flood risk management. *Environmental Modelling & Software, 111*(2019), 483-492. doi: 10.1016/j.envsoft.2018.10.015

Abebe, Y. A., Ghorbani, A., Nikolic, I., Vojinovic, Z., & Sanchez, A. (2019b). Flood risk management in Sint Maarten – A coupled agent-based and flood modelling method. *J Environ Manage, 248*(2019), 109-317. doi: https://doi.org/10.1016/j.jenvman.2019.109317

Agency, E. (2013). Flood Map - your questions answered. Rotherham: Environment Agency. doi: www.environment-agency.gov.uk/homeandleisure/31662.aspx

Ahamed, A., & Bolten, J. D. (2017). A MODIS-based automated flood monitoring system for southeast asia. *International Journal of Applied Earth Observation and Geoinformation, 61*(2017), 104-117. doi: 10.1016/j.jag.2017.05.006

Ahmad, T., Pandey, A. C., & Kumar, A. (2018). Flood hazard vulnerability assessment in Kashmir Valley, India using geospatial approach. *Physics and Chemistry of the Earth, Parts A/B/C, 105*(2018), 59-71. doi: 10.1016/j.pce.2018.02.003

Akbari, A., Mozafari, G., Fanodi, M., & Maliheh, H. S. (2014). Impact of Landuse Change on River Floodplain Using Public Domain Hydraulic Model. *Modern Applied Science, 8*(2014), 80-86. doi: 10.5539/mas.v8n5p80

Azouagh, A., El Bardai, R., Hilal, I., & Stitou El Messari, J. (2018). Integration of GIS and HEC-RAS in Floods Modeling of Martil River (Northern Morocco). *European Scientific Journal, ESJ, 14*(12), 130-142. doi: 10.19044/esj.2018.v14n12p130

Bamberg, S., Masson, T., Brewitt, K., & Nemetschek, N. (2017). Threat, coping and flood prevention – A meta-analysis. *Journal of Environmental Psychology, 54*(2017), 116-126. doi: 10.1016/j.jenvp.2017.08.001

Batista, C. M. (2018). Coastal Flood Hazard Mapping. *Springer, Cham*(2018), 1-11. doi: 10.1007/978-3-319-48657-4_356-1

Ben Khalfallah, C., & Saidi, S. (2018). Spatiotemporal floodplain mapping and prediction using HEC-RAS - GIS tools: Case of the Mejerda river, Tunisia. *Journal of African Earth Sciences, 142*(2018), 44-51. doi: 10.1016/j.jafrearsci.2018.03.004

Bezak, N., Sraj, M., Rusjan, S., & Mikos, M. (2018). Impact of the Rainfall Duration and Temporal Rainfall Distribution Defined Using the Huff Curves on the

Hydraulic Flood Modelling Results. *Geosciences, 8*(69), 1-15.

Bhat, M. S., Alam, A., Ahmad, B., Kotlia, B. S., Farooq, H., Taloor, A. K., & Ahmad, S. (2019). Flood frequency analysis of river Jhelum in Kashmir basin. *Quaternary International, 507*(2019), 288-294. doi: https://doi.org/10.1016/j.quaint.2018.09.039

Bhola, P., Leandro, J., Videkhina, I., & Disse, M. (2018). Dynamic Risk Mapping in Fluvial Flood Application Using a Two-dimensional Hydrodynamic Model Incorporating the Model Parameter Uncertainties. *Technische Universität München*. doi: 10.13140/RG.2.2.12812.36481

Bhola, P., Nair, B., Leandro, J., Rao, S., & Disse, M. (2018). Flood inundation forecasts using validation data generated with the assistance of computer vision. *Hydroinformatics, 21*(2019), 240-256. doi: 10.2166/hydro.2018.044

Buchori, I., Pramitasari, A., Sugiri, A., Maryono, M., Basuki, Y., & Sejati, A. W. (2018). Adaptation to coastal flooding and inundation: Mitigations and migration pattern in Semarang City, Indonesia. *Ocean & Coastal Management, 163*(2018), 445-455. doi: 10.1016/j.ocecoaman.2018.07.017

Cao, C., Xu, P., Wang, Y., Chen, J., Zheng, L., & Niu, C. (2016). Flash Flood Hazard Susceptibility Mapping Using Frequency Ratio and Statistical Index Methods in Coalmine Subsidence Areas. *Sustainability, 8*(948), 1-18. doi: 10.3390/su8090948

Chen, W., Hong, H., Li, S., Shahabi, H., Wang, Y., Wang, X., & Ahmad, B. B. (2019). Flood susceptibility modelling using novel hybrid approach of reduced-error pruning trees with bagging and random subspace ensembles. *Journal of Hydrology, 575*(2019), 864-873. doi: https://doi.org/10.1016/j.jhydrol.2019.05.089

Chim, K., Tunnicliffe, J., Shamseldin, A., & Ota, T. (2019). Land Use Change Detection and Prediction in Upper Siem Reap River, Cambodia. *Hydrology, 6*(64), 1-23.

Chung, S., Takeuchi, J., Fujihara, M., & Oeurng, C. (2019). Flood damage assessment on rice crop in the Stung Sen River Basin of Cambodia. *Paddy and Water Environment, 17*(2019), 255-263. doi: 10.1007/s10333-019-00718-1

Cochrane, T. A., Arias, M. E., & Piman, T. (2014). Historical impact of water infrastructure on water levels of the Mekong River and the Tonle Sap system. *Hydrology and Earth System Sciences, 18*(11), 4529-4541. doi: 10.5194/hess-18-4529-2014

Coquet, M., Mercier, D., & Fleury-Bahi, G. (2019). Assessment of the exposure to coastal flood risk by inhabitants of French coasts: The effect of spatial optimism and temporal pessimism. *Ocean & Coastal Management, 177*(2019), 139-147. doi: https://doi.org/10.1016/j.ocecoaman.2019.05.004

Criado, M., Martinez-Grana, A., San Roman, J. S., & Santos-Frances, F. (2018). Flood Risk Evaluation in Urban Spaces: The Study Case of Tormes River (Salamanca, Spain). *Int J Environ Res Public Health, 16*(1), 1-19. doi: 10.3390/ijerph16010005

Degiorgis, M., Gnecco, G., Gorni, S., Roth, G., Sanguineti, M., & Taramasso, A. C. (2012). Classifiers for the detection of flood-prone areas using remote sensed elevation data. *Journal of Hydrology, 470-471*(2012), 302-315. doi: https://doi.org/10.1016/j.jhydrol.2012.09.006

Demir, V., & Kisi, O. (2016). Flood Hazard Mapping by Using Geographic Information System and Hydraulic Model: Mert River, Samsun, Turkey. *Advances in Meteorology, 2016*, 1-9. doi: 10.1155/2016/4891015

Dysarz, T., Wicher-Dysarz, J., Sojka, M., & Jaskuła, J. (2019). Analysis of extreme flow uncertainty impact on size of flood hazard zones for the Wronki gauge station in the Warta river. *Acta Geophysica, 67*(2019), 661-676. doi: 10.1007/s11600-019-00264-8

Echogdali, F. Z., Boutaleb, S., Jauregui, J., & Elmouden, A. (2018). Cartography of Flooding Hazard in Semi-Arid Climate: The Case of Tata Valley (South-East of Morocco). *Journal of Geography & Natural Disasters, 08*(01), 1-11. doi: 10.4172/2167-0587.1000214

El-Naqa, A., & Jaber, M. (2018). Floodplain Analysis using ArcGIS, HEC-GeoRAS and HEC-RAS in Attarat Um Al-Ghudran Oil Shale Concession Area, Jordan. *Journal of Civil & Environmental Engineering, 08*(05). doi: 10.4172/2165-784x.1000323

Elkhrachy, I. (2015). Flash Flood Hazard Mapping Using Satellite Images and GIS Tools: A case study of Najran City, Kingdom of Saudi Arabia (KSA). *The Egyptian Journal of Remote Sensing and Space Science, 18*(2), 261-278. doi: 10.1016/j.ejrs.2015.06.007

Erena, S. H., Worku, H., & De Paola, F. (2018). Flood hazard mapping using FLO-2D and local management strategies of Dire Dawa city, Ethiopia. *Journal of Hydrology: Regional Studies, 19*, 224-239. doi: 10.1016/j.ejrh.2018.09.005

Ezz, H. (2018). Integrating GIS and HEC-RAS to model Assiut plateau runoff. *The Egyptian Journal of Remote Sensing and Space Science, 21*(2018), 219-227. doi: https://doi.org/10.1016/j.ejrs.2017.11.002

Farooq, M., Shafique, M., & Khattak, M. S. (2018). Flood frequency analysis of river swat using Log Pearson type 3, Generalized Extreme Value, Normal, and Gumbel Max distribution methods. *Arabian Journal of Geosciences, 11*(216), 1-10. doi: 10.1007/s12517-018-3553-z

Farooq, M., Shafique, M., & Khattak, M. S. (2019). Flood hazard assessment and mapping of River Swat using HEC-RAS 2D model and high-resolution 12-m TanDEM-X DEM (WorldDEM). *Natural Hazards, 97*(2), 477-492. doi: 10.1007/s11069-019-03638-9

Gao, Z., Long, D., Tang, G., Zeng, C., Huang, J., & Hong, Y. (2017). Assessing the potential of satellite-based precipitation estimates for flood frequency analysis in ungauged or poorly gauged tributaries of China's Yangtze River basin. *Journal of Hydrology, 550*(2017), 478-496. doi: https://doi.org/10.1016/j.jhydrol.2017.05.025

Ghanbarpour, M. R., Salimi, S., & Hipel, K. W. (2013). A comparative evaluation of flood mitigation alternatives using GIS-based river hydraulics modelling and multicriteria decision analysis. *Journal of Flood Risk Management, 6*(2013), 319–331. doi: 10.1111/jfr3.12017

Habte, A., Teka, D., & Teka, K. (2017). Integration of Remote Sensing and Hydraulic Models to Identify Flood Prone Areas in Woybo River Catchment, South Western Ethiopia. *Geography & Natural Disasters, 07*(1), 1-13. doi: 10.4172/2167-0587.1000190

Hadipour, V., Vafaie, F., & Kerle, N. (2019). An indicator-based approach to assess

social vulnerability of coastal areas to sea-level rise and flooding: A case study of Bandar Abbas city, Iran. *Ocean & Coastal Management*, 105077. doi: https://doi.org/10.1016/j.ocecoaman.2019.105077

Hazarika, M. K., Bormudoi, A., Kafle, T. P., Samarkoon, L., Nuon, K., Savuth, Y., & Narith, R. (2007). Flood Hazard Mapping in Four Provinces of Cambodia Under the Mekong River Basin. *ResearchGate*.

Heimhuber, V., Hannemann, J. C., & Rieger, W. (2015). Flood Risk Management in Remote and Impoverished Areas—A Case Study of Onaville, Haiti. *Water, 7*(12), 3832-3860. doi: 10.3390/w7073832

Hong, H., Panahi, M., Shirzadi, A., Ma, T., Liu, J. P., Zhu, A. X., Chen, W., Kougias, I., & Kazakis, N. (2018). Flood susceptibility assessment in Hengfeng area coupling adaptive neuro-fuzzy inference system with genetic algorithm and differential evolution. *Science of The Total Environment, 621*(2018), 1124-1141. doi: https://doi.org/10.1016/j.scitotenv.2017.10.114

Horritt, M. S., & Bates, P. D. (2002). Evaluation of 1D and 2D numerical models for predicting river flood inundation. *Journal of Hydrology, 268*(2002), 87-99. doi: https://doi.org/10.1016/S0022-1694(02)00121-X

Islam, B., Muhammad, S., Tazeem, K., & Iffat, T. M. (2015). Flood hazard assessment using hydro-dynamic model and GIS/RS tools: A case study of Babuzai-Kabal tehsil Swat Basin, Pakistan. *Himalayan Earth Sciences*.

Jodar-Abellan, A., Valdes-Abellan, J., Pla, C., & Gomariz-Castillo, F. (2019). Impact of land use changes on flash flood prediction using a sub-daily SWAT model in five Mediterranean ungauged watersheds (SE Spain). *Sci Total Environ, 657*(2019), 1578-1591. doi: 10.1016/j.scitotenv.2018.12.034

Kasiviswanathan, K. S., He, J., & Tay, J.-H. (2017). Flood frequency analysis using multi-objective optimization based interval estimation approach. *Journal of Hydrology, 545*(2017), 251-262. doi: https://doi.org/10.1016/j.jhydrol.2016.12.025

Kawasaki, A., Takamatsu, M., He, J., Rogers, P., & Herath, S. (2010). An integrated approach to evaluate potential impact of precipitation and land-use change on streamflow in Srepok River Basin. *Theory and Applications of GIS, 18*(2010), 117-128. doi: 10.5638/thagis.18.117

Kheradmand, S., Seidou, O., Konte, D., & Barmou Batoure, M. B. (2018). Evaluation of adaptation options to flood risk in a probabilistic framework. *Journal of Hydrology: Regional Studies, 19*(2018), 1-16. doi: https://doi.org/10.1016/j.ejrh.2018.07.001

Kim, K., Pant, P., & Yamashita, E. (2018). Integrating travel demand modeling and flood hazard risk analysis for evacuation and sheltering. *International Journal of Disaster Risk Reduction, 31*, 1177-1186. doi: 10.1016/j.ijdrr.2017.10.025

Kishore, N., Marques, D., Mahmud, A., Kiang, M. V., Rodriguez, I., Fuller, A., Ebner, P., Sorensen, C., Racy, F., Lemery, J., Maas, L., Leaning, J., Irizarry, R. A., Balsari, S., & Buckee, C. O. (2018). Mortality in Puerto Rico after Hurricane Maria. *N Engl J Med, 379*(2), 162-170. doi: 10.1056/NEJMsa1803972

Kumar, R., Singh, R., Gautam, H., & Pandey, M. K. (2018). Flood hazard assessment of August 20, 2016 floods in Satna District, Madhya Pradesh, India. *Remote Sensing Applications: Society and Environment, 11*, 104-118. doi: 10.1016/j.rsase.2018.06.001

Lazare, K. K., Alexis, B. L., Berthe, Y. A., Alex, K. Z., Seraphin, K. K., Felix, K. K., & Berenger, K. (2019). 1D-2D Hydraulic Modeling of a Diversion Channel on the Cavally River in Zouan-Hounien, Cote d'Ivoir. *Journal of Water Resource and Protection, 11*(08), 1036-1048. doi: 10.4236/jwarp.2019.118061

Li, D., Long, D., Zhao, J., Lu, H., & Hong, Y. (2017). Observed changes in flow regimes in the Mekong River basin. *Journal of Hydrology, 551*(2017), 217-232. doi: 10.1016/j.jhydrol.2017.05.061

Liu, J., Xu, Z., Chen, F., Chen, F., & Zhang, L. (2019). Flood Hazard Mapping and Assessment on the Angkor World Heritage Site, Cambodia. *Remote Sensing, 11*(1), 98. doi: 10.3390/rs11010098

Logah, F. Y., Amisigo, A. B., Obuobie, E., & Kankam-Yeboah, K. (2017). Floodplain hydrodynamic modelling of the Lower Volta River in Ghana. *Journal of Hydrology: Regional Studies, 14*(2017), 1-9. doi: https://doi.org/10.1016/j.ejrh.2017.09.002

Lyu, H.-M., Shen, S.-L., Zhou, A., & Yang, J. (2019). Perspectives for flood risk assessment and management for mega-city metro system. *Tunnelling and Underground Space Technology, 84*(2019), 31-44. doi: 10.1016/j.tust.2018.10.019

Macchione, F., Costabile, P., Costanzo, C., & De Santis, R. (2019). Moving to 3-D flood hazard maps for enhancing risk communication. *Environmental Modelling & Software, 111*(209), 510-522. doi: 10.1016/j.envsoft.2018.11.005

Mahmoud, S. H., & Gan, T. Y. (2018). Urbanization and climate change implications in flood risk management: Developing an efficient decision support system for flood susceptibility mapping. *Sci Total Environ, 636*(2018), 152-167. doi: 10.1016/j.scitotenv.2018.04.282

Manfre, L. A., Hirata, E., Silva, J. B., Shinohara, E. J., Giannotti, M. A., Larocca, A. P. C., & Quintanilha, J. A. (2012). An Analysis of Geospatial Technologies for Risk and Natural Disaster Management. *ISPRS International Journal of Geo-Information, 1*(2), 166-185. doi: 10.3390/ijgi1020166

Markert, K. N., Griffin, R. E., Limaye, A. S., & Mcnider, T. R. (2018). Spatial Modeling of Land Cover/Land Use Change and Its Effects on Hydrology Within the Lower Mekong Basin. *ResearchGate*(2018), 667-698. doi: 10.1007/978-3-319-67474-2_29

Maskong, H. (2019). Flood Hazard Mapping Using on-Site Surveyed Flood Map, Hecras V.5 and Gis Tool: A Case Study of Nakhon Ratchasima Municipality, Thailand. *International Journal of GEOMATE, 16*(54), 1-8. doi: 10.21660/2019.54.81342

Massazza, G., Tamagnone, P., Wilcox, C., Belcore, E., Pezzoli, A., Vischel, T., Panthou, G., Housseini Ibrahim, M., Tiepolo, M., Tarchiani, V., & Rosso, M. (2019). Flood Hazard Scenarios of the Sirba River (Niger): Evaluation of the Hazard Thresholds and Flooding Areas. *Water, 11*(5), 1-22.

Mihu-Pintilie, A., Cimpianu, C. I., Stoleriu, C. C., Perez, M. N., & Paveluc, L. E. (2019). Using High-Density LiDAR Data and 2D Streamflow Hydraulic Modeling to Improve Urban Flood Hazard Maps: A HEC-RAS Multi-Scenario Approach. *Water, 11*(9), 1-24.

Mishra, A. K., Bairagi, S., Velasco, M. L., & Mohanty, S. (2018). Impact of access to capital and abiotic stress on production efficiency: Evidence from rice farming

in Cambodia. *Land Use Policy, 79*(2018), 215-222. doi: 10.1016/j.landusepol.2018.08.016

Mochizuki, J., Vitoontus, S., Wickramarachchi, B., Hochrainer-Stigler, S., Williges, K., Mechler, R., & Sovann, R. (2015). Operationalizing Iterative Risk Management under Limited Information: Fiscal and Economic Risks Due to Natural Disasters in Cambodia. *International Journal of Disaster Risk Science, 6*(4), 321-334. doi: 10.1007/s13753-015-0069-y

Mohammed, I. N., Bolten, J. D., Srinivasan, R., & Lakshmi, V. (2018). Satellite observations and modeling to understand the Lower Mekong River basin streamflow variability. *J Hydrol (Amst), 564*, 559-573. doi: 10.1016/j.jhydrol.2018.07.030

Mohammed, I. N., Bolten, J. D., Srinivasan, R., & Lakshmi, V. (2018). Satellite observations and modeling to understand the Lower Mekong River Basin streamflow variability. *Journal of Hydrology, 564*, 559-573. doi: https://doi.org/10.1016/j.jhydrol.2018.07.030

Mokhtar, E. S., Pradhan, B., Ghazali, A. H., & Helmi, Z. M. S. (2018). Assessing flood inundation mapping through estimated discharge using GIS and HEC-RAS model. *Arabian Journal of Geosciences, 11*(682), 1-20. doi: 10.1007/s12517-018-4040-2

Mosquera-Machado, S., & Ahmad, S. (2007). Flood hazard assessment of Atrato River in Colombia. *Water Resources Management, 21*(3), 591-609. doi: 10.1007/s11269-006-9032-4

Motevalli, A., & Vafakhah, M. (2016). Flood hazard mapping using synthesis hydraulic and geomorphic properties at watershed scale. *Stochastic Environmental Research and Risk Assessment, 30*(2016), 1889-1900. doi: 10.1007/s00477-016-1305-8

Moya Quiroga, V., Kure, S., Udo, K., & Mano, A. (2016). Application of 2D numerical simulation for the analysis of the February 2014 Bolivian Amazonia flood: Application of the new HEC-RAS version 5. *RIBAGUA - Revista Iberoamericana del Agua, 3*(2016), 25-33. doi: https://doi.org/10.1016/j.riba.2015.12.001

Muthusamy, M., Rivas Casado, M., Salmoral, G., Irvine, T., & Leinster, P. (2019). A Remote Sensing Based Integrated Approach to Quantify the Impact of Fluvial and Pluvial Flooding in an Urban Catchment. *Remote Sensing, 11*(5), 577.

Nor, D., Adnan, N., Ainul, Z., Zulkarnain, H., & Mokhtar, E. (2014). Geospatial Flood Inundation Modelling and Estimation of Sungai Muda Kedah Floodplain, Malaysia. *ResearchGate*.

Nyda, C., & Millington, A. (2015). Drought Monitoring for Rice Production in Cambodia. *Climate, 3*(4), 792-811. doi: 10.3390/cli3040792

Oddo, P. C., Ahamed, A., & Bolten, J. D. (2018). Socioeconomic Impact Evaluation for Near Real-Time Flood Detection in the Lower Mekong River Basin. *Hydrology, 5*(2018), 23. doi: 10.3390/hydrology5020023

Okazumi, T., Tanaka, S., Kwak, Y., Shrestha, B. B., & Sugiura, A. (2013). Flood vulnerability assessment in the light of rice cultivation characteristics in Mekong River flood plain in Cambodia. *Paddy and Water Environment, 12*(S2), 275-286. doi: 10.1007/s10333-013-0403-1

Orsini-Zegada, L., & Escalante-Sandoval, C. (2016). Flood frequency analysis using

synthetic samples. *Atmósfera, 29*(4), 299-309. doi: https://doi.org/10.20937/ATM.2016.29.04.02

Orton, P. M., Conticello, F. R., Cioffi, F., Hall, T. M., Georgas, N., Lall, U., Blumberg, A. F., & Macmanus, K. (2018). Flood hazard assessment from storm tides, rain and sea level rise for a tidal river estuary. *Natural Hazards*, 1-29. doi: 10.1007/s11069-018-3251-x

Oubennaceur, K., Chokmani, K., Nastev, M., Lhissou, R., & El alem, A. (2019). Flood risk mapping for direct damage to residential buildings in Quebec, Canada. *International Journal of Disaster Risk Reduction, 33*(2019), 44-54. doi: https://doi.org/10.1016/j.ijdrr.2018.09.007

Parhi, P. K. (2018). Flood Management in Mahanadi Basin using HEC-RAS and Gumbel's Extreme Value Distribution. *Journal of The Institution of Engineers (India): Series A, 99*(4), 751-755. doi: 10.1007/s40030-018-0317-4

Park, K., & Lee, M.-H. (2019). The Development and Application of the Urban Flood Risk Assessment Model for Reflecting upon Urban Planning Elements. *Water, 11*(920), 1-17.

Patel, C. G., & Gundaliya, P. J. (2016). Floodplain Delineation Using HECRAS Model. *Open Journal of Modern Hydrology, 06*(01), 34-42. doi: 10.4236/ojmh.2016.61004

Petit-Boix, A., Sevigne-Itoiz, E., Rojas-Gutierrez, L., A., Barbassa, A., P., Josa, A., Rieradevall, J., & Gabarrell, X. (2017). Floods and consequential life cycle assessment: Integrating flood damage into the environmental assessment of stormwater Best Management Practices. *Journal of Cleaner Production, 162*(2017), 601-608. doi: https://doi.org/10.1016/j.jclepro.2017.06.047

Pokhrel, Y., Shin, S., Lin, Z., Yamazaki, D., & Qi, J. (2018). Potential Disruption of Flood Dynamics in the Lower Mekong River Basin Due to Upstream Flow Regulation. *Sci Rep, 8*(2018), 1-13. doi: 10.1038/s41598-018-35823-4

Puno, G. R., Amper, R. A. L., Opiso, E. M., & Cipriano, J. A. B. (2019). Mapping and analysis of flood scenarios using numerical models and GIS techniques. *Spatial Information Research*, 1-12. doi: 10.1007/s41324-019-00280-2

Qiang, Y. (2019). Disparities of population exposed to flood hazards in the United States. *J Environ Manage, 232*(2019), 295-304. doi: 10.1016/j.jenvman.2018.11.039

Quirogaa, V. M., Kurea, S., Udoa, K., & Manoa, A. (2017). Application of 2D numerical simulation for the analysis of the February 2014 Bolivian Amazonia flood: Application of the new HEC-RAS version 5. *Ribagua, 3*(1), 25-33. doi: 10.1016/j.riba.2015.12.001

Rahmati, O., Zeinivand, H., & Besharat, M. (2016). Flood hazard zoning in Yasooj region, Iran, using GIS and multi-criteria decision analysis. *Geomatics, Natural Hazards and Risk, 7*(3), 1000-1017. doi: 10.1080/19475705.2015.1045043

Rishiraj, D., Senaka, B., & Atiq, K. A. (2015). Assessing Gaps and Strengthening Early Warning System to Manage Disasters in Cambodia. *Integrated Disaster Risk Management, 5*(2), 167-175. doi: 10.5595/idrim.2015.0104

Rojas, O., Mardones, M., Rojas, C., Martínez, C., & Flores, L. (2017). Urban Growth and Flood Disasters in the Coastal River Basin of South-Central Chile (1943–2011). *Sustainability, 9*(2), 1-21.

Samanta, S., Pal, D. K., & Palsamanta, B. (2018). Flood susceptibility analysis through

remote sensing, GIS and frequency ratio model. *Applied Water Science, 8*(2), 66. doi: 10.1007/s13201-018-0710-1

Sami, G., Hadda, d., & Mahdi, K. (2016). Flood Hazard Map in the City of Batna (Algegia) by Hydraulic Modeling Approch. *Analele Universităţii din Oradea, Seria Geografie*(2016), 86-93.

Sarann, L., Lengthong, K., Demerre, S., & Sokchhay, H. (2018). Flood Mapping along the Lower Mekong River in Cambodia. *Engineering Journal, 22*(1), 269-278. doi: 10.4186/ej.2018.22.1.269

Sein, K. (2016). Flood Hazard Mapping using Hydraulic Model and GIS: A Case Study in Mandalay City, Myanmar. *Suan Sunandha Rajabhat University Journal of Science and Technology, 03*. doi: 10.14456/ssstj.2016.4

Shao, W., Keim, B. D., Xian, S., & O'connor, R. (2019). Flood hazards and perceptions – A comparative study of two cities in Alabama. *Journal of Hydrology, 569*(2019), 546-555. doi: 10.1016/j.jhydrol.2018.11.070

Shrestha, S., & Lohpaisankrit, W. (2017). Flood hazard assessment under climate change scenarios in the Yang River Basin, Thailand. *International Journal of Sustainable Built Environment, 6*(2), 285-298. doi: 10.1016/j.ijsbe.2016.09.006

Sohan, G. (2013). Application of a 2D Hydrodynamic Model for Assessing Flood Risk from Extreme Storm Events. *Climate*. doi: 10.3390/cli1030148

Speckhann, G. A., Borges Chaffe, P. L., Fabris Goerl, R., Abreu, J. J., & Altamirano Flores, J. A. (2018). Flood hazard mapping in Southern Brazil: a combination of flow frequency analysis and the HAND model. *Hydrological Sciences Journal, 63*(1), 87-100. doi: 10.1080/02626667.2017.1409896

Su, W. Z., Xiaodong Wang, Zhen Su, Xiaohui Huang, Jianxi Yang, Siquan Liu, Sanchao. (2011). Analyzing disaster-forming environments and the spatial distribution of flood disasters and snow disasters that occurred in China from 1949 to 2000. *Mathematical and Computer Modelling, 54*(3), 1069-1078. doi: https://doi.org/10.1016/j.mcm.2010.11.037

Taha, M. M. N., Elbarbary, S. M., Naguib, D. M., & El-Shamy, I. Z. (2017). Flash flood hazard zonation based on basin morphometry using remote sensing and GIS techniques: A case study of Wadi Qena basin, Eastern Desert, Egypt. *Remote Sensing Applications: Society and Environment, 8*(2017), 157-167. doi: 10.1016/j.rsase.2017.08.007

Talisay, B. A. M., Puno, G. R., Amper, R. A. L., Talisay, B. A. M., Puno, G. R., & Amper, R. A. L. (2019). Flood hazard mapping in an urban area using combined hydrologic-hydraulic models and geospatial technologies. *Global J. Environ. Sci. Manage, 5*(2), 139-154. doi: 10.22034/gjesm.2019.02.01

Tan, M. L., Ibrahim, A., Yusop, Z., Chua, V. P., & Chan, N. W. (2017). Climate change impacts under CMIP5 RCP scenarios on water resources of the Kelantan River Basin, Malaysia. *Atmospheric Research, 189*(2017), 1-10. doi: 10.1016/j.atmosres.2017.01.008

Tangdamrongsub, N., Ditmar, P. G., Steele-Dunne, S. C., Gunter, B. C., & Sutanudjaja, E. H. (2016). Assessing total water storage and identifying flood events over Tonlé Sap basin in Cambodia using GRACE and MODIS satellite observations combined with hydrological models. *Remote Sensing of Environment, 181*(2016), 162-173. doi: 10.1016/j.rse.2016.03.030

Teng, J., Jakeman, A. J., Vaze, J., Croke, B. F. W., Dutta, D., & Kim, S. (2017). Flood

inundation modelling: A review of methods, recent advances and uncertainty analysis. *Environmental Modelling & Software, 90*(2017), 201-216. doi: https://doi.org/10.1016/j.envsoft.2017.01.006

Trung, L. D., Duc, N. A., Nguyen, L. T., Thai, T. H., Khan, A., Rautenstrauch, K., & Schmidt, C. (2018). Assessing cumulative impacts of the proposed Lower Mekong Basin hydropower cascade on the Mekong River floodplains and Delta – Overview of integrated modeling methods and results. *Journal of Hydrology*(2018). doi: 10.1016/j.jhydrol.2018.01.029

Try, S., Lee, G., Yu, W., & Oeurng, C. (2018). Delineation of flood-prone areas using geomorphological approach in the Mekong River Basin. *Quaternary International*. doi: 10.1016/j.quaint.2018.06.026

Try, S., Lee, G., Yu, W., & Oeurngd, C. (2019). Delineation of flood-prone areas using geomorphological approach in the Mekong River Basin. *Quaternary International, 503*, 79-86. doi: 10.1016/j.quaint.2018.06.026

Ty, T. V., Sunada, K., Ichikawa, Y., & Oishi, S. (2012). Scenario-based Impact Assessment of Land Use/Cover and Climate Changes on Water Resources and Demand: A Case Study in the Srepok River Basin, Vietnam—Cambodia. *Water Resources Management, 26*(5), 1387-1407. doi: 10.1007/s11269-011-9964-1

Unfpa. (2018). United Nations Population Fund (accessed on 29 August, 2018). . doi: https://www.unfpa.org/.

Usher, K., Redman-Maclaren, M. L., Mills, J., West, C., Casella, E., Hapsari, E. D., Bonita, S., Rosaldo, R., Liswar, A. K., & Zang, Y. A. (2015). Strengthening and preparing: enhancing nursing research for disaster management. *Nurse Educ Pract, 15*(1), 68-74. doi: 10.1016/j.nepr.2014.03.006

Vathana, S. (2013). Impact of Disasters and Role of Social Protection in Natural Disaster Risk Management in Cambodia. *ERIA, 10*(2013), 1-32.

Vichet, N., Kawamura, K., Phan Trong, D., Van On, N., Gong, Z., Lim, J., Khom, S., & Bunly, C. (2019). MODIS-Based Investigation of Flood Areas in Southern Cambodia from 2002–2013. *Environments, 6*, 57. doi: 10.3390/environments6050057

Vivekanandan, N. (2015). Frequency Analysis of Annual Maximum Flood Discharge Using Method of Moments and Maximum Likelihood Method of Gamma and Extreme Value Family of Probability Distributions. *Mathematics and Computational Science, 1, No. 3, 2015, pp. 141-146*.

Vojtek, M., & Vojtekova, J. (2016). Flood hazard and flood risk assessment at the local spatial scale: a case study. *Geomatics, Natural Hazards and Risk, 7*(6), 1973-1992. doi: 10.1080/19475705.2016.1166874

Vojtek, M., Petroselli, A., Vojtekova, J., & Asgharinia, S. (2019). Flood inundation mapping in small and ungauged basins: sensitivity analysis using the EBA4SUB and HEC-RAS modeling approach. *Hydrology Research, 50*(4), 1002-1019. doi: 10.2166/nh.2019.163

Waghwala, R. K., & Agnihotri, P. G. (2019). Flood risk assessment and resilience strategies for flood risk management: A case study of Surat City. *International Journal of Disaster Risk Reduction*(2019), 1-13. doi: 10.1016/j.ijdrr.2019.101155

Walalite, T., Dekker, S. C., Schot, P. P., & Wassen, M. J. (2018). Unraveling the ecological functioning of the monsoonal Songkhram river floodplain in Thailand

by integrating data on soil, water, and vegetation. *Ecohydrology & Hydrobiology, 18*(1), 10-21. doi: 10.1016/j.ecohyd.2017.09.005

Wan Deraman, W. H. A., Abd Mutalib, N. J., & Mukhtar, N. Z. (2017). Determination of return period for flood frequency analysis using normal and related distributions. *Journal of Physics: Conference Series, 890*(2017), 1-11. doi: 10.1088/1742-6596/890/1/012162

Wang, Y., Liu, G., Guo, E., & Yun, X. (2018). Quantitative Agricultural Flood Risk Assessment Using Vulnerability Surface and Copula Functions. *Water, 10*(9), 1-16. doi: 10.3390/w10091229

Wang, Y., Yang, J., Chang, J., & Zhang, R. (2019). Assessing the drought mitigation ability of the reservoir in the downstream of the Yellow River. *Sci Total Environ, 646*(2019), 1327-1335. doi: 10.1016/j.scitotenv.2018.07.316

Wang, Z., Yao, W., Wang, M., Xiao, P., Yang, J., Zhang, P., Tang, Q., Kong, X., & Wu, J. (2019). The Influence of River Channel Occupation on Urban Inundation and Sedimentation Induced by Floodwater in Mountainous Areas: A Case Study in the Loess Plateau, China. *Sustainability, 11*(3), 761.

Wierzbicki, G., Ostrowski, P., Falkowski, T., & Mazgajski, M. (2018). Geological setting control of flood dynamics in lowland rivers (Poland). *Sci Total Environ, 636*(2018), 367-382. doi: 10.1016/j.scitotenv.2018.04.250

Wing, O. E. J., Sampson, C. C., Bates, P. D., Quinn, N., Smith, A. M., & Neal, J. C. (2019). A flood inundation forecast of Hurricane Harvey using a continental-scale 2D hydrodynamic model. *Journal of Hydrology X, 4*(2019), 1-17. doi: https://doi.org/10.1016/j.hydroa.2019.100039

Wu, Y. B., Xue, L. Q., & Liu, Y. H. (2019). Local and regional flood frequency analysis based on hierarchical Bayesian model in Dongting Lake Basin, China. *Water Science and Engineering, 12*(4), 253-262. doi: https://doi.org/10.1016/j.wse.2019.12.001

Xiao, Y., Yi, S., & Tang, Z. (2017). Integrated flood hazard assessment based on spatial ordered weighted averaging method considering spatial heterogeneity of risk preference. *Science of The Total Environment, 599-600*(2017), 1034-1046. doi: https://doi.org/10.1016/j.scitotenv.2017.04.218

Xu, H., Ma, C., Lian, J., Xu, K., & Chaima, E. (2018). Urban flooding risk assessment based on an integrated k-means cluster algorithm and improved entropy weight method in the region of Haikou, China. *Journal of Hydrology, 563*(2018), 975-986. doi: 10.1016/j.jhydrol.2018.06.060

Yin, J., Zhao, Q., Yu, D., Lin, N., Kubanek, J., Ma, G., Liu, M., & Pepe, A. (2019). Long-term flood-hazard modeling for coastal areas using InSAR measurements and a hydrodynamic model: The case study of Lingang New City, Shanghai. *Journal of Hydrology, 571*(2019), 593-604. doi: https://doi.org/10.1016/j.jhydrol.2019.02.015

Yousuf Gazi, M., Ashraful Islam, M., & Hossain, S. (2019). Flood-Hazard Mapping in a Regional Scale – Way Forward to the Future Hazard Atlas in Bangladesh. *Malaysian Journal of Geosciences, 3*(1), 01-11. doi: 10.26480/mjg.01.2019.01.11

Yu, W., Kim, Y., Lee, D., & Lee, G. (2019). Hydrological assessment of basin development scenarios: Impacts on the Tonle Sap Lake in Cambodia. *Quaternary International, 503*, 115-127. doi: 10.1016/j.quaint.2018.09.023

Zeleňáková, M., Fijko, R., Labant, S., Weiss, E., Markovič, G., & Weiss, R. (2019). Flood risk modelling of the Slatvinec stream in Kruzlov village, Slovakia. *Journal of Cleaner Production, 212*(2019), 109-118. doi: 10.1016/j.jclepro.2018.12.008

Zhao, G., Xu, Z., Pang, B., Tu, T., Xu, L., & Du, L. (2019). An enhanced inundation method for urban flood hazard mapping at the large catchment scale. *Journal of Hydrology, 571*(2019), 873-882. doi: 10.1016/j.jhydrol.2019.02.008

Zhou, Q., Leng, G., Su, J., & Ren, Y. (2019). Comparison of urbanization and climate change impacts on urban flood volumes: Importance of urban planning and drainage adaptation. *Sci Total Environ, 658*(2019), 24-33. doi: 10.1016/j.scitotenv.2018.12.184

Zin, W. W., Kawasaki, A., Takeuchi, W., San, Z. M. L. T., Htun, K. Z., Aye, T. H., & Win, S. (2018). Flood Hazard Assessment of Bago River Basin, Myanmar. *Journal of Disaster Research, 13*(1), 14-21. doi: 10.20965/jdr.2018.p0014

Resports

Cred. (2017). Natural Disaster 2017.

Moe. (2019). Situation of Environmental Report in Cambodia.

Mrc. (2018). Flood Sector Key Findings Report Flood Protection Structures and Floodplain Infrastructure.

Websites

Mowrm. (2019). National Flood Frorecasting Center., from http://www.mowram-nffc.org/index.php

Ncdm. (2018). Disaster Loss Database in Cambodia by National Committee Disaster Management. Disaster Loss Database Retrieved 31 Dec 2019 http://camdi.ncdm.gov.kh/DesInventar/profiletab.jsp?countrycode=kh855&continue=y

Thesis

Ali, A. B. M. (2018). *Flood Inundation Modeling and Hazard Mapping under Uncertainty in the Sungai Johor Basin, Malaysia.* (Doctor), Delft University of Technology, Netherlands.

APPENDIXS

APPENDIX A Water discharge historical recording from MoWRM (Cambodia, 2018)

Years	Kampong Cham Gaugin Station			Years	Chruy Changvar Gauging Station		
	Average	Minimum	Maximum		Average	Minimum	Maximum
1989	11498	1906	34939	1989	11530	1174	32358
1990	13737	2008	41262	1990	12965	891	35520
1991	12934	2050	48383	1991	12386	1814	38924
1992	10122	1688	37775	1992	9813	881	33628
1993	10340	1207	34094	1993	9872	406	30907
1994	13769	1548	44889	1994	12586	484	37632
1995	12288	1436	45058	1995	11446	406	37243
1996	13675	1835	51324	1996	12734	1243	39328
1997	13095	2084	49852	1997	12103	1254	40082
1998	8600	1641	29491	1998	8438	559	27484
1999	13644	1480	42024	1999	12874	484	36330
2000	16734	2061	48230	2000	15104	997	38388
2001	15868	2381	51919	2001	14311	1564	39308
2002	15748	2255	50398	2002	13929	1550	38025
2003	11228	2575	42958	2003	10442	1914	36028
2004	12288	1730	43296	2004	11062	793	36144
2005	13472	1963	46018	2005	12031	782	37705
2006	13120	2249	43743	2006	12060	1439	36754
2007	12391	1947	39622	2007	11538	758	34480
2008	13906	2337	40386	2008	12985	1498	35190
2009	13174	2309	44043	2009	12180	1166	37118
2010	9724	1861	35905	2010	9017	518	32096
2011	16022	2206	50295	2011	14051	705	39023
2012	11134	2789	35802	2012	10440	2203	31649
2013	13074	1942	50967	2013	11832	1132	39612
2014	12740	3343	51866	2014	11513	2628	40556
2015	8916	2467	30812	2015	8216	1730	27402
2016	10329	1921	36179	2016	9210	692	30893
2017	13672	2751	42629	2017	12072	2012	35243
2018	14164	2772	47900	2018	11832	1242	36928

APPENDIX B Water level of gauge station Kampong Cham and Chruy Changvar

Year	Maximum of Kampong Cham water level					Max.	Maximum of PP water level						Max.
	June	July	Aug	Sep	Oct		Year	June	July	Aug	Sep	Oct	
2008	10.23	11.56	14.38	14.05	12.94	14.38	2008	5.95	7.01	9.01	9.32	9.28	9.32
2009	7.84	13.01	14.2	14.03	15.16	15.16	2009	4.54	7.73	8.61	9.02	9.92	9.92
2010	4.08	8.19	12.42	13.43	11.96	13.43	2010	2.45	4.69	7.43	8.08	8.49	8.49
2011	8.32	12.69	15.24	16.02	15.22	16.02	2011	4.69	7.69	9.50	10.85	10.86	10.86
2012	7.68	10.28	12.71	13.46	11.5	13.46	2012	4.23	5.93	7.76	8.56	8.53	8.56
2013	7.49	11.81	13.67	15.97	15.58	15.97	2013	4.13	6.87	8.40	10.26	10.26	10.26
2014	9.00	13.65	15.93	12.4	12.34	15.93	2014	5.00	8.19	9.82	8.60	8.65	9.82
2015	5.97	8.94	12.16	11.43	9.97	12.16	2015	3.14	4.91	7.09	7.00	6.70	7.09
2016	7.23	9.40	11.69	13.31	11.86	13.31	2016	3.61	5.27	6.94	8.13	7.97	8.13
2017	8.00	14.54	14.62	12.87	12.25	14.62	2017	4.67	8.71	8.86	8.64	8.59	8.86